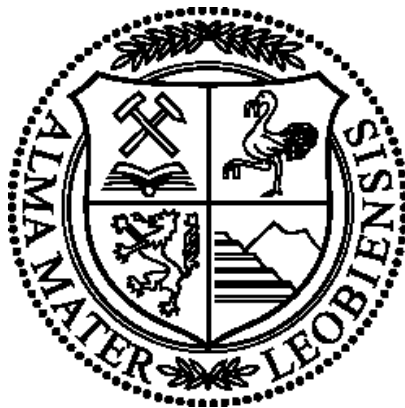# „Low Migration Photoinitiators for Thiol-ene and Water Based Systems"

PhD Thesis

Dissertation

by

DI Meinhart Roth

Chair of Chemistry of Polymeric Materials

University of Leoben

Thesis Supervisor:

Assoc. Prof. Dipl-Ing. Dr. tech Thomas Grießer

November 2015

KURZFASSUNG

Die vorliegende Arbeit beschäftigt sich mit migrationsarmen Photoinitiatoren für biokompatible Thiol-En und UV härtender wasserbasierende Harzformulierungen.

Es wurden neuartige Initiatoren synthetisiert und charakterisiert, welche zum Ziel hatten, die Migration des Initiators selbst, als auch jene der entstehenden Spalt- und Nebenprodukte zu verringern.

Dahingehend wurden drei unterschiedliche Strategien verfolgt, welche zu einer signifikanten Reduktion der migrierenden Substanzen führten.

Hierbei handelte es sich einerseits um polymerisierbare Initiatoren, deren Beweglichkeit durch Copolymerisation eingeschränkt wurde, sowie um oligomere bzw. polymere Substanzen, welche auf Grund ihres erhöhten Molekulargewichtes eine reduzierte Mobilität aufweisen.

Die synthetisierten Typ 1 und Typ 2 Photoinitiatoren wurden für Wasser und Thiol-En basierende Harzsysteme evaluiert und hinsichtlich ihrer photochemischen Reaktivität umfassend untersucht.

Durch die Modifizierung mit Vinylcarbonat- und Alkin-Funktionalitäten konnten ausgezeichnete Ergebnisse, hinsichtlich des Migrationsverhaltens der photoreaktiven Subtanzen in Thiol-En basierenden Harzen erzielt werden, während auch eine signifikante Verbesserung der Migrationsstabilität für oligomere kohlenhydratbasierende Photoinitiatoren in wässrigen Formulierungen verzeichnet werden konnte. Alternativ wurden ebenfalls makromolekulare Initiatoren untersucht welche eine interessante Option für herkömmliche Initiatorsysteme darstellen.

Darüber hinaus wurden neuartige, niederviskose auf Silizium basierende Mercaptoverbindungen hergestellt und mit kommerziell erhältlichen Thiolen verglichen, um deren Eignung für Thiol-Ene Harzsysteme zu evaluieren.

Diese neuen Monomere führten zu einer deutlichen Steigerung der Lagerstabilität der photoreaktiven Formulierungen und zu einer signifikanten Verbesserung der mechanischen Eigenschaften der resultierenden Polymere.

ABSTRACT

The present work deals with the topic of low migration photoinitiators for biocompatible thiol-ene and UV curable water based resins. The focus was set on the synthesis and characterization of novel photoinitiators, to enable a migration reduction of unreacted photoreactive species and related cleavage products.

To realize an improvement in terms of migration stability three different strategies were pursued.

Among these were polymerizable photoinitiators, which lead to a decrease of the initiator mobility by copolymerization of the photoreactive species as well as oligomeric and polymeric photoinitiators which reduce the unwanted migration as a consequence of their enhanced molecular weight.

The synthesized type 1 and type 2 photoinitiators were evaluated for their usability in thiol-ene and water based resins and characterized referring to their photochemical performance.

Attributed to the modification of the novel Initiators with vinyl carbonate and alkyne functionalities excellent results in terms of migrations stability could be obtained for thiol-ene based resins, whereas also a significant improvement for the carbohydrate based initiators in aqueous formulations could be observed. Furthermore macromolecular photoinitiators were investigated, which might be a promising alternative to conventional initiator systems.

Additionally new, low viscous silicon based mercapto compounds were synthesized and compared with commercially available thiols to evaluate their suitability for corresponding thiol-ene resins. These novel monomers led to a significant enhancement in term of storage stability of the related resins and the obtained polymers exhibited improved mechanical properties.

ACKNOWLEDGEMENT

Writing the acknowledgement of your thesis is the most challenging part of the whole work, because you have to consider every single person who supported you in the past three years.

Furthermore, I would like to thank the guys from the MBZS (TU-Graz), who gave me the possibility to write my thesis in their rooms. Finally, I have to thank my family and my girlfriend who always encouraged me in bad times in the past years.

"This work is dedicated to my little nephew who was born in December 2014"

STATUTORY DECLARATION

I declare in lieu of oath, that I wrote this thesis and performed the associated research myself, using only literature cited in this volume

Leoben. November 2015   Dipl.-Ing. Meinhart Roth

INDEX

1 <u>Motivation and outline</u>

The market of high performance photopolymers materials is continuously growing and opening up new fields for industrial and medical applications.[1] Especially, the topic of 3D-printing attracts the public interest, which is obviously a result of its fascinating approach, for smart manufacturing on demand. Its potential, for the design of patient-specific anatomical data individualized implants, scaffolds or tissue engineering applications, is certainly the future of modern implantology. However, before 3D-printing can be used routinely in plastic and reconstructive surgery, it is essential to overcome several technological limitations, which requires ground breaking innovative solutions.[2,3]

Photoinitiators are an indispensable component of photoreactive resins, to obtain appropriate and rapid monomer conversion. Attributed to the usually poor biocompatibility of synthetic monomers, low migration behavior is desirable for cured resins, which requires efficient photoinitiators.

Beside the development of new materials for 3D-printing, the field of UV-curable inkjet inks is a key application for photoreactive resins. In this context, especially product safety aspects are in the focus of public attention. Forced by various food scandals in the past, the migration of ink components became an inevitable topic for food packaging industries.[4,5] Great efforts are being made to realize improved systems, in terms of low migration behavior and biocompatibility, to supply safe and competitive products.

In this work strategies and solutions for novel photoinitiators are reported, which might be promising candidates for low migration applications. The focus was set on thiol-ene based systems, which might be a new approach suitable for 3D-printing, whereas also water based systems are an interesting opportunity for the printing of food packaging materials.

The thesis comment on the synthesis and photochemical characterization of the designed compounds and include comprehensive migration studies of the investigated photoinitiators.

The relevance of the provided results might be highlighted by the fact that parts of the work have been patented.

2 Fundamentals and state of the art

2.1 Photochemistry and photoreactions

In general electromagnetic radiation can be absorbed, emitted or scattered by matter.[6] According to the first law of photochemistry, known as the Grotthuss-Draper law, light must be absorbed that a chemical reaction can occur. [7]
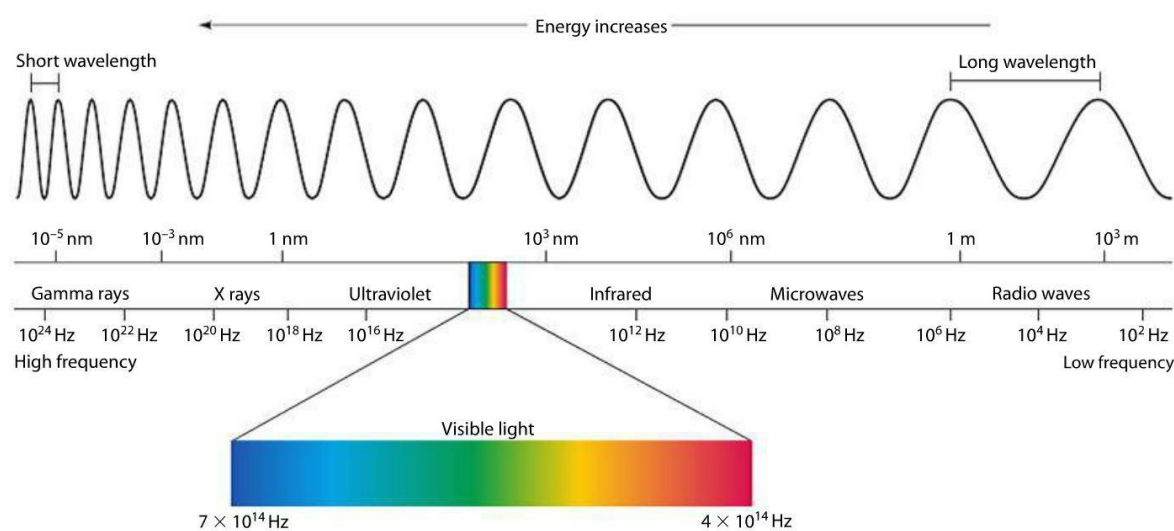
Figure 1: Electromagnetic spectrum[8]

When a molecule gets excited from its ground state (E_0) to a electronically excited state (E_1), the energy of the emitted electromagnetic radiation (E=hv) has to equal the difference between the ground state and the excited state.

(1) $$E_1 - E_o = h\nu$$

The absorption of radiation is a one quantum process, which implicates that for one absorbed photon only one molecule gets excited. This behavior is known as the photochemical equivalence law, or the second law of photochemistry, discovered by Johannes Stark and Albert Einstein.[9]
Accordingly, the efficiency of a photochemical reaction can be defined by the overall quantum yield (Φ), which is proportional to the quotient of the number of reacting molecules (n_A) and the number of absorbed photons (n_Q).

(2)
$$\phi = \frac{n_A}{n_Q}$$

The Stark-Einstein law is restricted to photochemical reactions, which occur at interactions with moderate light intensities. In the case of high-intensity laser experiments, two photon or even multiple absorption can be observed, which lead to quantum yields higher than one ($\Phi > 1$).

Based on these fundamental laws, the electronic transitions, which are a result of absorption and emission processes, can be illustrated by the Jablonski diagram.

In consideration of the selection rules, which constrain the possible transitions of the system, the Jablonski diagram gives a survey of the electronic processes, which are attributed to interaction with electromagnetic radiation.
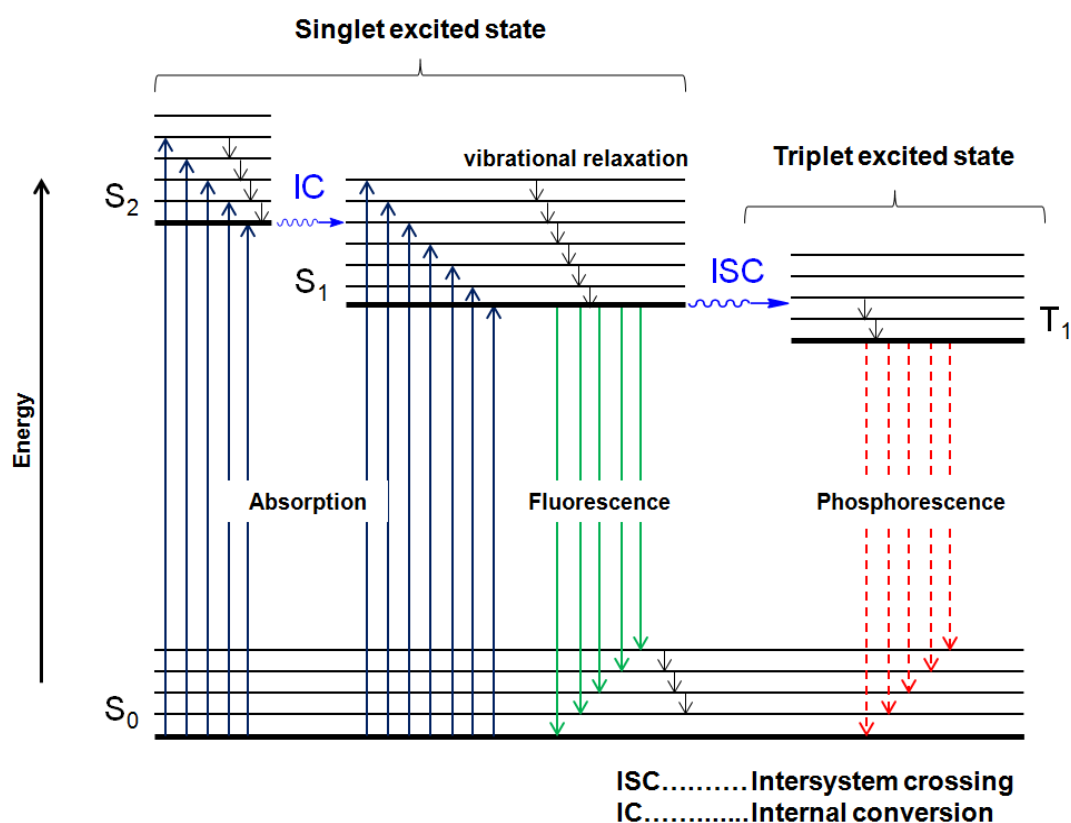
Figure 2: Jablonski diagram[10]

If a molecule gets excited from the ground state S_0 to the unstable excited state S_2, non-radiative decay processes, which are known as internal conversion (IC) and vibrational relaxation, can occur. The system returns to the lowest vibrational S_1 singlet state, which can either relax to the ground state under fluorescence light emission, or undergo a

intersystem crossing to the triplet state (T_1). The transition to the triplet state is associated to a change of the electronic spin orientation, which can be seen as a "forbidden" transition, due to the change of the spin multiplicity. Although the singlet-triplet transition violates the selection rule ($\Delta S=0$), the spin changing transitions (ICS and phosphorescence decay) can be observed as a result of the spin-orbit coupling. The spin-orbit coupling describes the interaction of the spin magnetic moment with the magnetic field arising from the orbital angular momentum and is more distinctive in the presence of heavy atoms (e.g. sulfur)[11]and larger molecules[12]

Therefore longer excitation life times (10^{-4} s) can be observed for the triplet state, as a consequence of the kinetically inhibited transition to the ground state. Due to this behavior the majority of the photochemical reactions originate from the excited triplet state. [13–16]

2.2 *Photopolymers*

The concept of photoreactive resins was already used in antiquity for the caulking of wooden ships and mummification. The utilized material, called "bitumen of Judea", was cross-linked by sunlight induced photo-oxidation processes, which lead to a hardening and insolubilization.[1]

Today photoreactive materials are commonly used as photoresists, printer inks and varnishes and the amount of applications is still increasing. Especially, for the purpose of 3D-printing there is a hugh demand for highly reactive, biocompatible and tough materials, which leads to the continuous development of new or improved systems. Among these numerous photoreactive materials, three for this work relevant systems are introduced and discussed in further detail.

2.2.1 Acrylate and methacrylate systems

Acrylates and methacrylates have a high industrial relevance for a broad range of applications, which is attributed to their unique photoreactivity. They have made significant inroads in replacing thermally cured and solvent based technologies, which can be mainly ascribed to their superiority in terms of energy requirements and VOCs reduction.[1] Especially, in the field of inkjet inks, solvent free formulations lead to higher film abrasion resistance and lower ink waste, as a result of enhanced open times (time between several printing steps) and more consistent ink qualities (no solvent evaporation) which is obviously the reason for their market leading position. Attributed to the huge amount of available acrylate monomers, ink formulations can be optimized regarding their physical properties and the field of application. The adjustment of the viscosity and surface tension are crucial to guarantee satisfying printability, whereas the number of acrylate functionalities and the structure of the monomer backbone are responsible for the film quality and resistance.[17] Nevertheless, all acrylate and methacrylate formulations have in common, that they are polymerizable in a radical chain growth mechanism, which can be subdivided into initiation, propagation and termination step (see Figure 3).

In the first step, the photoinitiator gets excited by electromagnetic radiation, which leads to the generation of reactive radicals. The monomer is activated by the reactive species and propagates the polymerization, until a termination reaction occurs, or the monomer supply is depleted. The termination can be initialized, when either two reactive polymer chains join together (combination) or the radical is annihilated by hydrogen addition and double bond formation (disproportionation). Furthermore, chain transfer reactions can be observed, which lead to the deactivation of the polymer chain and the activation of

another polymer fragment by electron transfer. Usually these reactions are responsible for the formation of polymer side chains.

$$\text{Photoinitiator} + h\nu \longrightarrow R^{\bullet}$$
$$R^{\bullet} + M \longrightarrow RM^{\bullet}$$

Initiation

$$RM^{\bullet} + M_n \longrightarrow RM^{\bullet}_{n+1}$$

Propagation

combination
$$RM^{\bullet}_n + {}^{\bullet}M_mR \longrightarrow RM_nM_mR$$

disproportionation
$$RM^{\bullet}_n + {}^{\bullet}M_mR \longrightarrow RM_n + M_mR$$

Termination
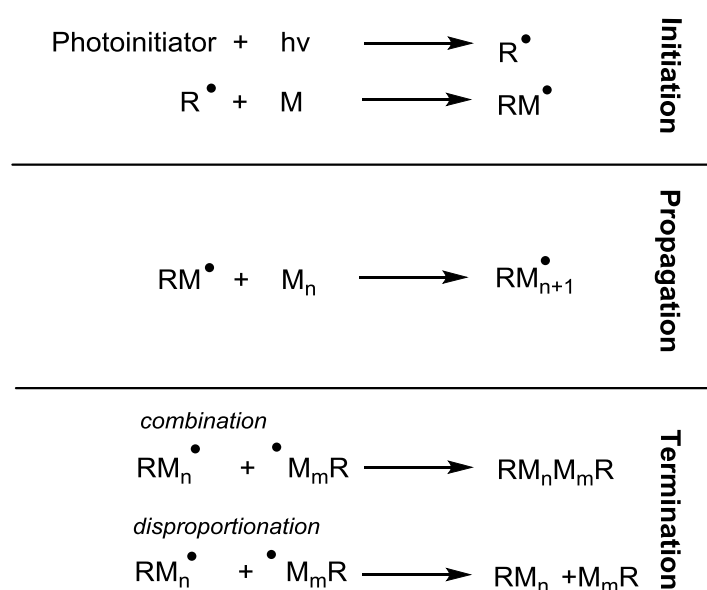
Figure 3: Radical chain growth mechanism

Despite the outstanding reactivity of the acrylate functionalities, these systems suffer from some essential drawbacks. The homopolymerization of acrylates and methacrylates is significantly inhibited in the presence of oxygen and heterogeneous high-density regions are formed at low double bond conversion.[18,19] Due to the huge amount of uncured monomers, which is a result of the reduced conversion of approximately 80% [20,21], migration effects of the unbound species can be observed. In case of UV-curable inks for printing on food packing materials this can lead to the contamination of the packaged goods due to the migration of uncured monomers, which limits the usability of acrylate formulations.[22]

Methacrylates are in the focus of public attention due to their broad field of applications in dental medicine.[23] Their cyctotoxicity is presumably lower compared to acrylates, although the actual harmfulness is not entirely clarified. A multitude of publications discuss their usability for medical applications critically, whereas several questions are still open. However, it is proven that the exposure with multifunctional methacrylates and acrylates can induce a sensitization, which leads to a delayed contact dermatitis. The reasons for that can be found in the thiol michael addition of the acrylates to the thiol and amine functionalities of the proteins.[21]

The studies investigating the carcinogenicity are partially contradictory, which is mainly attributed to the lack of appropriate long-term studies. [24–28]

It can be concluded that, beside the unique properties regarding the photoreactivity of acrylate formulations, disadvantage in terms of cyctotoxicity and migration behavior limit the usability of these formulations. To overcome these essential drawbacks, there is an enhanced demand for alternative systems, which combine high reactivity and biocompatibility.

2.2.2 Thiol-ene systems

In contrast to the radical chain grow homopolymerization of acrylates, the polymerization of thiol-ene systems is based on a step growth mechanism. This implicates that, if the ene monomer is not homopolymerizable, high monomer conversion can only be observed in a stoichiometric mixture of a reactive ene and a convenient thiol. Furthermore, the reactivity of the utilized ene and thiol functionalities is significantly influenced by their electronic environment. Electronically rich enes exhibit high reactivities, whereas electronically poor double bonds are rather slow regarding their reaction speed.[19,29,30]
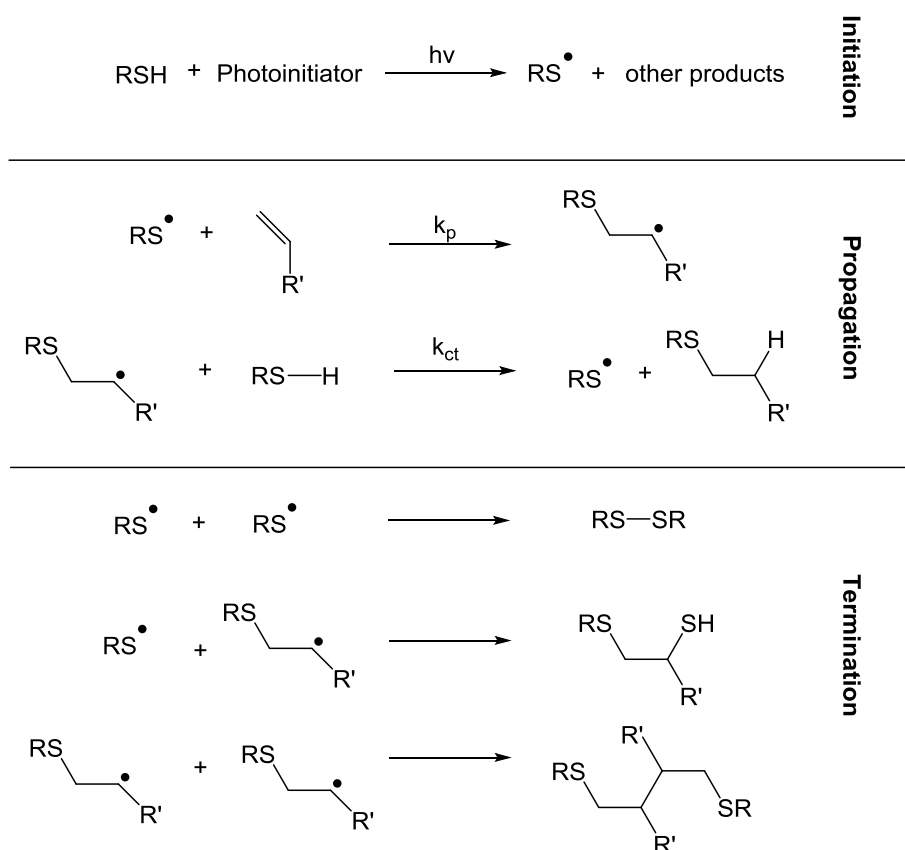
Figure 4: Mechanism of the thiol-ene reaction[31]

For the mercaptans the stability of the sulfur-hydrogen bond is decisive for the reactivity whereas the nucleophilic character of the thiol is dependent on the neighboring

functionalities. Electron withdrawing groups favor hydrogen abstraction, which lead subsequently to an enhanced reactivity (see chapter 5.3.2) [32]

The polymerization mechanism can be subdivided, analogously to the homopolymerization of Acrylates (see chapter 2.2.1), into three different reactions steps, namely initiation, propagation and termination which are depicted in Figure 4.

The thiyl radical is generated after hydrogen abstraction, by the formed radical of the applied photoinitiator upon UV light, which leads to an anti-Markovnikov addition of the thiyl radical to the ene monomer. The carbon centered radical leads, upon hydrogen abstraction to another thiyl radical which propagates the polymerization. Termination occurs by radical -radical coupling of either two thiyl or carbon centered radicals or by recombination of one of each groups.[31,33–35,35]

The superiority of thiol-ene formulations is accentuated by high double bond conversions, which is obviously a consequence of the delayed gelation point induced by the step growth polymerization mechanism and the low oxygen inhibition of the polymerization.[36,37] Thus, the unfavored migration of uncured monomers is rather low and the formed networks exhibit high homogeneity and low polymer shrinkage compared to acrylate systems[18]. However the glass-transition temperatures (T_g) are rather low which is attributed to the high flexibility of the generated thio-ether bonds and the reduced crosslinking of the loose thiol-ene network[38]. The most important drawbacks are the reduced storage stability (dark-reaction) of thiol-ene based resins and the strong odor of low molecular thiols, which limit the field of possible applications drastically. Regarding the shelf-life of thiol-ene systems, different strategies are reported in the literature which enable the stabilization of unpigmented formulations.[39] However these methods are usually on the expense of the reactivity and the unwanted gelation is only slightly delayed.
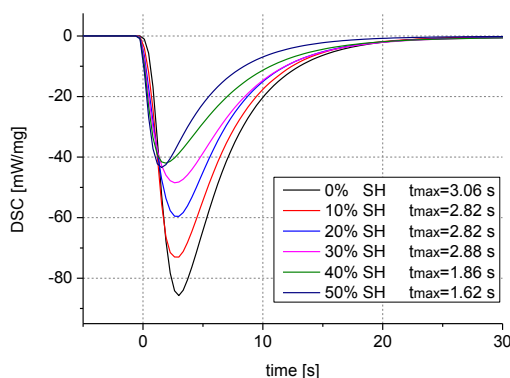
Figure 5: Acceleration of the reaction speed (t_{max}) of butandiol divinylcarbonate by thiol addition

Nevertheless thiol-ene chemistry can also be utilized for the acceleration of rather unreactive monomers. For instance vinyl carbonates systems, which exhibit inappropriate homopolymerization speed but high biocompatibility, can be optimized regarding their reactivity by the addition of multifunctional thiols. The reason for the reduced performance of the homopolymerization can be found in the lack of resonance stabilization of the formed radicals of the vinyl carbonates which are additionally prone to side reactions like H-abstractions. To overcome this essential drawback the addition of abstractable hydrogens (thiols) that form subsequently highly reactive radicals (thiyl radicals) is an appropriate solution to accelerate the polymerization process.[40]

The obtained dual polymerization, homopolymerization as well as thiol-ene reaction, leads therefore to increased reaction speeds and higher monomer conversion compared to the vinyl carbonate formulations which are polymerized in a chain growth mechanism.[21,41]

Thus, vinyl carbonates in combination with multifunctional thiols were chosen for the evaluation of low migration photoinitiators.

2.2.3 UV curable water based resins

Aqueous polymer dispersions are a versatile alternative to conventional acrylate formulations. The applications range from coatings and binders to adhesives which makes them to a versatile field of technology.[42]

The main difference between photoreactive water based coatings and the conventional photo-curable systems lies in the avoidance of monomers as reactive diluents. Polymers are dispersed into water and the photoreactive groups are usually attached to the polymer backbone.[43] Therefore, unwanted migration of resin components can be minimized, which enables the application for food packaging materials. The resin properties can be adjusted by the tailor-made synthesis of the dispersed polymer. For that purpose, polymers like polyesters, polyethers, polyacrylates and polyurethanes can be utilized, whereas the preparation of the corresponding dispersions is rather complex and requires a high degree of preparative knowledge. Nevertheless, a tremendous amount of polymer dispersions are commercially available. Most of them are based on polyurethane, which might be explained by their easily adjustable mechanical properties. In general they consists of flexible polyols and rigid isocyanates which are polymerized in a step-growth polymerization. After neutralization and dispersion in water the PUDs are modified by amines as chain-extenders which enables microphase separations of the hard and soft segments of polymer. This effect is responsible for the outstanding mechanical stability of the polyurethanes and expands the field possible applications drastically.[44,45]

Furthermore the opportunity for self stabilization is an important feature that avoids the necessity of additional stabilizers and expands the applicability of this class of coatings.[46]
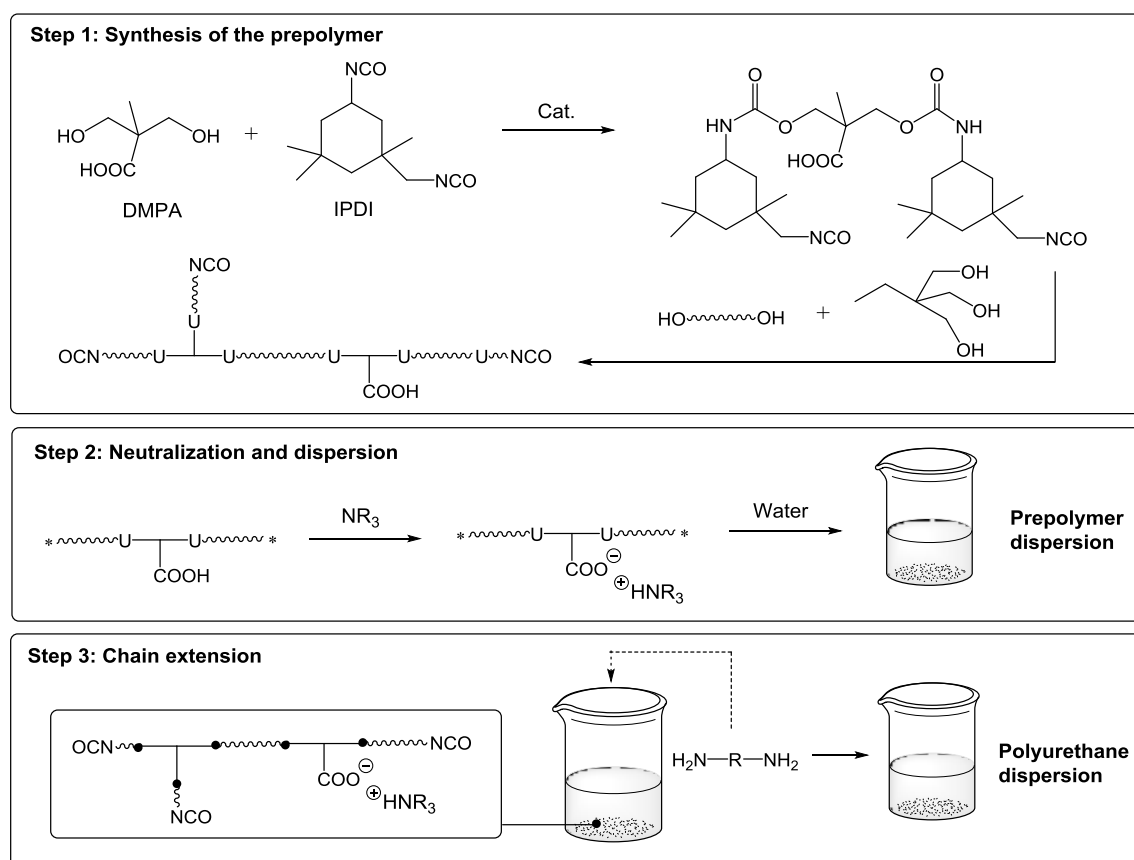
Figure 6: Scheme of the polyurethane dispersion preparation (U...urethane-group; IPDI... isophorone diisocyanate; DMPA ...dimethylol propionic acid [43]

The scheme of the preparation procedure is depicted in Figure 6, which is subdivided into three different steps. First a multifunctional isocyanate (IPDI) is reacted with dimethylol propionic acid (DMPA), which is neutralized in step two by the addition of an amine. The incorporation of ionic or hydrophilic functionalities in polyurethane dispersions lead to better shelf-life stabilities, which is attributed to the repulsive forces of the ionic functionalities. They prevent coagulation and sedimentation of the polyurethane particles and additionally lead to an elevated solvent resistance of the obtained films. In step three, the excess of isocyanate groups is reacted with difunctional amines, which is known as the chain extension reaction. It leads to a significant increase of the molecular weight of the polyurethane particles, whereas the influence on particle size and resin viscosity is neglectable.[47,48]

Another outstanding feature of polyurethane dispersions are their excellent film forming properties.[49]
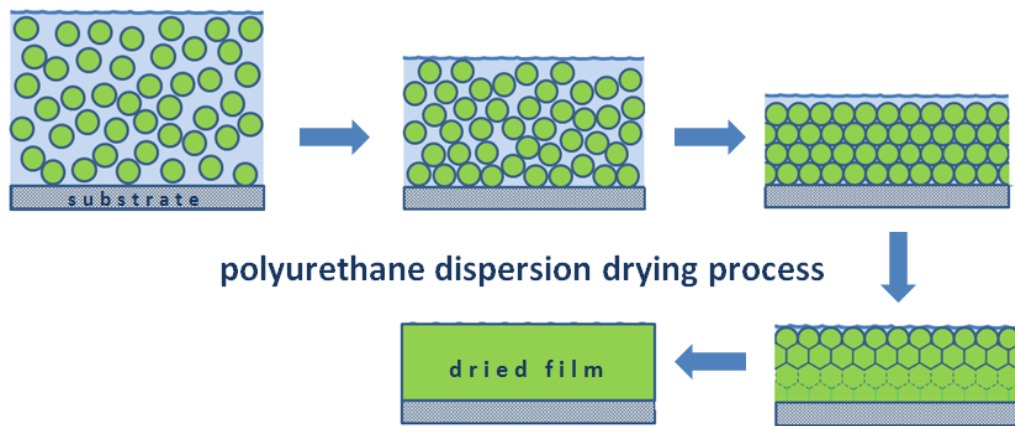
Figure 7: Polyurethane dispersion drying process[50]

After the application on a substrate, the film is dried to remove the excess of water to obtain a resistant polymer film (Figure 7).[49] With the continuous evaporation of the solvent a coagulation of the polymer particles can be observed which supports the formation of a homogenous polymer surface. This procedure might be supported by additional photochemical curing steps, which can be applied before and/or after the drying process. Photoreactive moieties, which are attached to the polymer backbone, are crosslinked by UV light and lead to higher scratch resistance of the obtained polymer films.[51]

2.3 *Photoinitiators*

2.3.1 Theory and basics

Photoinitiators are a crucial component of photoreactive resins to realize satisfying curing velocities and high monomer conversion. To obtain ideal resin performance, it is essential to choose a suitable photoreactive species, which exhibits (I) an absorption maximum that fits to the applied light source and (II) high solubility in the investigated resin. Furthermore, the field of application has to be taken into consideration, according to the preferred type of curing (depth or surface curing) whereby also combinations are commonly used.[52]

After the absorption of UV light, photoinitiators are excited to the reactive singlet state. They can return to lower energy levels by fluorescence light emission or by intersystem crossing, which lead, to a triplet state transition. In the absence of quenching reactions, the excited triplet state is the starting point for radical production. In general, three different initiation pathways can be divided, namely cleavage of type I photoinitiators, electron transfer by charge-transfer complexes (CTC) and hydrogen donation to type II photoinitiators (see Figure 8).[52,53]
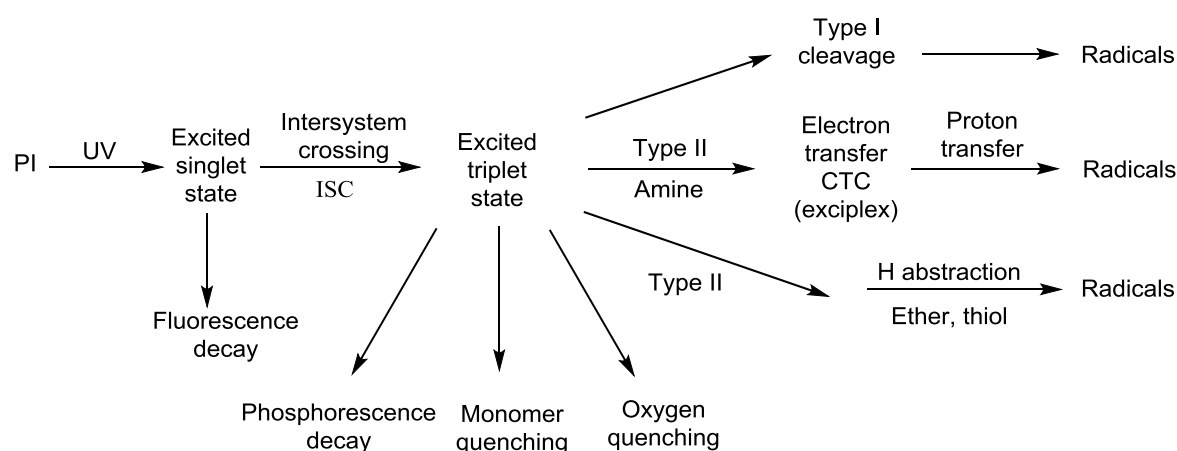
Figure 8: Reactive and deactivating processes in the production of radicals[52]

Quenching reactions usually dependent on the life time of the excited triplet state. If the system looses energy by phosphorescence decay, or the triplet life time is inherently short, quenching reactions are more unlikely. Therefore, type II photoinitiators, which exhibit elevated triplet life times, are more susceptible to inhibition. In general, two main quenching reactions can be observed, the monomer quenching and the oxygen quenching. The latter only plays a minor role, as a consequence of the usually low oxygen

concentration in the formulation.[52] The influence of the monomer is obviously more decisive for the resulting curing performance and was studied extensively by Lemee et al.[54]. They focused on monomer quenching reactions of type II photoinitiators and compared the influence of electron rich and electron poor double bond featuring monomers. In general, they propose four essential quenching mechanisms of benzophenones in methacrylate based resins which can lead to a deactivation of the excited triplet state. The formation of 1,4-biradicals followed by the generation of an oxetane is postulated as the predominate reaction (see Figure 9) for these systems.
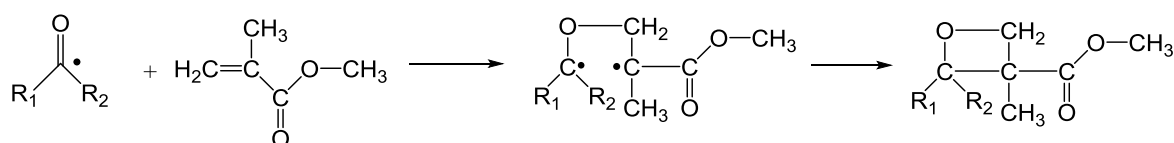
Figure 9: Formation of 1,4-biradicals in methacrylate systems[55]

Additionally the energy transfer from the ketone to the olefin, the hydrogen abstraction by the ketone and the electron transfer process have to be taken into consideration, depended on to the applied monomer system.[55,56]

2.3.2 Type I photoinitiators

After the absorption of electromagnetic radiation type I photoinitiators undergo a photolysis of a C-C bond (usually Norrish type I reaction), which leads to the generation of reactive radicals (see Figure 10). Unimolecular photoinitiators, which implicates that no co-initiator is required, exhibit decent initiation rates and due to their short triplet state life times they are insensitive towards monomer or oxygen quenching (see chapter 2.3.1). Probably the most important representative of this group are the acetophenones and their derivatives, which are commonly used in several industrial applications. In general, they exhibit a strong absorption band between 250 and 300 nm, which is attributed to the π-π^* transition and a weaker one at 320 - 360 nm as a result of the "forbidden" n-π^* transition. Due to the delocalization or interactions of molecule orbitals of the substituents (R_1-R_3) and the chromophore, significant shifts of the absorption bands can be obtained.[53]
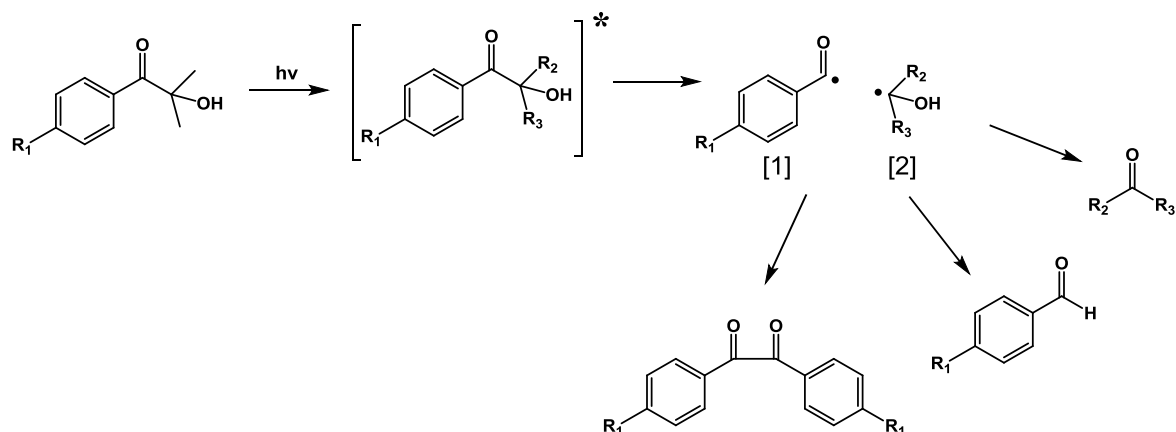
Figure 10: Norrish type I reaction - α-scission of the acetophenones and the corresponding cleavage products[53]

Acetophenones undergo an α-cleavage, which leads to the generation of two different radicals. The reactivity of these species is depending on the chemical structure of the radical (R_1-R_3), as well as on the electron density of the double bond of the available monomer (see chapter 2.2.2). Accordingly, it is reported in the literature that the initiation is predominately influenced by the ketyl radical [2] whereas the benzoyl radical [1] only plays a minor role for the initiator performance (see Figure 11).[56]

A second class of type I photoinitiators are the phosphine oxides, which feature a broad absorption, even to the visible part of the electromagnetic spectrum and no yellowing reactions during photopolymerization. These unique properties made them to an important group of photoreactive species which were studied in a multitude of publications. [57–61] Especially their photo-physical behavior was investigated extensively, which offers several explanations for their outstanding photochemical performance. In general, this group of photoinitiators can be subdivided into two types of initiators, namely the monoacylphosphine oxides and bis(acyl)phosphine oxides.
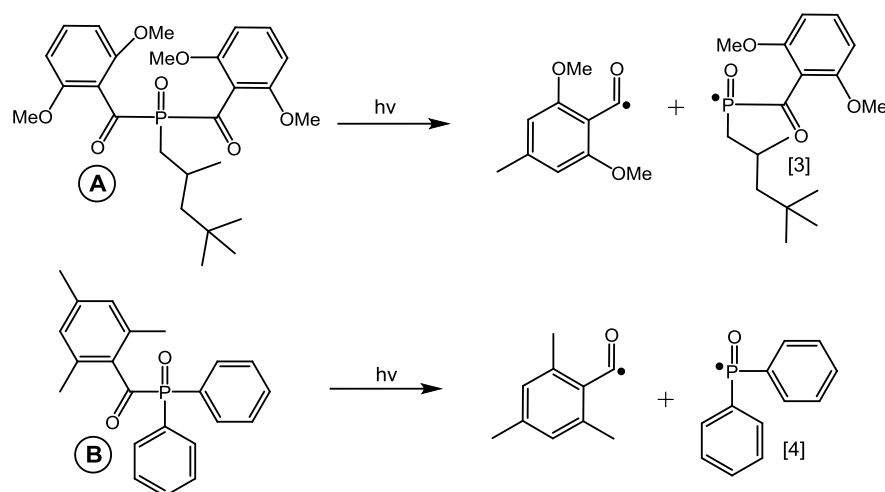
Figure 11: A: Bis(acyl)phosphine oxide, B: Monoacylphosphine oxide[62]

Both of them undergo rapid α-cleavage from a excited triplet state, which leads to the generation of two radicals. The triplet life time is rather short that it was postulated in older publications that the radical generation originates from the excited singlet state. In fact, a small fraction of α-cleavage from the excited singlet state cannot be excluded, although singlet radical pair recombination is faster than separation. Jockusch et al.[62] were able to examine the triplet generation by the utilization of triplet quenching reactions and it turned out, that the intersystem crossing is the limiting step of the radical generation.

Furthermore, it could be shown by Sluggett et al.[63] that the radical [4] was 2-6 times more reactive (dependent from the investigated monomer) than compound [3]. This effect can be explained by the sterically demanding substitutes of the alkyl modified species and emphasizes the individuality of every initiator system.
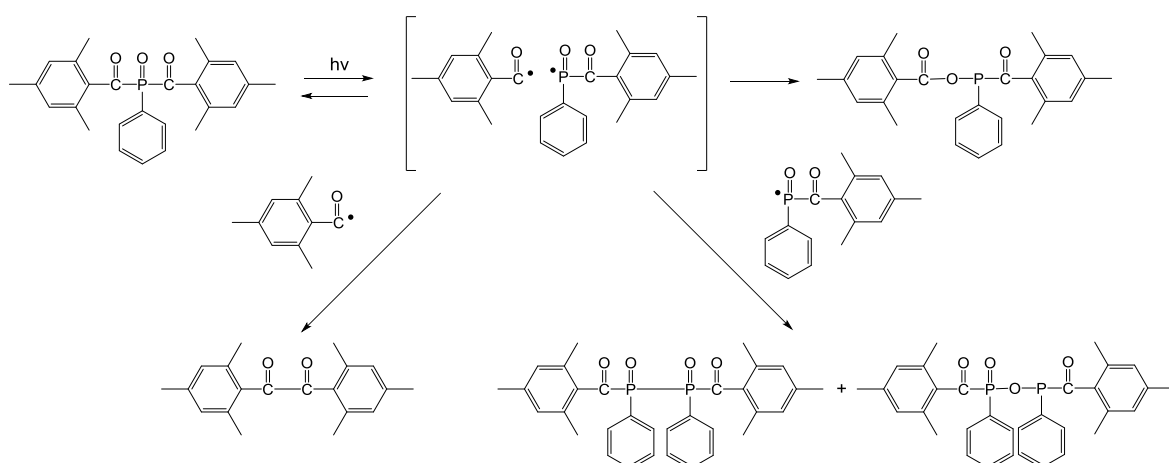
Figure 12: Cleavage and side products of bis(acyl)phosphine oxides[64]

Beside these important photo physical findings, the generation of the cleavage and side products, as a result of recombination of initiator fragments, was investigated. Accordingly, several compounds could be identified by ^{31}P, ^{13}C, ^{1}H-CINDP (chemically induced dynamic nuclear polarization) studies, which give information about the complex reactions which occur during the initiation process.[64] The generation of cleavage and side products have to be taken into consideration especially for migration studies and also the correlated safety aspects of photoreactive resins.

2.3.3 Type II photoinitiators

In contrast to the type I photoinitiators, type II photoinitiators are two component systems. To realize satisfying curing behavior a co-initiator is required, which is usually a hydrogen donating substance. In the literature a multitude of co-initiators are investigated extensively, with focus on tertiary amines and mercapto-compounds. The main classes of type II photoinitiators are based on benzophenone, thioxanthone, camphorquinone and ketocoumarine[65] whereas the initiation mechanism of the benzophenone is comprehensively elucidated in this work.
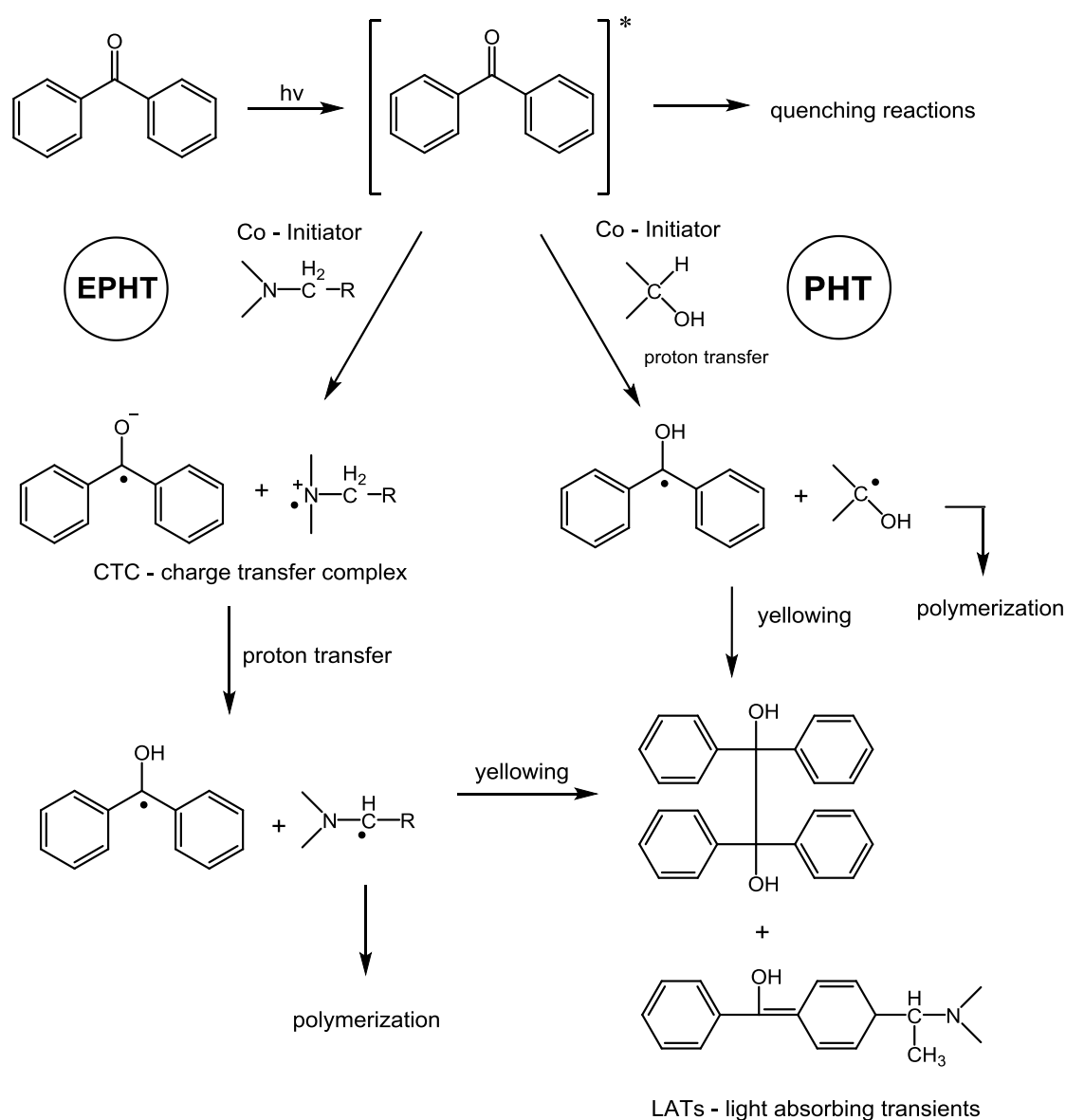
Figure 13: Initiation mechanism of the benzophenone (EPHT...electron proton hydrogen transfer; PHT...proton hydrogen transfer; LATs... light absorbing transients)[53]

As described in chapter 2.3.1, the initial point of the initiation process is the excited triplet state of benzophenone. In absence of possible quenching reactions, two main initiation processes can be subdived for the generation of the reactive radicals. In general, the applied co-initiator is decisive for the observed reaction pathway, whereas the redox properties of the reactants and the free-energy changes (ΔG) for the electron transfer have to be taken into consideration.[66] Amines and mercapto compounds usually react in an EPHT (electron proton hydrogen transfer) process, which leads to the formation of a CTC (charge transfer complex), which is followed by a proton transfer (see Figure 13).

In the case of an alcohol or silane proton donator, the initiation is dominated by a PHT-process (proton hydrogen transfer), which is mainly dependent on the bond dissociation energy of the co-initiator (H-donor). In contrast to EPHT process no charge transfer complex is formed, the radical generation is only influenced by hydrogen abstraction. In presence of both types of co-initiator the EPHT-process is favored, which also leads to higher initiation rates. This effect is mainly attributed to elevated interaction rates between the excited triplet state and the corresponding co-initiators and low susceptibility toward side and quenching reactions. Obviously, both of the described mechanisms always occur side by side, although the given principles can be seen as an estimation of the predominant process.[66] To give a secured prediction of initiation mechanism, several aspects have to be taken into consideration. For instance, the electron transfer rate, the ability of proton transfer of the CTC, the bond dissociation energy of the hydrogen donor and sterical influences.[53] Furthermore, the actual initiation efficiency is depended on the reactivity of the generated radicals. For the benzophenone/amine system two types of reactive species can be observed, although it is well known that the ketyl radical shows hardly any reactivity and is responsible for chain growth termination reactions.[67]

Moreover, the appearance of side reactions can lead to recombination processes of the ketyl radicals, which have negative effects on applicability of resins containing this type of photoinitiator. Consequently, the yellowing, which is definitely one of the most important drawbacks of the benzophenones, can be explained by the formation of recombination products. These compounds are called light absorbing transients (LATs) and exhibit a absorption maximum at 330 nm.[68]

2.4 *Migration of resin components*

The migration of resin components is an essential topic in terms of product safety and operational capability from the industrial point of view. Especially, in the field of inkjet inks for food packaging materials and medical applications of photopolymeric materials, migration aspects require highest attention. It is well known that several components of photoreactive resins are harmful or even toxic (see chapter 2.2.1).[26,69,70] Attributed to incomplete monomer conversion[20,71] or elevated contents of photoinitiators migration effects of the low molecular compounds can be observed. In particular, pigmented systems (inkjet inks) tend to contain elevated amounts of photoinitiating compounds to obtain satisfying curing behavior, although the monomer conversion is still low.[53]

Forced by various food scandals in the past, the amount of directives and guidelines regarding articles intended to come in contact with food increased significantly. In general, there are two basic regulations of the European Union which deal with the topic of food contamination namely Council Regulation EC No. 1935/2004 and EC Commission Regulation No. 2023/2006. They introduce important mechanisms regarding quality assurance and implement a guideline for "good manufacturing", whereas the special topic of inkjet ink migration is neglected. However, the commission regulation EU No 10/2011 and the Ordinance on Materials and Articles in Contact with Food (SR 817.023.21), consider contamination effects ascribed to inkjet ink components and provide a procedure for the investigation of the migration behavior. They regulate the testing of the related packaging material depending on the type of food and the expected storage temperature and time.[72,73] Furthermore, they give an extensive list of migrations limits, which refer to the highest permissible concentration in the analyzed food or food stimulants.
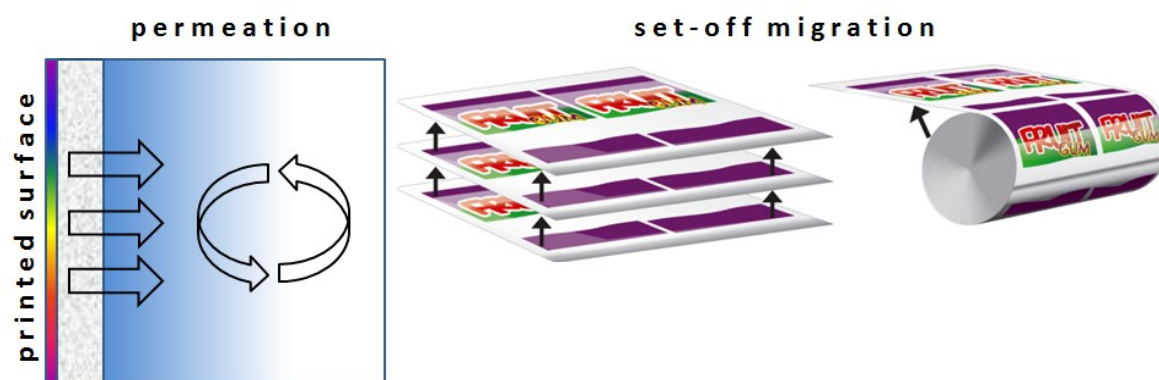
Figure 14: The different types of migration, left: Permeation through packaging material; right: Set off migration[74]

In this context, different types of migration have to be mentioned (see Figure 14). In general, migration can be subdived into set-off migration and permeation, which implicates the contamination pathway of the investigated food. The set-off type is a consequence of the conventional production method of food packaging material, which is usually stacked or rolled after the printing process. The inner surface of the packaging is contaminated by the other rolled layers, which finally leads to substantial concentration of inkjet ink components in the packaged product. The permeation describes the diffusion through the packaging material, which should not be underestimated in terms of product safety and potential risk assessment.[75,76]

3 Polymerizable photoinitiators

Parts of the work in this chapter have been patented -
AT201350557 - **Roth, M.;** Grießer, T.; Oesterreicher, A.; Edler, M.; Mostegel, F.; Gassner, M.; Billiani, J.; - Photoinitiators

Patent application:
WO2015031927 - **Roth, M.;** Grießer, T.; Oesterreicher, A.; Edler, M.; Mostegel, F.; Gassner, M.; Billiani, J.; - Photoinitiators

3.1 Introduction

In the last decades the photopolymerization was the matter of extensive research and found its place in various industrial applications. Especially in the field of coatings, varnishes and ink-jet inks photochemical reactions are in the focus of public attention, which leads to an increasing demand for eco-friendly and harmless products.[53,77,78]

Photoinitiators are essential components in photoreactive formulations to realize satisfying curing behavior and to obtain high monomer conversion during the illumination process.[79]

Incited by various food scandals, regarding the contamination of orange juice and baby milk with the photoinitiators ITX and benzophenone, the unfavorable migration behavior of these substances was discussed exhaustively in various publications.[80–82]

Benzophenone and its derivatives, which are commonly used as photoinitiators in photo curable resins but also as a chemical UV filter in sunscreens and cosmetics, are an important group of photoreactive species. Due to the versatile use of this substance class, a comprehensive amount of publications deals with the safety aspects of benzophenones and discusses their influence on the human body.[83,84]

In general, benzophenones are classified as endocrine disrupting substances, which indicates their negative impact on the human hormone balance. A multitude of publications report on the bioactivity and the disrupting capacity of this substance class and propose the potential risk to develop ovarian or testicular cancer as a result of the hormonal imbalance.[69,83,85,86] Furthermore, it was even named as the contact allergen of the year 2014 by the American Contact Dermatitis Society.[87]

In contrast to the extensive investigated benzophenone derivatives there are only a few studies which focus on other commonly used photoinitiators. Only C. G. Williams et al.[88] report on the biocompatibility of the commercially available photoinitiator Irgacure 2959

and discuss its tolerance over a wide range of cell types and initiator concentrations. They conclude that the hydroxy ketone photoinitiator shows high biocompatibility and they postulate a connection between the cellular proliferation and the cellular toxicity.

Based on these results the cyctotoxicity of the commercially available photoinitiator Irgacure TPO-L was evaluated and compared to Irgacure 2959 (see chapter 3.4.1) to estimate their usability for biocompatible resin formulations.

It could be observed that the Irgacure TPO-L (EC_{50} <0.16 mM) shows a significant lower biocompatibility compared to the Irgacure 2959 (EC_{50}=2.2 mM) (Figure 15), whereas cleavage or side products, which are generated during the illumination process, were not taken into consideration for this study. However it must be emphasized that also these undesired by-products can be harmful or even toxic substances.

For instance the 4-(2-hydroxyethoxy)benzaldhyde, which is one of the main cleavage products of the Irgacure 2959, is labeled as an irritant substance,[89] although the unreacted photoinitiator shows an acceptable biocompatibility.
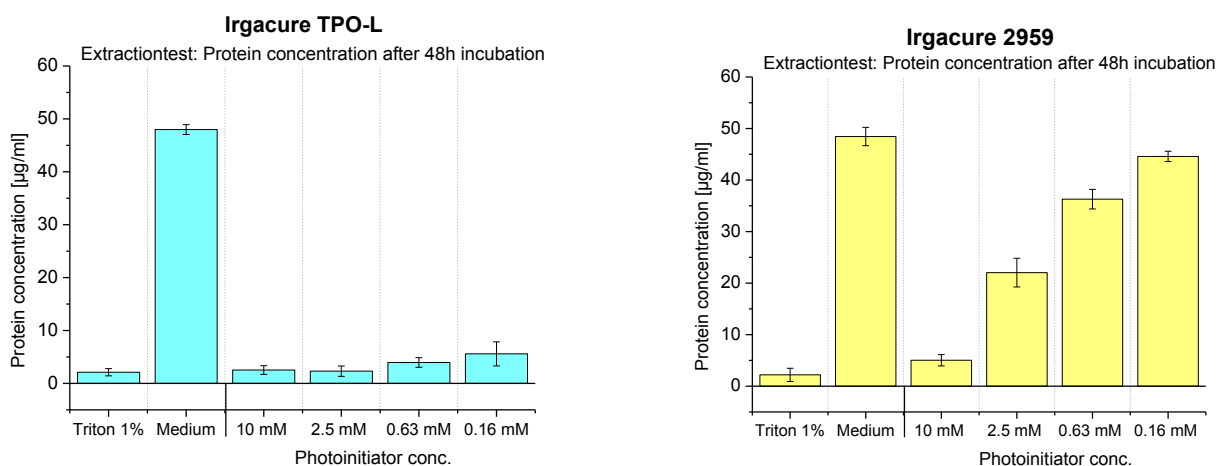
Figure 15: Biocompatibility of the commercially available photoinitiator Irgacure TPO-L and Irgacure 2959 (ISO 10993-5)

Consequently, several strategies were proposed to overcome the potential risk of this substance group.

Polymeric systems containing photoinitiating residues covalently bonded to a macromolecular backbone exhibit better migration stability, but suffer from low reactivity and poor compatibility with many resin systems.[90] These essential drawbacks, in particular the lack of reactivity, can be ascribed to a dilution of photoinitiating moieties in the polymeric backbone. That means that the required amount of polymeric photoinitiator is significantly higher to obtain a reactivity equivalent to the original photoinitiator.

Furthermore quenching effects due to the proximity of neighboring photoreactive groups are reported in the literature.[91–93]

Another possibility to reduce the unwanted migration of the photoinitiators are oligomeric photoreactive species. These are multifunctional photoinitiators, featuring several initiator units coupled to an arbitrary molecular backbone to increase the molecular weight. Usually the target formula weight is higher than 1000 g/mol in order to circumvent a toxicological classification, which is required in industrial applications for smaller molecules. The EU Scientific Committee for Food (SCF) considers high molecular weights as safe, because there is only a little adsorption in the gastrointestinal tract, thus no toxicological data are required for safety evaluation.[94,95]

However to realize low migration behavior the focus was set on polymerizable photoreactive species due to the high solubility in the most resin formulations and the straightforward synthetic pathways.

The concept of these photoinitiators is rather simple and was published for the first time in patent literature 1961 by the company Du Pont.[96] In general, the photoinitiating unit gets immobilized in a photopolymer by the copolymerization of a photo reactive group which is attached to the photoinitiator.[97] Consequently, the unwanted migration is being reduced as the photoreactive species is covalently bound into the polymer network and any type of diffusion processes is being excluded.

The amount of scientific publications which deal with the topic of polymerizable photoinitiators is rather low and most of them focus on the photochemical performance whereas the migration behavior is only discussed superficially.[98,99,99] Moreover they only provide data for acrylate resins and the polymerizable groups are limited to acrylate, methacrylate or aliphatic ene functionalities.

Thus, we extended the toolbox of polymerizable groups by the vinylcarbonate, thiol and alkyne moieties and investigated the photochemical performance, as well as the migration behavior in two different photoreactive resins.

In particular, we focused on the applicability of these novel photoinitiators in biocompatible thiol-ene based systems to realize low migration photoreactive formulations, suitable for food packaging materials and 3D printing resins.

3.2 *Results and Discussion*

3.2.1 Synthesis of polymerizable photoinitiators

The investigated benzophenone derivatives **1a - 1e** and **2d** were synthesized by a Steglich esterification (see Figure 16).[100]
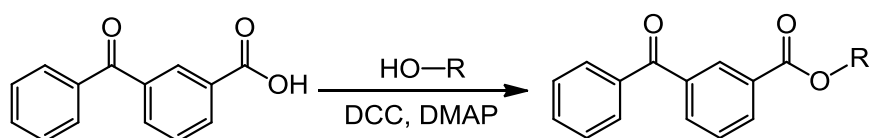
Figure 16: Reaction scheme of a Steglich esterification

The 3-benzoylbenzoic acid was reacted in the presence of 4-dimethylaminopyridine (DMAP) as a catalyst with *N,N'*-dicyclohexylcarbodiimide (DCC) to enhance the electrophilicity of the carboxylate group.
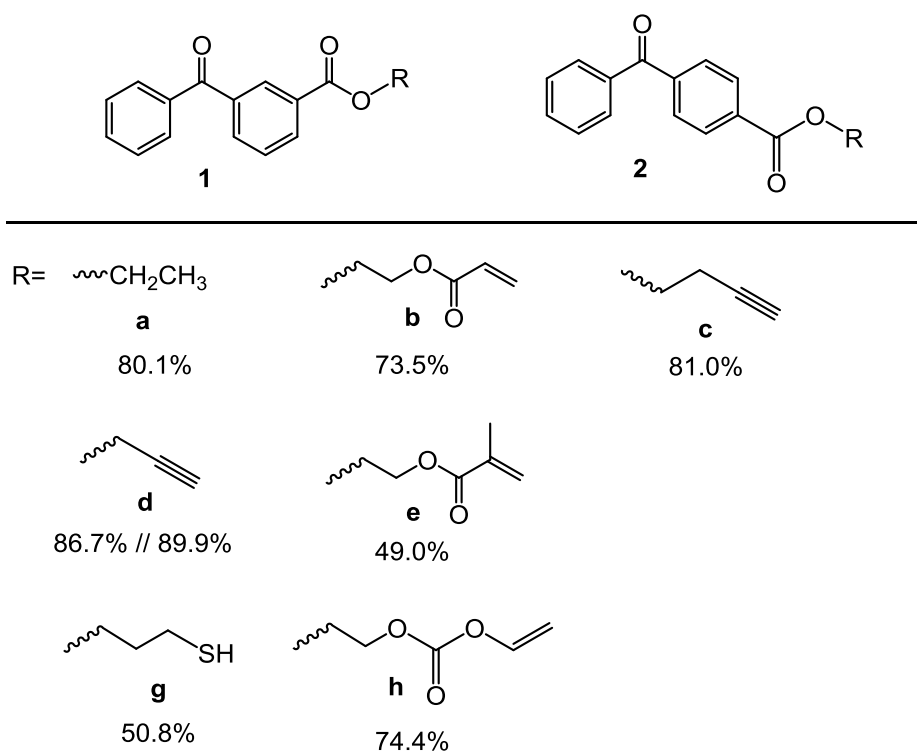
Figure 17: Structures of the synthesized benzophenone derivatives

In the reaction the DCC is attacked by the nucleophilic oxygen of the carboxylate and generates a highly reactive O-acyl intermediate which favors the nucleophilic attack of the

alcohol.[101] The compounds **1a** - **1e** and **2d** could be obtained after purification by column chromatography in decent yields and high purities (see Figure 16 and yields in Figure 17). The substances **1g** and **1h** were realized in a two step reaction. First the benzophenone carboxylic acid was converted by Steglich esterification (I) of 1-bromo propan-3-ol and ethylene glycol respectively, to obtain the precursor materials which were subsequently transformed to the corresponding photoinitiators.

An appropriate procedure to obtain compound **1g** was found in a mercapto - dehalogenation reaction (II), which was based on the in situ generation of the highly reactive tetrabutylammonium trimethylsilylthiolate.[102] For that reason the precursor material was reacted with hexamethyldisilathiane and an equimolar amount of tetrabutylammonium fluoride (TBAF) to obtain **1g** upon aqueous workup and chromatographic purification, in acceptable yields (51%) (see Figure 18).
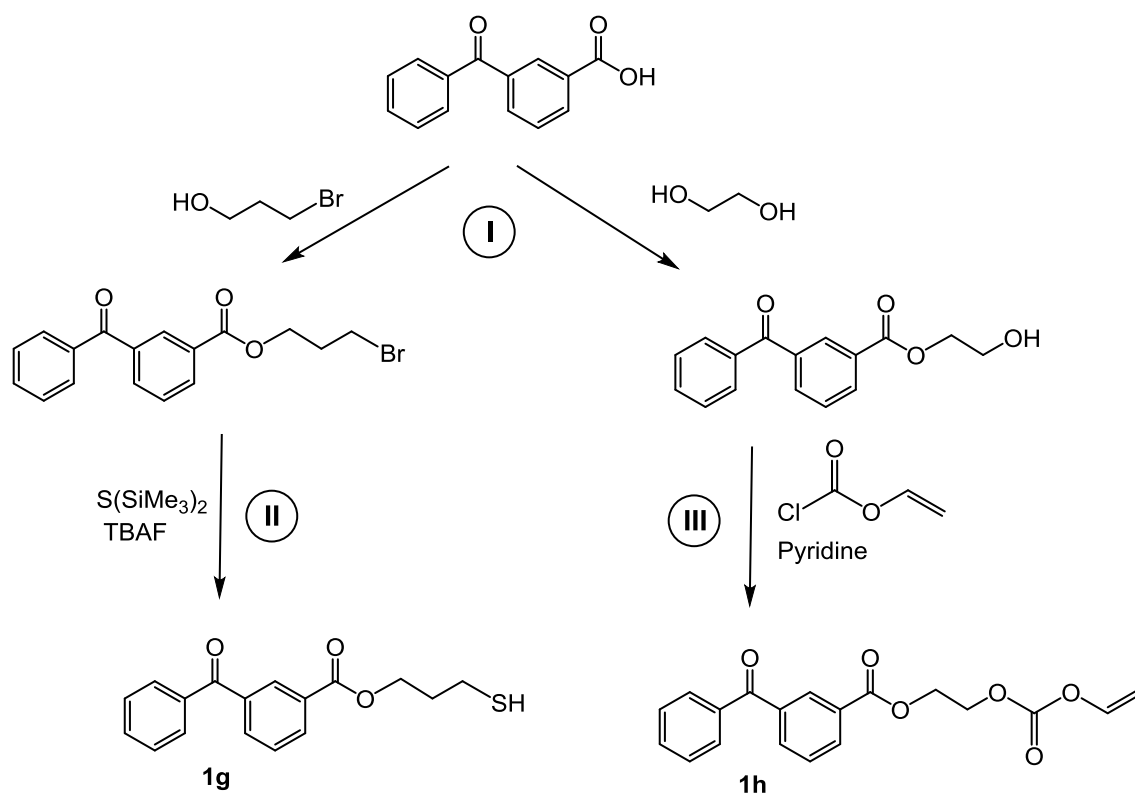
Figure 18: Synthetic pathway of the substances 1g and 1h

Substance **1h** was accessible by a straight-forward esterification (III) of the benzophenone ethylene alcohol and vinyl chloroformate in the presence of pyridine. The product could be isolated in appropriate yields (74%) and purities.

The compounds **3a** and **3b** were synthesized in a multi-step reaction (Figure 19). In the first step (I), the commercially available Irgacure 2959 was cleaved with the strong Lewis

acid AlI$_3$ to obtain the phenolic species of the photoinitiator.[103] This reaction suffered from low yield and a complex purification process to remove iodine impurities. For that reason an alternative synthetic pathway was required. Therefore the focus was set on a process which provided more synthetic steps, although higher purities could be obtained by a less time consuming purification process.
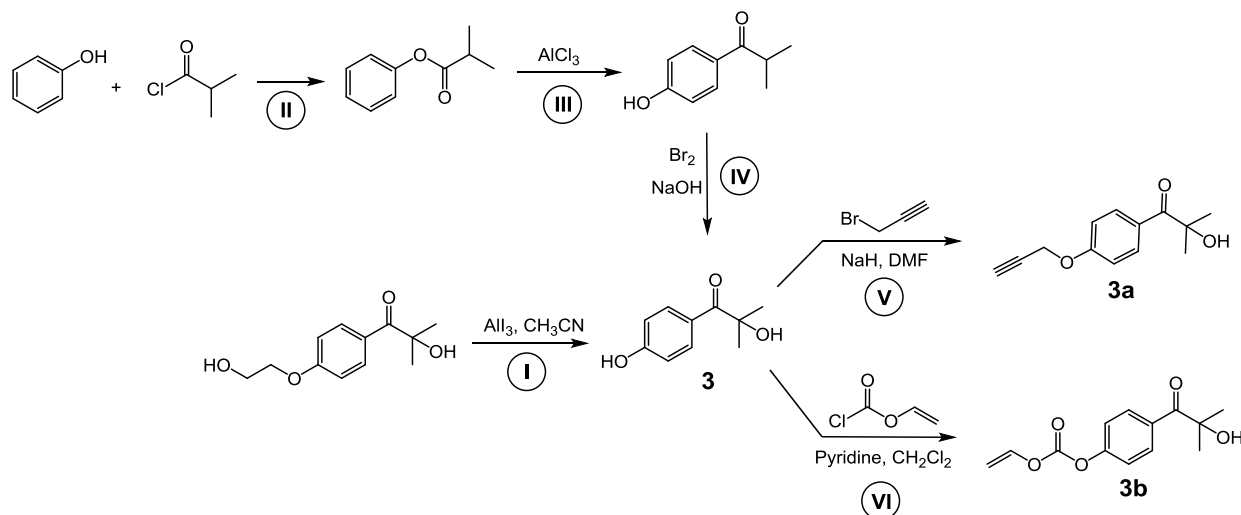
Figure 19: Synthetic pathway of polymerizable hydroxy ketone photoinitiators

The esterification (II) could be performed in quantitative yields and an excellent purity without further purification. In the next step (III) a Fries rearrangement[104] was conducted with a reasonable yield of 83% and the obtained product was converted by bromination and a subsequent nucleophilic substitution (IV) to the phenolic photoinitiator **3**.[105] This compound was used as a precursor molecule for the synthesis of the desired photoinitiators **3a** and **3b** which were obtained in one step reactions. **3a** was accessible by an etherification under basic conditions with propargyl bromine (V), whereas **3b** was synthesized by an esterification reaction with vinyl chloroformate in the presence of pyridine (VI). Both compounds could be obtained in decent yields (**3a**: 68%; **3b**: 75%) after purification by column chromatography.

The phosphine oxide derivatives **4a** and **4b** (Figure 20) were synthesized in a straightforward four step procedure. As a starting point the commercially available Irgacure TPO-L was converted with sodium iodine (I) to the corresponding salt which was isolated by filtration. This reaction step was followed by the generation of the phosphine acid derivative (II) under acidic conditions, which was dried by an azeotropic distillation before the crude product could be purified by recrystallization from toluene. The obtained phosphine acid derivative was reacted under elevated temperatures (110°C) with SOCl$_2$ in

the presence of a catalytic amount of DMF (III) to the corresponding acid chloride, which was converted (IV) into the alkyne derivative **4a** and into (V) the analog vinyl carbonate derivative **4b**. Both of them were accessible in appropriate yields (**4a**: 63%; **4b**: 50%) after the purification by column chromatography. [106]
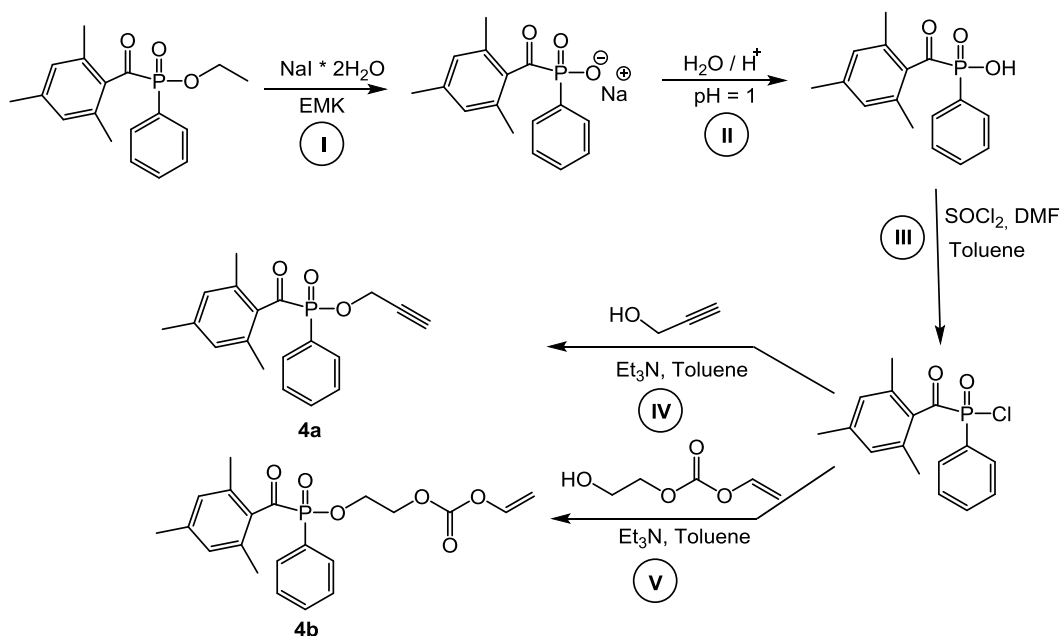
Figure 20: Synthetic pathway of polymerizable phosphine oxide photoinitiators

3.2.2 Photoreactivity of the polymerizable type II photoinitiators

The photochemical performance of the synthesized photoinitiators was characterized by means of Photo-DSC measurements (see 6.4). These studies were performed with two different photoreactive resins based on the conventional hexandiol diacrylate (HDDA) and a biocompatible thiol-ene system.

In detail, butandiol divinylcarbonate (BuVc) and trimethylolpropane tris(3-mercaptopropionate (TMPMP) were applied in an equimolar ratio regarding their functional groups to enable a thiol-ene step growth photopolymerization reaction.

This type of polymerization is, in contrast to the chain growth mechanism of the acrylic homopolymerization, not sensitive towards the presence of oxygen and leads to homogenous polymer networks.[33] Moreover, the delayed gelation and the lower polymer shrinkage are also consequences of the different polymerization mechanism.[31]

For the characterization of the benzophenone derivatives (**1a**-**1h**, **2d**) an equimolar (referring to the initiator concentration) amount of the co-initiator methyl diethanolamine

(MDEA) was added to the acrylate formulations. In case of the thiol-ene system the co-monomer TMPMP provides the required hydrogen donation.

In general, all the formulations included 5 mol% of the investigated photoinitiators and the Photo-DSC experiments were performed under nitrogen atmosphere and with a radiation intensity of 0.5 W/cm².

The crucial parameters which can be obtained by Photo-DSC measurements are the t_{max}, which is the time to reach the maximum heat of polymerization and the overall reaction enthalpy (ΔH), which is proportional to the peak area under the DSC curve. The t_{max} can be seen as the reaction speed of the photochemical reactions.[107] The double bond conversion (DBC) can be calculated from ΔH assuming that the theoretical heat of polymerization ($\Delta H0,p$) is known. For thiol-ene formulations, the determination of the DBC by means of photo-DSC is usually restricted to enes that show no homopolymerization, which can be observed in (meth)acrylate based thiol-ene systems.[32,40]

However, due to the low reactivity of the vinyl carbonates towards homopolymerization [41], a similar behavior to that of methacrylates in a thiol-ene systems was expected, which implicates that no homopolymerization can be observed in a resin with an equimolar ratio of ene and thiol functionalities. This assumption has been verified by RT-FTIR experiment. It could be demonstrated that the decrease of the thiol signal is proportional to the corresponding reduction of the ene of the vinylcarbonate, which is a clear indication that the homopolymerization is suppressed by the favored thiol-ene polymerization. For that reason it was possible to calculate the DBC of the BuVc/TMPMP polymerization by means of Photo-DSC measurements.

Due to overlapping IR signals and the fact that the reaction enthalpy for thiol-ene systems strongly depends on the structure of the ene (electron density), a monofunctional model thiol compound, i.e. butyl-mercaptopropionate, was used to estimate $\Delta H0,p$ of the thiol addition to the BuVc. In these experiments, the DBC was determined by means of NMR spectroscopy after dissolving the non-crosslinked thiol-ene adducts in $CDCl_3$. For the photoinduced addition of butyl-mercaptopropionate to BuVc the theoretical reaction enthalpy ($\Delta H0,p$) was found to be 231 kJ/mol (=280 J/g). For the HDDA based system $\Delta H0,p$ (148 kJ/mol = 707 J/g) was found elsewhere [108], to calculate the DBC.

The initiation of a photopolymerization is a complex photochemical process where several aspects have to be taken into consideration. Starting with the absorption of the emitted electromagnetic radiation and the associated generation of the reactive radicals, the hydrogen transfer of the co-initiator or quenching reactions of the excited states are playing an important role for a successful polymerization.[109] Furthermore, the specific structural properties of the applied monomers and at least the effect of the attached copolymerizable groups can change the initiation performance of the photoreactive

species drastically. Thus it is hardly possible to give a one dimensional explanation for the performance of a photoinitiator. However, significant tendencies can be discussed and allow conclusions on the reaction mechanism.

Table 1: Photoreactivity of the synthesized benzophenone derivatives (5 mol%) in a BuVc/TMPMP resin

	t_{max} [s]	$Peak_{max}$ [mW/mg]	Hp [J/g]	H_0p [J/g]	DBC [%]
Reference (1a)	4.62	29.49	229	280	82
BP-p-Propyne (2d)	4.68	21.36	260	280	93
BP-Butyne (1c)	4.86	22.75	230	280	82
BP-Propyne (1d)	5.22	21.90	240	280	86
BP-Acrylate (1b)	5.46	26.49	242	280	87
BP-Carbonate (1h)	7.62	19.12	236	280	85
BP-Thiol (1g)	11.04	5.98	141	280	51
BP-Methacrylate (1e)	18.30	11.66	224	280	80

The photoinitiators **1a**, **2d** and **1c** exhibits the best photochemical performance in the thiol-ene based system. The reference initiator **1a**, which is the benzophenone derivative without a polymerizable functionality, reaches the maximum of the reaction heat within 4.62 s, whereas the substances **2d** and **1c** show a slightly reduced reaction speed. The highest DBC is obtained with substance **2d**, approximately 13% higher than **1a** and **1c,** whereas the influence of the polymerizable functionality could not be taken into consideration. The superiority of the p-propyne modified species **2d** might be ascribed to the increased absorption of UV-light, which is further discussed in chapter 3.2.4. An influence on the reactivity of the photoinitiators by the incorporation of the alkyne functionality cannot be concluded due to the lack of reasonable correlations within the initiators **2d, 1c** and **1d**.

For the significant decrease of the DBC for the resin containing the thiol modified derivative **1g**, no reliable explanations can be given at the moment, however it will be part of further investigations. By UV-Vis spectroscopy a rather low extinction of substance **1g** could be observed (see 3.2.4), but this might not be the decisive factor for the considerable reduction of photoreactivity.

Table 2: Photoreactivity of the synthesized benzophenone derivatives (5 mol%) in a HDDA resin with 5 mol% MDEA

	t_{max} [s]	Peak$_{max}$ [mW/mg]	ΔH [J/g]	H$_0$p [J/g]	DBC [%]
BP-Thiol (1g)	4.14	48.10	454	707	64
BP-p-Propyne (2d)	5.16	46.07	521	707	74
BP-Acrylate (1b)	5.64	34.36	406	707	57
Reference (1a)	5.82	50.70	515	707	73
BP-Propyne (1d)	6.12	43.50	517	707	73
BP-Butyne (1c)	6.18	45.95	524	707	74
BP-Carbonate (1h)	6.42	31.64	412	707	58
BP-Methacrylate (1e)	8.76	30.78	418	707	59

For the acrylate based systems lower DBCs can be observed, which is attributed to the different reaction mechanism. In contrast to the thiol-ene formulation, acrylates react according to a radical chain growth mechanism, which leads to an accelerated gelation and subsequently to an inhomogeneous network of the polymer. The limited mobility of the active polymer chain and the monomers reduce the conversion of the reactive double bonds drastically and lead to a significant amount of uncured monomers.[33]

It is obvious that the thiol group of photoinitiator **1g** accelerates the photochemical reaction, which can be explained by the reaction mechanism of benzophenone photoinitiators (see chapter 2.3.3). To realize an appropriate initiation, it is essential to apply a co-initiator which is able to abstract a hydrogen to generate the desired radicals. The thiol group attached to the photoinitiator leads to an increase of abstractable hydrogens and subsequently to a lower t_{max}. The correlation between the amount of co-initiator and the polymerization speed was already reported in the literature and is in accordance with our observations.[110] Therefore, it must be noted that due to the hydrogen donating character of substance **1g**, a reliable comparison with the other synthesized photoinitiators is not possible.

However, the results also show a correlation between the reactivity of the polymerizable group and the monomer conversion. Obviously the photoinitiators **1b**, **1h** and **1e**, which are equipped with the acrylate, methacrylate and vinylcarbonate functionalities, lead to a significant reduction of the DBC compared to **2d, 1a, 1d** and **1c**. This can be ascribed to the limited mobility of the initiating compound, if the excited photoinitiator gets incorporated into the polymer network. In other words, the reactive species, which is responsible for an appropriate radical generation, gets bond to the polymer chain and is not able to provide a satisfying conversion of the co-initiator, which actually forms the decisive radical.

In comparison the alkyne modified photoinitiators as well as the reference initiator, are not polymerized during the homopolymerization of the acrylates which is leading to a significant increase of the DBC due to the elevated mobility of the photoreactive species.

The lack of reactivity of the alkyne functionalities in the acrylate homopolymerization was proven by additional RT-FTIR studies. In this experiments no conversion of the triple bond could be observed in the investigated system.

In contrast to the free radical polymerization of the acrylates the limitation in terms of photoinitiator mobility is less pronounced in the thiol-ene system. This is attributed to the step growth polymerization mechanism which exhibits a higher mobility of the reactive oligomers during the polymerization.[31] Therefore, higher monomer conversions and low t_{max} values are obtained.

3.2.3 Photoreactivity of the polymerizable type I photoinitiators

In order to realize maximal monomer conversion, usually a mixture of type I and type II photoinitiators are applied in photoreactive resins (further explanations see chapter 3.2.4). Therefore the focus was also set on type I photoinitiators, which were modified with alkyne and vinylcarbonate functionalities, to realize low migration behavior. After the successful synthesis they were characterized by photo-DSC measurements and compared with commercially available photoinitiators (Irgacure TPO-L and Irgacure 2959). The new substances as well as the reference initiators were tested in thiol-ene formulations based on BuVc, TMPMP (equimolar amount regarding functional groups) and 5 mol% PI.

All of the synthesized type I photoinitiators exhibited a far better reaction speed than benzophenone derivatives and high monomer conversion, which is mainly attributed to the different initiation mechanism (Table 3 and Table 4). It is well known that due to the straightforward scission process, higher initiation rates can be obtained compared to the rather complex reaction pathway of the type II photoinitiators (see chapter 2.3.3).[53,111,112]

However, it must be mentioned that due to the cleavage of the photoreactive species only the unreacted photoinitiator and a reduced percentage of the cleavage products get incorporated into the polymer network. Nevertheless the migration of the unreacted initiator can be decreased, which accentuates the superiority of these modified type I photoinitiators.

Within the group of phosphine oxide photoinitiators quantitative monomer conversion could be observed, whereas the t_{max} of the polymerizable phosphines was slightly increased (see Table 3).

Table 3: Photoreactivity of the synthesized phosphine oxide derivatives (5 mol%) in a BuVc/TMPMP resin

	t_{max} [s]	$Peak_{max}$ [mW/mg]	Hp [J/g]	H_0p [J/g]	DBC [%]
Irgacure TPO-L	1.38	43.28	279	280	100
Phos-VC (4b)	1.74	41.63	285	280	100
Phos-Alkyne (4a)	2.22	33.46	302	280	100

In the case of the hydroxy ketone derivatives similar behavior, regarding the t_{max} could be observed, although a reduction of DBC also became apparent (Table 4).

The differences in terms of reaction speed (t_{max}) of the novel polymerizable hydroxyketone photoinitiators, might be explained by the conversion of the polymerizable functionality. In consideration of the results of the RT-FTIR measurements (see chapter 3.2.5) and the migration studies (see chapter 3.2.6) it could be demonstrated that the triple bond is converted quantitatively whereas a significant amount of the vinylcarbonate modified species could be detected in the migration studies. Thus, a higher mobility of the radicals of substance **4b** is expectable which leads to lower t_{max}.

The diverging results of the DBC might be a result of an elevated crosslinking, due to the alkyne functionality of substance **3a,** which is able to undergo a reaction with two thiol moieties. [113,114] Therefore higher monomer conversion might be expectable, whereas this assumption requires additional experiments to be proved.

Table 4: Photoreactivity of the synthesized hydroxy ketone derivatives (5 mol%) in a BuVc/TMPMP resin

	t_{max} [s]	$Peak_{max}$ [mW/mg]	Hp [J/g]	H_0p [J/g]	DBC [%]
Irgacure2959	1.74	42.13	250.10	280	90
PI-I-VC (3b)	2.04	34.94	220.80	280	79
PI-I-Alkyne (3a)	2.34	26.15	243.10	280	87

3.2.4 Characterization of the polymerizable photoinitiators by UV-Vis spectroscopy

The absorption of electromagnetic radiation is a key factor for the reactivity of photo initiating systems. It is proportional to the generation of reactive radicals and consequently to the initiator performance. To achieve satisfying curing behavior of an investigated resin and to obtain high quantum yields the emission spectrum of the applied light source has to fit to the absorption maximum of the photoinitiator. Especially in the case of pigmented systems or the presence of photoactive additives, phenomena like an inner filter effect, light scattering or photo quenching reactions have to be taken into consideration.[53]

Therefore the synthesized photoinitiators were characterized by UV-Vis spectroscopy (see 6.3) and compared with the reference substances **1a**, Irgacure 2959 and Irgacure TPO-L. The reference photoinitiator **1a** exhibits two significant absorption maxima at a wavelength of 221 nm and 251 nm. The spectrum of substance **1d** is similar to the reference substance although a decrease of absorption intensity can be observed. In the case of the butyne derivative **1c** a bathochromatic shift to 270 nm appeared in the measured spectra, which might be attributed to an inductive effect of the triple bond over the one carbon extended alkyl spacer to the aromatic system. The spectra of para- substituted benzophenone differs from the other spectra,- it possesses just one absorption maximum with a slightly increased π - π* transition band at 255 nm, which can be explained by the different substitution pattern of the photoinitiator.
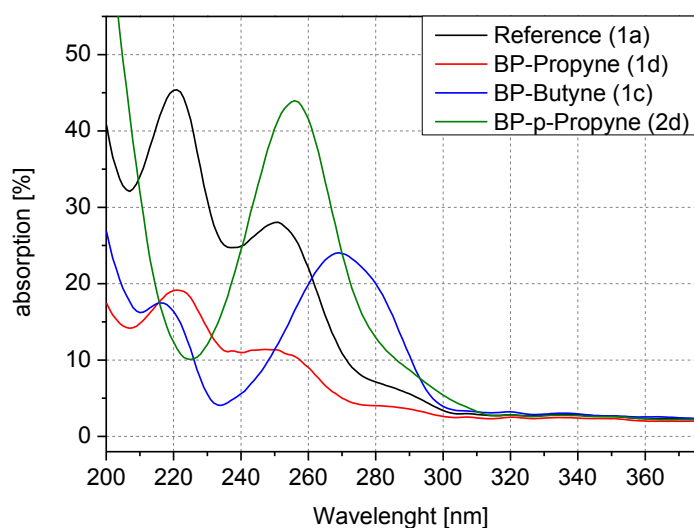
Figure 21: UV-Vis spectra of the alkyne modified benzophenones compared with the reference substance 1a

The synthesized substances **1b**, **1e**, **1h** which are equipped with the homo-, as well as thiol-ene polymerizable functionalities exhibit similar absorption spectra (221 nm and 251 nm) as the reference substance (Figure 22). Only the vinylcarbonate substituted photoinitiator shows decreased absorption intensity compared to the substances **1b**, **1e** and **1a**. However it still absorbs far better than the thiol modified initiator. (Figure 23)
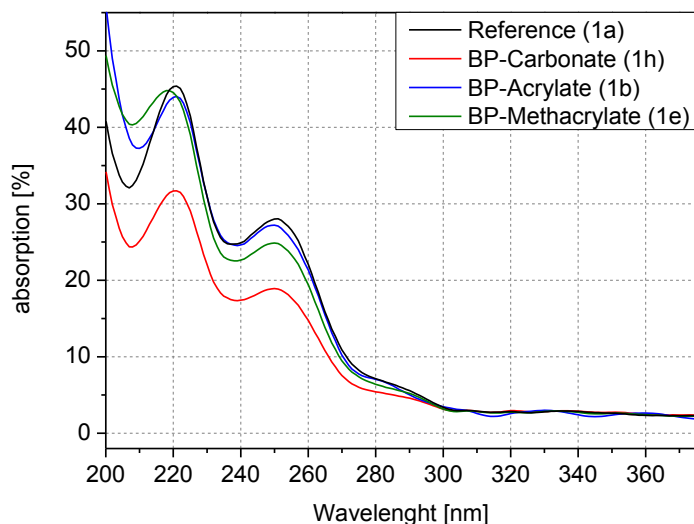
Figure 22: UV-Vis spectra of the acrylate and vinylcarbonate modified benzophenones compared with the reference substance 1a
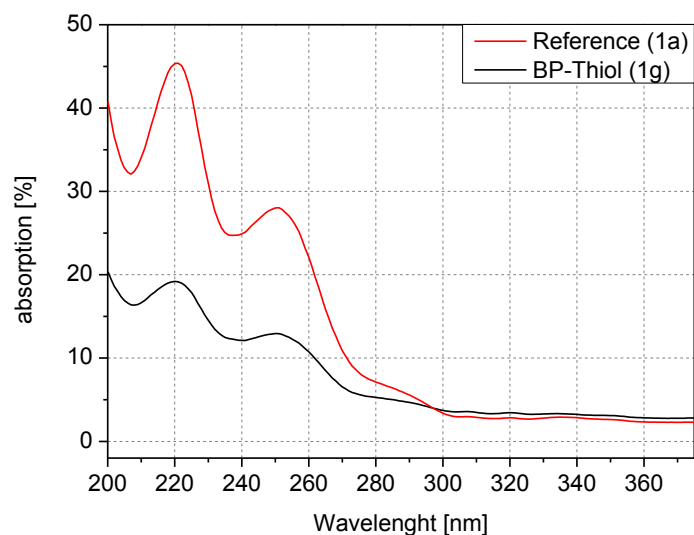
Figure 23: UV-Vis spectra of the thiol modified benzophenone compared with the reference substance 1a

To give reliable estimations regarding the photochemical reactivity based on the UV/Vis absorption spectra is hardly possible due to the complex initiation mechanism. But it can be determined that substances which exhibit a reduced light absorption, usually suffer from low photoreactivity.[53] This also correlates to the results in Chapter 3.2.2 where it could be shown that the substance **1h** and **1g** are less reactive than **2d**.

In order to realize satisfying surface curing as well as quantitative monomer conversion in deeper regions of photoreactive varnishes or printer inks, it is necessary to provide photoinitiators, which absorb at different wavelengths. Substances, which exhibit their absorption maxima at lower wavelengths, are responsible for the curing of the surface of the applied formulation films. Substances which absorb in the red shifted or even visible part of the spectrum lead to depth curing. The reasons for that can be found in the penetration depth of the electromagnetic radiation which is proportional to the wavelength and the energy of the applied radiation.[52] Consequently, the modified hydroxy ketone (surface curing) and phosphine oxide photoinitiators (depth curing) which cover both groups of curing agents were evaluated regarding their absorption spectra. The absorption of the initiator **3a** is comparable to the reference substance which possesses two maxima at 219 nm and 274 nm, only the absorption intensity is slightly increased for the alkyne modified species. The other hydroxy ketone derivative **3b** exhibits just one blue-shifted, intensified absorption maximum at 246 nm (Figure 24).
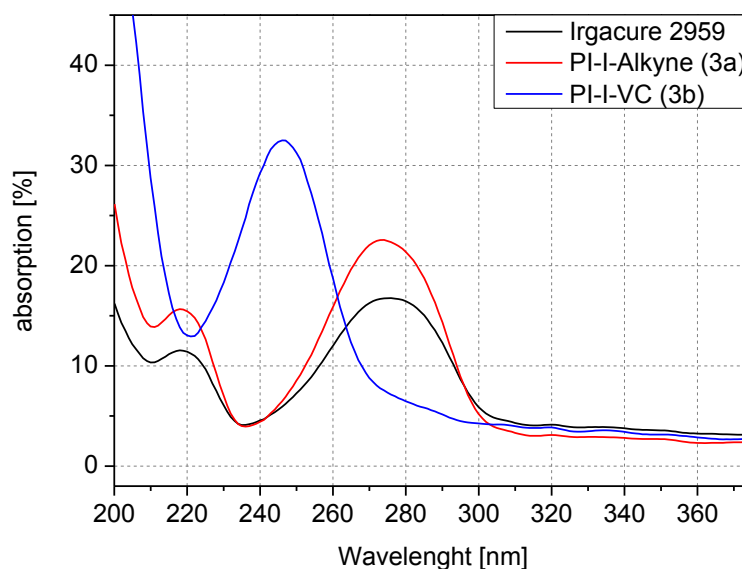
Figure 24: UV-Vis spectra of the alkyne and vinylcarbonate modified hydroxy ketones compared with the reference substance Irgacure 2959
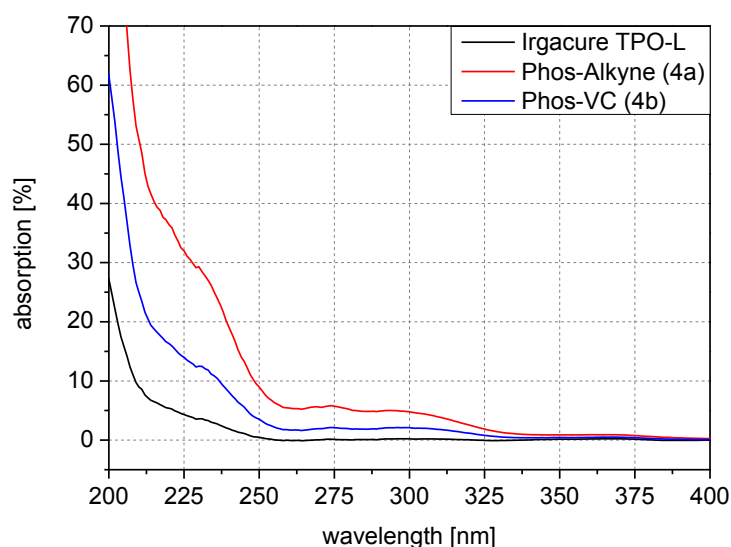
Figure 25: UV-Vis spectra of the alkyne and vinylcarbonate modified phosphine oxides compared with the reference Irgacure TPO-L

The phosphine oxide photoinitiators are commonly used as depth curing agents due to their long tailing absorption band into near ultraviolet or even visible regions of the electromagnetic spectrum. Their outstanding absorption behavior correlates with the measured spectra in Figure 25, whereas the modified substances **4a** and **4b** exhibit even higher extinctions than the commercially available Irgacure TPO-L.

3.2.5 Characterization of the alkyne conversion by RT – FTIR spectroscopy

Real-time Fourier transformed IR spectroscopy is a versatile tool to characterize chemical reactions during an illumination process and enables comprehensive kinetic studies of photopolymerizations (see chapter 6.2).

In detail the conversion of the polymerizable functionality of the alkyne modified photoinitiators (**1d, 1c, 2d, 3a, 4b**) was investigated to prove itsincorporation into the polymer network during the photochemical reaction. These kinetic studies were facilitated by the distinctive and isolated signal of the terminal alkyne which enabled an exact integration over the entire reaction time.

The reduction of the relevant C-H stretching band, which appears at the region between 3250 - 3330 cm^{-1}, was observed over a period of 3.5 min and was characterized by 69 IR-spectra per minute. The synthesized photoinitiators were tested in the same thiol-ene system (BuVc/TMPMP), explained in chapter 3.2.2 and 3.2.2.
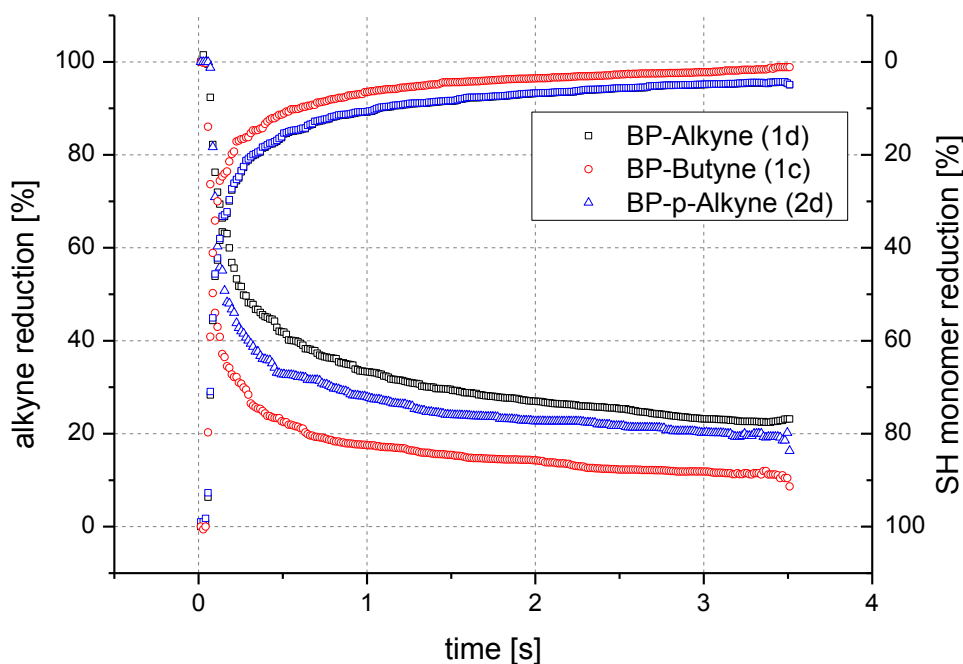
Figure 26: Conversion of the alkyne functionality attached to the benzophenone photoinitiators during the illumination process and the related thiol reduction

As shown in Figure 26 the conversion of triple bonds is influenced by the length of the alkyl spacer and the type of substitution pattern of the aromatic system. This observation is a consequence of the significant variation of the reaction speed of the terminal alkynes in thiol-yne systems which is reported in the literature by Fairbanks et al.[114]. They propose a reduced reactivity of the propargyl esters compared to aliphatic alkynes because of the electron withdrawing effect of the carbonyl functionality. Therefore, the increased conversion of the butyne (substance **1e**) can be attributed to two different phenomena. On the one hand the inductive effect of the ester group is reduced, which leads to an accelerated reactivity and on the other hand the triple bond is better accessible according to sterical reasons. Additionally the correlation between the yne reactivity and the curing behavior of thiol-ene monomer system has to be discussed. Obviously the conversion of the triple bond is influenced by the progress of the thiol-ene polymerization. If the polymerization reaches the gelation point, the mobility of the radicals is reduced and subsequently the conversion of yne as well as the ene gets slowed down rapidly. Therefore, it is essential that the yne reaction is finished before the overall conversion of the system gets slowed down by the gelification of the resin.

Concluding, it can be postulated, that the faster the conversion of the alkyne functionality, the higher the conversion of the alkyne in the thiol-ene system. Accordingly the amount of the remaining triple bonds of substance **1c** is reduced to 11% whereas 23% of the alkynes are detectable in the formulation of photoinitiator **1d**. In the case of **2d** a slight decrease to 19% of the polymerizable functionality can be observed, which can be ascribed to the sterical favored para-position of the triple bond.
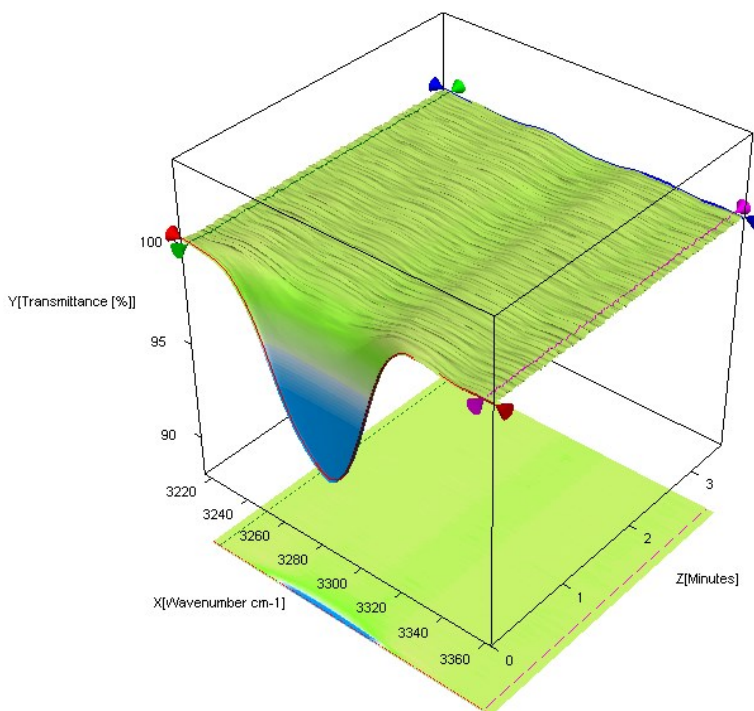
Figure 27: 3D model of the triple bond conversion (3280 cm^{-1}) during photopolymerization.

Based on the results of the benzophenone derivatives, the same studies were performed for the type I photoinitiators **3a** and **4a**. Surprisingly both of them exhibited a quantitative conversion of the alkyne functionality despite reasonable amounts of phosphine oxide photoinitiator could be detected in the migration studies (see chapter 3.2.6.1). Nevertheless it is obvious that the initiation of the type I photoinitiators exceeds the performance of the benzophenone derivatives, which results in a complete conversion of the reactive triple bonds and the overall conversion. This observation is in accordance with the results of the Photo-DSC measurements in chapter 3.2.3, where the quantitative conversion of the BuVc/TMPMP system, containing type I photoinitiators could be demonstrated.
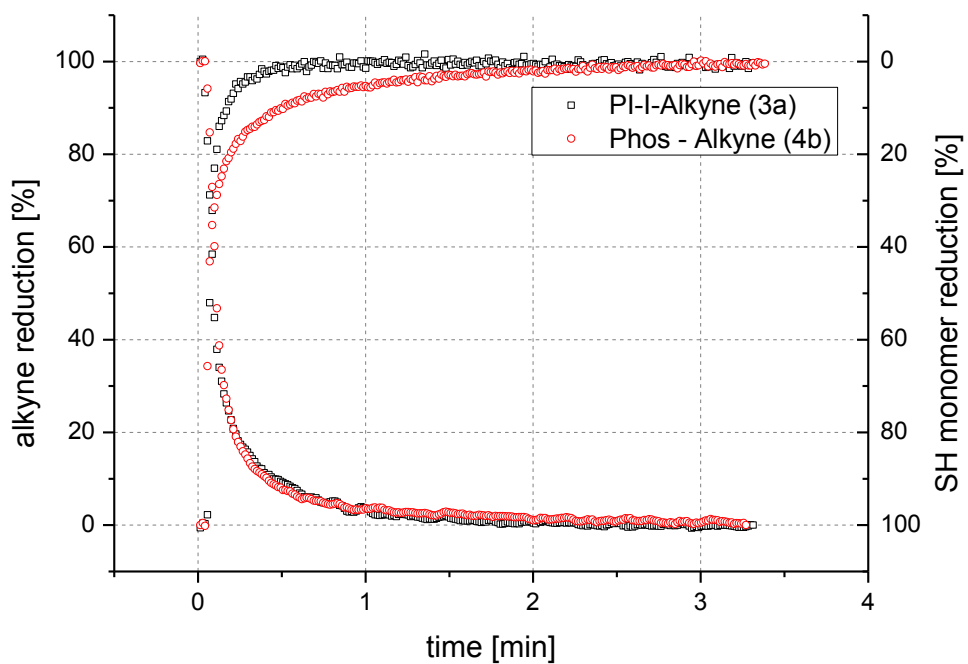
Figure 28: Conversion of the alkyne functionality attached to the hydroxy ketone and phosphine oxide photoinitiator during the illumination process and the related thiol reduction

3.2.6 Migration studies of the polymerizable photoinitiators

To obtain representative and reproducible values for the migration of the polymerizable photoinitiators, a defined procedure for the sample preparation was developed. The aim was to design a robust process, in order to reduce the observational error of inhomogeneous illumination and inconsistent curing conditions (oxygen inhibition, curing temperature etc.). Consequently the sample preparation was performed with the Photo-DSC under N_2 atmosphere with a radiation intensity of 5 W/cm². The increased illumination intensity was chosen to reach the highest possible monomer conversion and because of the increased volume of the investigated resin (same thiol-ene formulation as in 3.2.2 and 3.2.3). In general 20 mg of the photoreactive formulation were cured in a Photo-DSC crucible and the obtained polymers were extracted with ethanol at 50°C for 96h and continuous shaking. Subsequently the polymers were removed from the extracts, the excess of solvent was removed at 50°C and the residue was re-dissolved in a defined volume of ethanol.

3.2.6.1 Characterization of the migration behavior of benzophenone and hydroxy ketone derivatives by GC-MS

In the literature, there are only a few publications which provide studies of the migration behavior of polymerizable photoinitiators. In general, they focus on the photochemical performance of the synthesized substances, whereas the aspect of the photoreactive functionality is not further discussed. In detail only the studies of Davies et al. [97,115] and Sun et al. [97,115] deal with the complex topic of photoinitiator migration, although the correlations between migration, monomer conversion and reactivity of the polymerizable group is not elucidated in their work.

In present studies the migration behavior of the benzophenone and the hydroxy ketone photoinitiators was characterized by means of GC-MS measurements. The sample preparation was performed according to the description in chapter 3.2.6 and the applied GC-MS parameters are summarized in chapter 6.8.

For the quantification of the migrating photoinitiators a calibration was performed for every investigated substance. The detection limits, the coefficients of determination, as well as the molar mass of the observed ions of the MS - detector (see Figure 29), are concluded in Table 5.

209.22 g/mol

Figure 29: Fragmentation of the benzophenone derivatives

To compare the migration behavior of the different modified benzophenone derivatives they were cured in an acrylate and a thiol-ene based system (BuVc/TMPMP). The detailed compositions of the photoreactive formulations was elucidated in chapter 3.2.2 5 mol% photoinitiator were used in all formulations.

Table 5: Detection limits of the benzophenone photoinitiator, coefficient of determination of the calibration and the molecular weight of the detected photoinitiator fragment

Photoinitiator	detection limit [µg/mL]	R² - calibration	fragment [g/mol]
BP-Acrylate (1b)	0.11	0.9869	209
BP-Methacrylate (1e)	0.30	0.9868	209
BP-Thiol (1g)	0.41	0.9905	209
BP-Butyne (1c)	0.64	0.9858	209
BP-Propyne (1d)	0.26	0.9916	209
BP-p-Propyne (2d)	0.33	0.9857	209
BP-Reference (1a)	0.17	0.9952	209
BP-Carbonate (1h)	0.24	0.9982	209

For each polymer sample, four extractions were performed to obtain representative results and to enable the calculation of the corresponding standard deviation of the observed migration.

Table 6: Photoinitiator concentration in the investigated extracts of the acrylate and thiol-ene system

Photoinitiator	Resin: HDDA/MDEA		Resin: BuVc/TMPMP	
	conc. [µg/mL]	± SD [µg/mL]	conc. [µg/mL]	± SD [µg/mL]
BP-Acrylate (1b)	18.92	4.45	25.82	3.99
BP-Methacrylate (1e)	10.77	6.90	34.72	9.02
BP-Thiol (1g)	92.98	19.26	251.62	4.07
BP-Butyne (1c)	50.51	10.21	3.55	0.15
BP-Propyne (1d)	66.89	12.26	3.36	1.16
BP-p-Propyne (2d)	134.32	41.82	2.07	0.59
BP-Reference (1a)	73.79	6.64	142.20	16.04
BP-Carbonate (1h)	84.50	5.46	7.30	6.35

For the detailed discussion of the benzophenone migration three different aspects have to be taken into consideration. The first is the monomer conversion of the resin, which is expressed by the DBC of the photoreactive formulation (see chapter 3.2.2). The second is the reactivity of the polymerizable group in the investigated acrylate or thiol-ene system and finally the influence of the polymerization mechanism and the subsequent material properties (network density, etc.) of the investigated formulation should not be neglected.
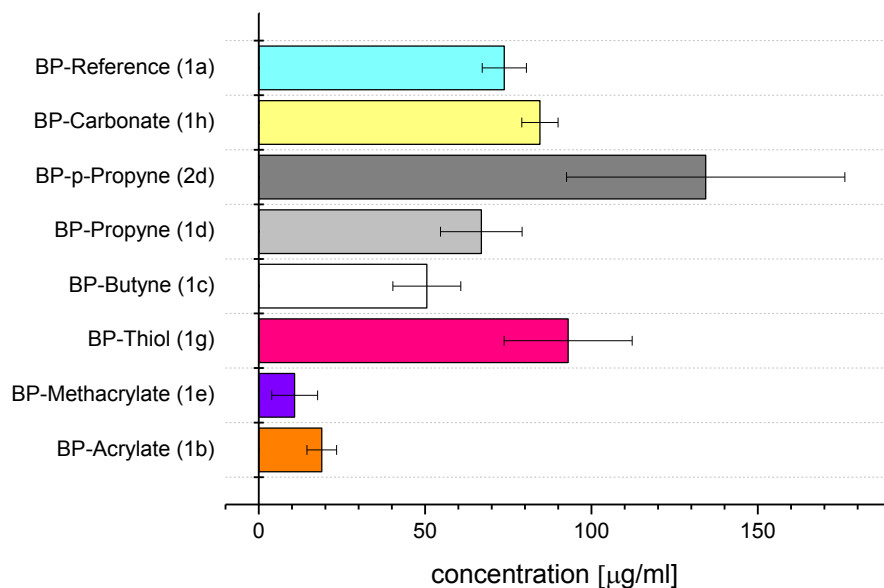
Figure 30: Photoinitiator concentration in the ethanolic extracts of the acrylate resins

In the first system (HDDA/MDEA), the extracts exhibited the lowest photoinitiator concentration for the acrylate and methacrylate modified substances (see Figure 30). These results can be explained by the ability to copolymerize the acrylate and methacrylate group **1e** and **1b,** respectively. They can be sufficiently involved in the radical polymerization of the resin, which is decisive for the reduced mobility of the initiating units.

However, due to this immobilization the polymerization suffers from low conversion rates which is illustrated by the DBC of **1e** (59%) and **1b** (57%) (see chapter 3.2.2). Obviously the influence of the polymerization mechanism (chain growth vs. step growth mechanism), the corresponding mobility of the initiating compounds (see chapter 3.2.2) and the resulting monomer conversion are responsible for the migration behavior of the photoinitiators.

Further the compatibility between the resin and the polymerizable groups of the photoinitiators has to be taken into consideration. It is well known that copolymerization of methacrylates with vinyl carbonates is rather poor due to the opposite position in the Q-e

scheme. [116] Accordingly the different amounts of migrated initiators within the group of the polymerizable species **1b**, **1e** and **1h** can be explained. The lower amount of the methacrylate and acrylate modified species compared to vinyl carbonate derivative is therefore a logical consequence of a higher compatibility of the reactive groups.

Nevertheless the detected amount of the photoinitiators **1e** and **1b** in the extracts of the acrylate based resins was significantly higher compared to the best results which could be obtained for thiol-ene systems. (see Figure 31)

In case of the alkyne functionalized substances the increased migration could be expected due to the lack of reactivity of the triple bond in the acrylate system which was proven by additional RT-FTIR measurements. In those experiments different concentrations of the alkyne modified photoinitiators were added to an acrylate based resin and illuminated with highest possible light intensity. It could be demonstrated that the triple bond, which exhibits a significant signal at the region between 3250 - 3330 cm^{-1} in the FTIR-spectrum, shows no reactivity at all.

Surprisingly, a high concentration of the thiol modified benzophenone could be observed, although it exhibits the highest reactivity in the acrylate system. At the moment no reliable explanation for this phenomenon can be given, however it will be part of further investigations.
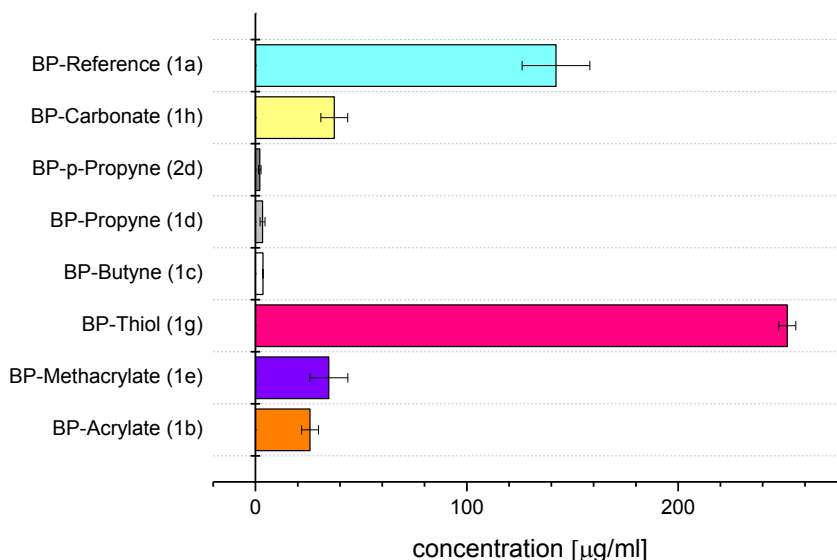
Figure 31: Photoinitiator concentration in the ethanolic extracts of the thiol-ene resin

In the second investigated system completely different migration rates of the photoinitiators could be detected (see Figure 31). The best performance regarding the extractable amount of photoinitiators exhibited the alkyne modified substances, which is in accordance with the results of chapter 3.2.5. In this part of the work it could be shown by

means of RT-FTIR measurements that the triple bonds of the photoinitiators **2d**, **1d** and **1c** were copolymerized during the photopolymerization. This implicates an incorporation into the polymer network and a subsequent immobilization.

For the substances **1b**, **1e** and **1h** a reduced initiator mobility could be observed compared to the reference photoinitiator **1a**. This can be attributed to the reactivity of the functional groups (acrylate, methacrylate, vinylcarbonate) which are attached to the photoinitiator. These moieties react according to a different reaction mechanism compared to the triple bonds of **2d**, **1d** and **1c** and lead to a reduced migration.

For the thiol modified photoinitiator the highest migration values can be observed, which cannot be explained at the moment. Further experiments will clarify the observed migration behavior.

Comparing the results of the two different investigated systems, clear tendencies of the migration behavior referring to the network properties can be observed. The acrylate homopolymerization forms heterogeneous, high-density regions at low double bond conversions, in contrast to the thiol-ene systems which lead to high monomer conversions and homogenous but lower crosslinked polymeric networks.[117] The subsequent influence on the permeation of the photoinitiating species can be depicted by the measured concentrations of reference photoinitiator. In the thiol-ene system nearly the triple amount of this substance could be detected (see Table 7) although a remarkable higher DBC could be reached.

Therefore, the outstanding results of alkyne modified initiators, which exhibited a concentration in range of 0.1% to 0.4% in the ethanolic extracts, have to be emphasized (see Table 7).

Table 7: Percentage of the migrated photoinitiator referred to the complete amount of applied photoinitiator

Photoinitiator	Resin: HDDA/MDEA Migration [%]	Resin: BuVc/TMPMP Migration [%]
BP-Acrylate (1b)	1.38	2.35
BP-Methacrylate (1e)	0.76	3.03
BP-SH (1g)	7.29	24.70
BP-Butyne (1c)	4.25	0.38
BP-Propyne (1d)	5.92	0.37
BP-p-Propyne (2d)	9.42	0.18
BP-Reference (1a)	6.78	16.49
BP-Carbonate(1h)	5.90	0.63

Based on the results of the benzophenone derivatives the migration behavior of the synthesized substance **3a** and **3b** in thiol-ene formulations was also investigated. First a GC-MS method had to be developed for a reliable quantification of the investigated substances. The corresponding parameters, including the detected fragments of the characterized hydroxy ketones are summarized in Table 34 in chapter 6.8 and Table 8.

Table 8: Photoinitiator concentration in the investigated extracts of the thiol-ene system, including the detection limit of the method, the coefficient of determination of the calibration and the molecular weight of the detected photoinitiator fragments

Photoinitiator	conc. [µg/mL]	± SD [µg/mL]	detec. limit [µg/mL]	R² -cali.	fragment [g/mol]
Irgacure 2959	217.92	41.7	0.07	0.9955	121, 181
PI-I-Alkyne (3a)	< 0.15		0.15	0.9900	131, 159, 175
PI-I-VC (3b)	15.11	2.4	1.18	0.9990	121

The results of the migration studies confirmed the expected superiority of the modified photoinitiators regarding their migration behavior. On the one hand it could be shown that the amount of the migrated photoinitiator for the vinylcarbonate derivative could be reduced by 93%, on the other hand the concentration of the alkyne initiator was even below the detection limit (>0.15 µg/ml) (see Figure 32).
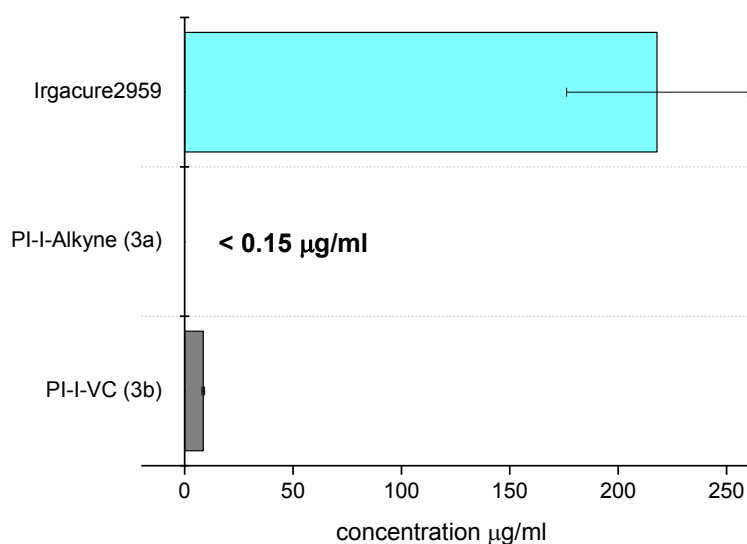
Figure 32: Photoinitiator concentration in the ethanolic extracts of the thiol-ene resin

Concluding it has to be emphasized that it was possible to design highly reactive photoinitiators for thiol-ene systems, which accentuate their superiority with their outstanding migrations behavior and their excellent monomer conversion compared to

53

conventional initiator systems. In consideration of these features these new substances pave the way towards low migration and biocompatible thiol-ene applications.

3.2.6.2 Characterization of the migration behavior of phosphine oxide derivatives by ICP-MS Analysis

For the ICP-MS measurements a closed acidic digestion was performed to dissolve the phosphorus containing samples in aqueous medium (see chapter 6.11). The ICP-MS analysis were carried out at the Chair of General and Analytical Chemistry of the Montanuniversität Leoben.

Table 9: Phosphorus concentration in the ethanolic extracts of the investigated polymers

Photoinitiator	P conc. [µg/mL]	± SD [µg/mL]
Irgacure TPO-L	28.41	0.07
Phos-Alkyne (4a)	17.22	0.79
Phos-VC (4b)	17.50	0.97
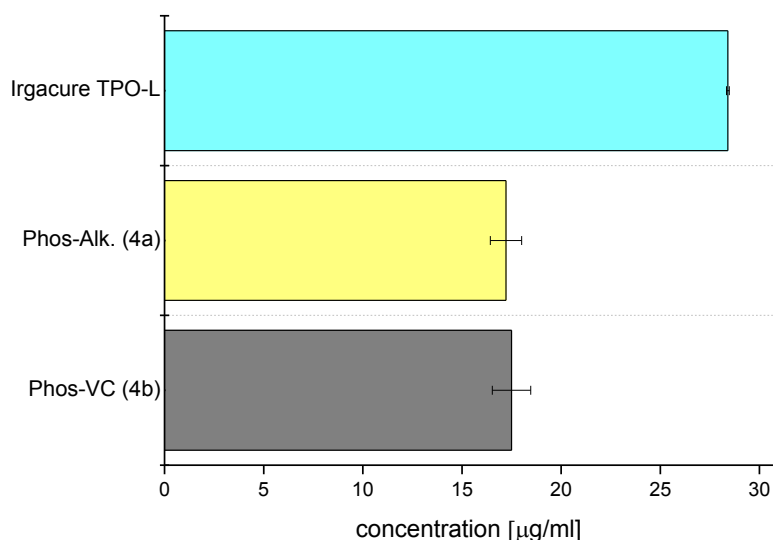
Figure 33: Phosphorus concentration in the ethanolic extracts of the investigated polymers

The results of the ICP - MS indicated a reduction of the phosphorus concentration in the analyzed extracts of the polymerizable photoinitiators. However the amount of the detected phosphorus was higher than it has been expected according to the RT-FTIR measurements of the alkyne modified photoinitiator (see Table 9). This observation is an evidence for additional cleavage and side reactions after the incorporation of the alkyne

functionality whereas this assumption requires further investigation to give a reliable explanation.

Nevertheless a reduction by 40% of extractable phosphorus compounds could be realized for the functionalized photoinitiators which a significant improvement to the commercially available photoinitiator. Further optimizations regarding the migration behavior of the phosphine oxide photoinitiators might be possible by modification with more than one polymerizable moieties. However these functionalizations could be at the expense of the photoreactivity due to the reduced mobility of the initiating fragments.

3.2.6.3 Determination of phosphorus concentration in the core of a polymer sample after Soxhlet extraction by XPS measurements

To investigate the migration behavior of the phosphine oxide photoinitiators, the phosphorus concentration on the surface of the cutting area of a polymer sample was analyzed before and after an ethanolic Soxhlet extraction by XPS. The sample preparation was performed according to the description in Figure 34 to guarantee a representative distribution of the photoinitiator over the whole polymer sample (see 6.7).

The different measured resin compositions contained the synthesized photoinitiators **4a**, **4b** and the reference substance Irgacure TPO-L and were characterized regarding the extractability of phosphorus containing compounds. This included the unreacted photoinitiators as well as the phosphorus containing cleavage and side products of the photoreactive species.
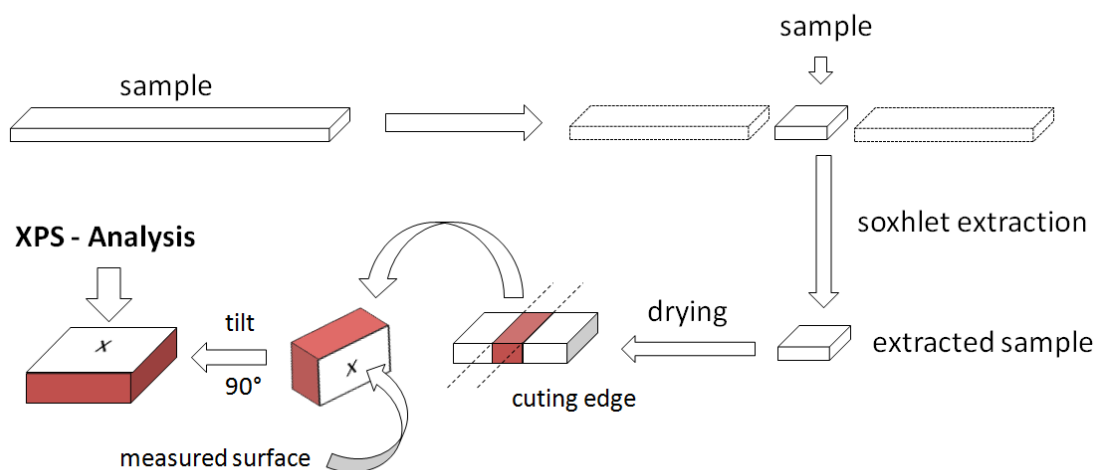
Figure 34: Sample preparation for XPS - analysis of the phosphorus concentration.

The Soxhlet extraction was performed with resin formulations consisting of BuVc/TMPMP (equimolar regarding functional groups) and 5 mol% photoinitiator. After an additional drying step the macromolecular samples were characterized by XPS measurements.

To compare the phosphorus concentration, the focus was set on the P2p signal of the photoinitiators, which appeared at 133 eV.[118]
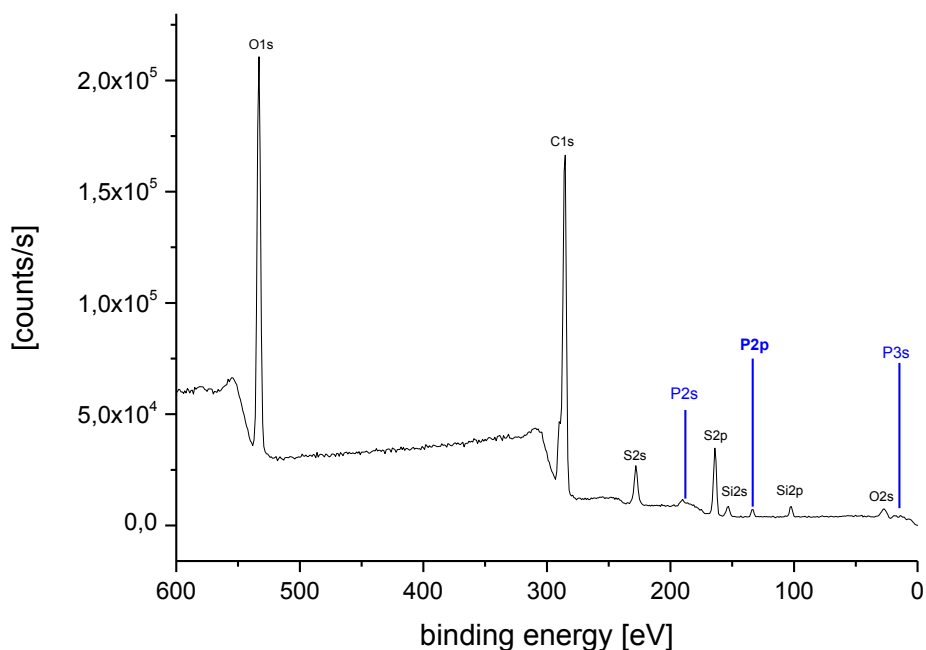
Figure 35: Survey scan of the of the Irgacure TPO-L containing polymer after ethanolic extraction
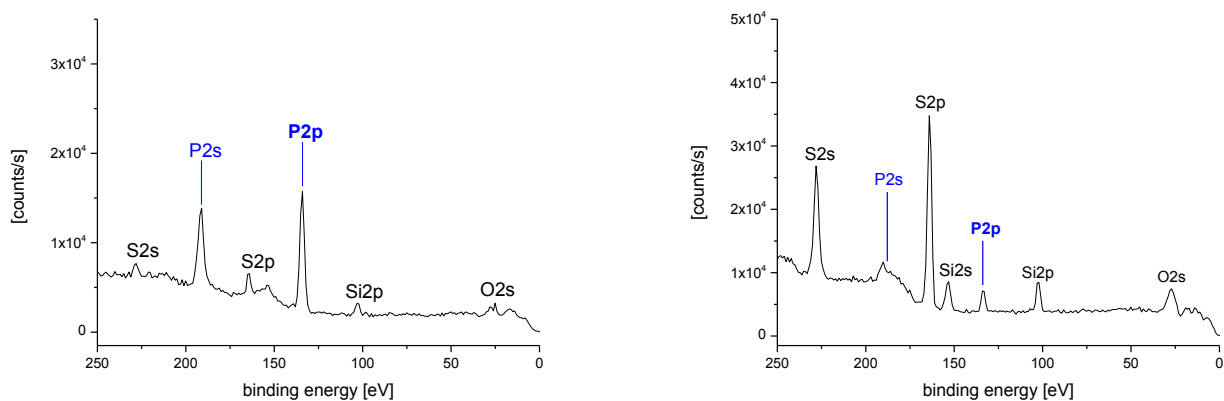
Figure 36: Survey scan before extraction (left) and after extraction (right)

The atom% which are summarized in Table 10 and Table 11 were obtained by the calculation of the average value of three measured points on the polymer surface before and after the ethanolic Soxhlet extraction.

Due to the significant changes of the carbon and sulfur signal, which is attributed to the monomer migration, a reliable referencing and calculation of the phosphorus concentration is not possible. Only a qualitative statement on the migration of the phosphorus containing compounds can be given.

Nevertheless it is obvious, that the amount of extractable phosphorus compounds is influenced significantly by the applied photoinitiator. In the case of the commercially available Irgacure TPO-L, the P2p signal was drastically reduced (Figure 36), whereas the content of phosphorus containing compounds of the other resins was only slightly changed.

Table 10: Sulfur and phosphorus content (atom %) on the surface of the cutting area before the extraction

Substance	P2p [atom %]	S2p [atom %]	C1s [atom%]
Phos VC (4b)	1,82	3,49	62,01
Phos Alkyne (4a)	1,08	4,09	62,31
Irgacure TPO-L	6,21	1,04	75,03

Table 11: Sulfur and the phosphorus content (atom %) on the surface of the cutting area after the extraction

Substance	P2p [atom %]	S2p [atom %]	C1s [atom%]
Phos VC (4b)	1,44	3,58	60,46
Phos Alkyne (4a)	0,76	5,33	62,95
Irgacure TPO-L	0,75	5,66	60,31

This is a clear indication that the polymerizable photoinitiators **4a** and **4b** were incorporated into the polymer network and the associated migration of the phosphorus compounds could be diminished. These results are in accordance with the observed conversion of the alkyne functionality in chapter 3.2.5 and the ICP-MS measurements in chapter 3.2.6.2.

3.3 *Conclusion*

In chapter 3 the synthesis and characterization of polymerizable photoinitiators was discussed comprehensively. The focus was set on benzophenone, hydroxy ketone and phosphine oxide photoinitiators, which were modified with polymerizable moieties. Their photochemical performance was evaluated in two different types of resin formulations, whereas the usability in a biocompatible thiol-ene system was elucidated extensively. Especially, the conversion of the reactive triple bonds was studied by real-time FTIR spectroscopy, to illustrate the expected incorporation process of the functionalized photoinitiators in the thiol-ene network. Furthermore, the extractability of the novel substances was investigated and quantified by GC-MS and ICP-MS analyses. Moreover, the phosphorus concentration on the surface of the cutting area in the center of polymer sample was studied by means of XPS measurements, before and after an ethanolic extraction.

Concluding the results, the photochemical performance as well as the migration behavior of the alkyne functionalized species in thiol-ene formulations have to be highlighted. They exhibit polymerization velocities (t_{max}) and monomer conversions which are comparable to conventional photoinitiators, although their migration behavior exceeds the commercially available substances. Especially, the investigated hydroxy ketone derivatives exhibited excellent low-migration features, which make them interesting candidates for biocompatible applications.

Regarding the initiation process of the polymerizable photoinitiators, it was possible to gain important insights for the understanding of the investigated systems. In particular in acrylate formulations, a significant breakdown in the monomer conversion was observable for the polymerizable photoinitiator species. This result is a clear indication, that the initiator mobility plays an important role for the initiation process in acrylate resins. In contrast to the thiol-ene formulations, which react in a step growth mechanism, the reactive polymer chain is limited regarding its mobility. Therefore, the bound photoinitiator is inhibited in its diffusion, which leads to a reduction of reactive radicals and subsequently to low monomer conversion. Attributed to the different polymerization mechanism, this effect cannot be observed in the thiol-ene formulations. Although the incorporation of alkyne functionalities could be proven, the reactive polymer fragments of the thiol-ene reaction exhibit higher mobility, within the investigated resin. This theory is supported by the fact that thiol-ene formulations also exhibit delayed gelation points, which is a result of the increased mobility of the system.[33]

For to phosphine oxide photoinitiators a significant improvement, regarding the amount of extractable phosphor compounds could be obtained. However the effect of the polymerizable functionalities was not that distinctive, due to the complex scission process of phosphine oxide photoinitiators. Nevertheless the capability for low migration applications, as a result of the migration reduction by 40%, is definitely imaginable.

3.4 *Experimental*

Unless otherwise stated, all reagents were purchased from Sigma–Aldrich, TCI, VWR, Acros, Bruno-Bock or Roth and were used without further purification.

3.4.1 Biocompatibility

These studies were carried out by CYTOX (Bayreuth, Germany) in compliance with the required standards of ISO 10993-5, which evaluates the in vitro biocompatibility using L929 - Mouse fibroblast cells. Consequently, L929 cells were incubated in a defined media with increasing concentrations of the photoinitiators for 48 hours at 37°C with 5% CO_2. The concentration where the half of the cells remained alive compared to the negative control (cell culture medium) was assessed as cell viability (EC_{50}). Additionally a cytotoxic tenside solution was applied as a positive control. (Triton)

3.4.2 Synthesis of Benzophenone derivatives

3.4.2.1 3-Bromopropyl-3-benzoylbenzoate
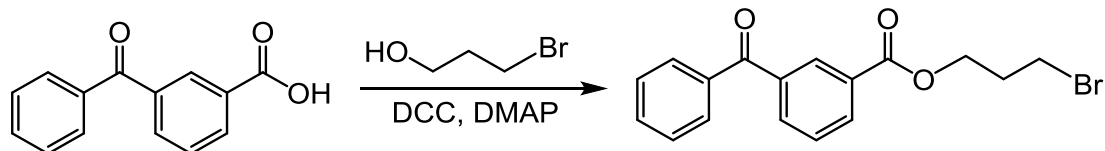
N,N'-Dicyclohexylcarbodiimide (DCC) (2.18 g, 10.6 mmol) was added to mixture of 3-benzoylbenzoic acid (2.0 g, 8.84 mmol), 4-(dimethylamino)pyridine (DMAP) (129.6 mg), and 3-bromopropan-1-ol (35.36 mmol, 4.Eq) in 60 mL of CH_2Cl_2 at 0 °C. After 1h the ice bath was removed and the mixture was allowed to stir for additional 16h. The white precipitate was separated by filtration and the organic layer was diluted with 5% hydrochloric acid, neutralized with saturated $NaHCO_3$ solution and dried over sodium sulfate. After the solvent was evaporated under reduced pressure the crude product was purified by flash column chromatography (silica gel, cyclohexane / ethyl acetate = 10:1).

Yield: 1.25 g (40.72%)

^{1}H-NMR (δ, 400 MHz, CDCl$_3$, 25 °C):
8.43 (s, 1H, AR); 8.26 (d, 1H, AR); 7.99 (d, 1H, AR); 7.79 (d, 2H, AR); 7.58 (m, 2H, AR); 7.50 (m, 2H, AR); 4.49 (t, 2H, CH$_2$); 3.53 (t, 2H, CH$_2$); 2.32 (m, 2H, CH$_2$) ppm

^{13}C-NMR (δ, 100 MHz, CDCl$_3$, 25 °C):
195.59 (1C, C=O); 165.50 (1C, C=O); 137.92 (1C, AR); 136.89 (1C, AR); 134.12 (1C, AR); 133.073 (1C, AR); 132.78 (1C, AR); 130.88 (1C, AR); 129.96 (3C, AR); 128.54 (1C, AR); 128.40 (3C, AR); 63.03 (1C, CH$_2$); 31.62 (1C, CH$_2$); 29.20 (1C, CH$_2$) ppm

3.4.2.2 3-Mercaptopropyl 3-benzoylbenzoate (1g)
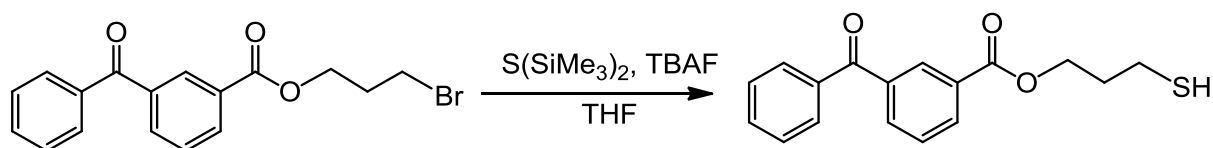
3-Bromopropyl-3-benzoylbenzoate (0.250 g; 1.44 mmol) and hexamethyldisilathiane (0.154 g; 0.86 mmol) were dissolved in degassed THF and cooled to -10°C. A solution of tetrabutylammonium fluoride (0.273 g; 0.86 mmol) in degassed THF was added to the mixture and stirred for further 30 minutes at -10°C. Afterwards the cooling bath was removed and the reaction was allowed to stir for additional 20h at room temperature (RT). The reaction was diluted with saturated NH_4Cl- solution (3 x30 mL) and the organic layer was dried over Na_2SO_4. The solvent was evaporated under reduced pressure and the residue was purified by flash chromatography (silica gel, cyclohexane / ethyl acetate=7:1), to obtain the title compound as a colorless oil.

Yield: 0.97 g (50.8%)

^{1}H-NMR (δ, 400 MHz, CDCl$_3$, 25 °C):

8.42 (s, 1H, AR); 8.25 (d, 1H, AR); 7.99 (d, 1H, AR); 7.80 (d, 2H, AR); 7.59 (m, 2H, AR); 7.49 (m, 2H, AR); 7.05 (q, 1H, CH) 4.45 (m, 2H, CH$_2$); 2.07 (m, 2H, CH$_2$) ppm

^{13}C-NMR (δ, 100 MHz, CDCl$_3$, 25 °C):

195.71 (1C, C=O); 165.69 (1C, C=O); 137.99 (1C, AR); 136.99 (1C, AR); 134.14 (1C, AR); 133.14 (1C, AR); 132.84 (1C, AR); 130.96 (1C, AR); 130.05 (3C, AR); 128.59 (1C, AR); 128.47 (3C, AR); 63.37 (1C, CH$_2$); 32.83 (1C, CH$_2$); 21.20 (1C, CH$_2$) ppm

3.4.2.3 2-Hydroxyethyl 3-benzoylbenzoate
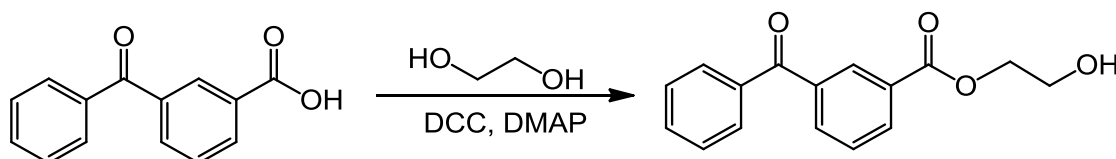
N,N'-Dicyclohexylcarbodiimide (DCC) (2.18 g, 10.6 mmol) was added to a mixture of 3-benzoylbenzoic acid (2.2 g, 8.84 mmol), 4-(dimethylamino)pyridine (DMAP) (129.6 mg), and 2.2 g ethane-1,2-diol (35.36 mmol, 4 Eq.) in 60 mL of CH_2Cl_2 at 0 °C. After 1h the ice bath was removed and the mixture was allowed to stir for additional 16h. The white precipitate was separated by filtration and the organic layer was diluted with 5% hydrochloric acid, neutralized with saturated $NaHCO_3$ solution and dried over sodium sulfate. After the solvent was evaporated under reduced pressure the crude product was purified by flash column chromatography (silica gel, cyclohexane / ethyl acetate = 8:1)

Yield: 2.1 g (83.0%)

^{1}H-NMR (δ, 400 MHz, CDCl$_3$, 25 °C):

8.45 (s, 1H, AR); 8.27 (d, 1H, AR); 7.98 (d, 1H, AR); 7.82 (d, 2H, AR); 7.59 (m, 2H, AR); 7.49 (m, 2H, AR); 4.48 (t, 2H, CH$_2$); 3.96 (t, 2H, CH$_2$); 3.47 (m, 1H, OH) ppm

^{13}C-NMR (δ, 100 MHz, CDCl$_3$, 25 °C):

195.65 (1C, C=O); 165.99 (1C, C=O); 137.89 (1C, AR); 136.83 (1C, AR); 134.18 (1C, AR); 133.16 (1C, AR); 132.78 (1C, AR); 130.87 (1C, AR); 129.93 (3C, AR); 128.48 (1C, AR); 128.38 (3C, AR); 66.90 (1C, CH$_2$); 61.13 (1C, CH$_2$) ppm

3.4.2.4 2-(((Vinyloxy)carbonyl)oxy)ethyl 3-benzoylbenzoate (1h)
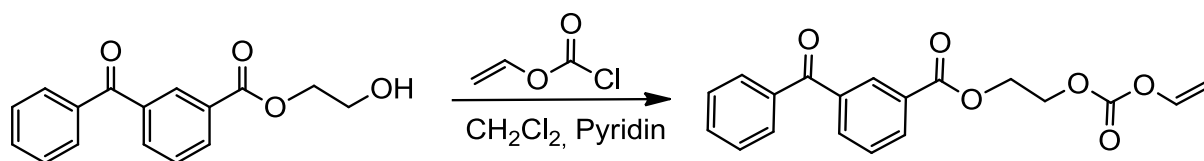
2-Hydroxyethyl-3-benzoylbenzoate (1.00 g; 4.82 mmol) and pyridine (0.5 mL) were dissolved in CH_2Cl_2 and cooled to 0°C. Vinyl chloroformate (0.51 g; 4.82 mmol) was slowly added to the mixture and was stirred for 30 minutes until the ice bath was removed. After the reaction time of 20h the mixture was diluted with 5% HCl (3x 50 mL) and the organic layer was dried over Na_2SO_4. The solvent was evaporated under reduced pressure and the residue was purified by flash chromatography (silica gel, cyclohexane / ethyl acetate = 5:1), to obtain the title compound as a brown solid

Yield: 0.97 g (74.4%)

^{1}H-NMR (δ, 400 MHz, CDCl$_3$, 25 °C):
8.45 (s, 1H, AR); 8.27 (d, 1H, AR); 7.98 (d, 1H, AR); 7.82 (d, 2H, AR); 7.59 (m, 2H, AR); 7.49 (m, 2H, AR); 7.05 (q, 1H,CH) 4.93 (m, 1H, CH$_2$); 4.65 (m, 1H, CH$_2$); 4.62 (q, 2H,CH$_2$); 4.54 (q, 2H,CH$_2$) ppm

^{13}C-NMR (δ, 100 MHz, CDCl$_3$, 25 °C):
195.55 (1C, C=O); 165.41 (1C, C=O); 152.53 (1C, C=O); 142.44 (1C, CH) 137.99 (1C, AR); 136.89 (1C, AR); 134.31 (1C, AR); 133.24 (1C, AR); 132.80 (1C, AR); 131.06 (1C, AR); 130.00 (3C, AR); 129.80 (1C, AR); 128.60 (1C, AR); 128.43 (3C, AR); 98.20 (1C, CH$_2$); 65.95 (1C, CH$_2$); 62.62 (1C, CH$_2$) ppm

3.4.2.5 Prop-2-yn-1-yl 3-benzoylbenzoate (1d)
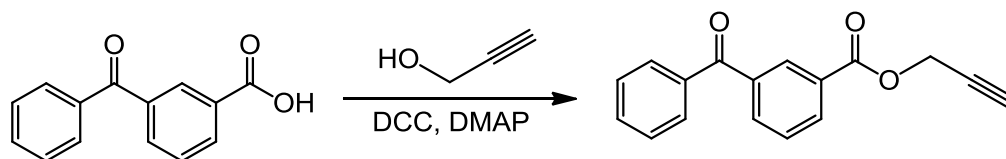
N,N'-Dicyclohexylcarbodiimide (DCC) (2.18 g, 10.6 mmol) was added to a mixture of 3-benzoylbenzoic acid (2.0 g, 8.84 mmol), 4-(dimethylamino)pyridine (DMAP) (129.6 mg), and 3.96 g propargyl alcohol (70.72 mmol, 4.11 mL) in 60 mL of CH_2Cl_2 at 0 °C. After 1h the ice bath was removed and the mixture was allowed to stir for additional 16h. The white precipitate was separated by filtration and the organic layer was diluted with 5% hydrochloric acid, neutralized with saturated $NaHCO_3$ solution and dried over sodium sulfate. After the solvent was evaporated under reduced pressure the crude product was purified by flash column chromatography (silica gel, cyclohexane / ethyl acetate = 8:1) to obtain the title compound as a white solid.

Yield: 2.03 g (86.7%)

^{1}H-NMR (δ, 400 MHz, CDCl$_3$, 25 °C):

8.45 (s, 1H, AR); 8.27 (d, 1H, AR); 7.98 (d, 1H, AR); 7.82 (d, 2H, AR); 7.59 (m, 2H, AR); 7.49 (m, 2H, AR); 4.95 (d, 2H, CH$_2$); 2.53 (t, 1H, -C≡C) ppm

^{13}C-NMR (δ, 100 MHz, CDCl$_3$, 25 °C):

195.59 (1C, C=O); 165.00 (1C, C=O); 138.07 (1C, AR); 136.93 (1C, AR); 134.44 (1C, AR); 133.3 (1C, AR); 132.85 (1C, AR); 130.04 (3C, AR); 129.69 (1C, AR); 128.67 (1C, AR); 128.49 (3C, AR); 75.27 (2C, C, CH); 52.76 (1C, CH$_2$) ppm

3.4.2.6 Ethyl-3-benzoylbenzoate (1a)
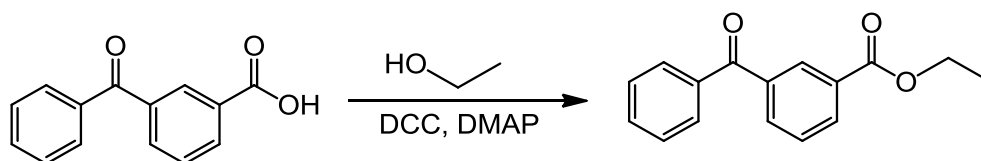
N,N'-Dicyclohexylcarbodiimide (DCC) (2.18 g, 10.6 mmol) was added to mixture of 3-benzoylbenzoic acid (2.0 g, 8.84 mmol), 4-(dimethylamino)pyridine (DMAP) (129.6 mg), and 2.18 g ethanol (44.20 mmol, 2.11 mL) in 60 mL of CH_2Cl_2 at 0 °C. After 1h the ice bath was removed and the mixture was allowed to stir for additional 16h. The white precipitate was separated by filtration and the organic layer was diluted with 5% hydrochloric acid, neutralized with saturated $NaHCO_3$ solution and dried over sodium sulfate. After the solvent was evaporated under reduced pressure the crude product was purified by flash column chromatography (silica gel, cyclohexane / ethyl acetate = 7:1) to obtain the title compound as a colorless oil.

Yield: 1.80 g (80.1%)

^{1}H-NMR (δ, 400 MHz, CDCl$_3$, 25 °C):
8.42 (s, 1H, AR); 8.23 (s, 1H, AR); 7.95 (s, 1H, AR); 7.77 (d, 2H, AR); 7.55 (m, 2H, AR); 7.46 (m, 2H, AR); 4.37 (d, 2H, CH$_2$); 1.36 (t, 3H, -CH$_3$) ppm

^{13}C-NMR (δ, 100 MHz, CDCl$_3$, 25 °C):
195.73 (1C, C=O); 165.74 (1C, C=O); 137.88 (1C, AR); 137.01 (1C, AR); 133.91 (1C, AR); 133.09 (1C, AR); 132.74 (1C, AR); 130.85 (1C, AR); 130.85 (1C, AR); 130.00 (3C, AR); 128.42 (3C, AR); 66.90 (1C, CH$_2$); 61.13 (1C, CH$_2$) ppm

3.4.2.7 But-3-in-1-yl 3-benzoylbenzoate (1c)
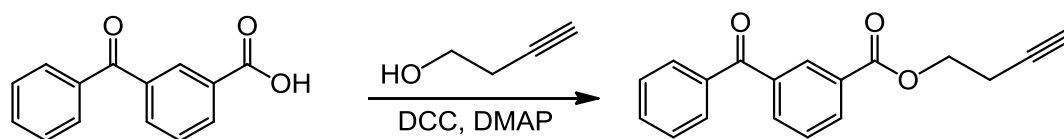
N,N'-Dicyclohexylcarbodiimide (DCC) (2.18 g, 10.6 mmol) was added to a mixture of 3-benzoylbenzoic acid (1.5 g, 6.63 mmol), 4-(dimethylamino)pyridine (DMAP) (97.0 mg), and 1.85 g 3-butyn-1-ol (26.52 mmol, 2.4 mL) in 60 mL of CH_2Cl_2 at 0 °C. After 1h the ice bath was removed and the mixture was allowed to stir for additional 16h. The white precipitate was separated by filtration and the organic layer was diluted with 5% hydrochloric acid, neutralized with saturated $NaHCO_3$ solution and dried over sodium sulfate. After the solvent was evaporated under reduced pressure the crude product was purified by flash column chromatography (silica gel, cyclohexane / ethyl acetate = 8:1) to obtain the title compound as a colorless oil.

Yield: 1.5 g (81%)

^{1}H-NMR: (δ, 400 MHz, 25°C, CDCl$_3$):
8.45 (s, 1H, AR); 8.28 (d, 1H, AR); 8.02 (d, 1H, AR); 7.79 (d, 2H, AR); 7.59 (m, 2H, AR); 7.50 (m, 2H, AR); 4.45 (t, 2H, CH$_2$); 2.68 (t, 2H, CH$_2$); 2.01 (t, 1H, -C≡C) ppm

^{13}C-NMR: (δ, 100 MHz, 25°C, CDCl$_3$):
195.59 (1C, C=O); 165.00 (1C, C=O); 138.07 (1C, AR); 136.93 (1C, AR); 134.44 (1C, AR); 133.3 (1C, AR); 132.85 (1C, AR); 130.04 (3C, AR); 129.69 (1C, AR); 128.67 (1C, AR); 128.49 (3C, AR); 75.27 (2C, C, CH); 52.76 (1C, CH$_2$) ppm

3.4.2.8 Prop-2-in-1-yl 4-benzoylbenzoate (2d)
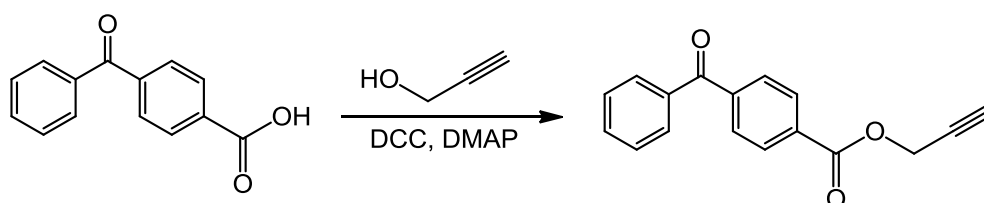
N,N'-Dicyclohexylcarbodiimide (DCC) (2.18 g, 10.6 mmol) was added to a mixture of 3-benzoylbenzoic acid (1.5 g, 6.63 mmol), 4-(dimethylamino)pyridine (DMAP) (97.0 mg), and 1.85 g propargyl alcohol (26.52 mmol, 2.4 mL) in 60 mL of CH_2Cl_2 at 0 °C. After 1h the ice bath was removed and the mixture was allowed to stir for additional 16h. The white precipitate was separated by filtration and the organic layer was diluted with 5% hydrochloric acid, neutralized with saturated $NaHCO_3$ solution and dried over sodium sulfate. After the solvent was evaporated under reduced pressure the crude product was purified by flash column chromatography (silica gel, cyclohexane / ethyl acetate = 8:1) to obtain the title compound as a white solid.

Yield: 2.1 g (89.9%)

^{1}H-NMR: (δ, 400 MHz, 25°C, CDCl$_3$):
8.45 (s, 1H, AR); 8.27 (d, 1H, AR); 7.98 (d, 1H, AR); 7.82 (d, 2H, AR); 7.59 (m, 2H, AR); 7.49 (m, 2H, AR); 4.97 (d, 2H, CH$_2$); 2.55 (t, 1H, -C≡C) ppm

^{13}C-NMR: (δ, 100 MHz, 25°C, CDCl$_3$):
195.59 (1C, C=O); 165.00 (1C, C=O); 138.07 (1C, AR); 136.93 (1C, AR); 134.44 (1C, AR); 133.3 (1C, AR); 132.85 (1C, AR); 130.04 (3C, AR); 129.69 (1C, AR); 128.67 (1C, AR); 128.49 (3C, AR); 75.27 (2C, C, CH); 52.76 (1C, CH$_2$); 52.76 (1C, CH$_2$) ppm

3.4.2.9 2-(Methacryloyloxy)ethyl 3-benzoylbenzoate (1e)
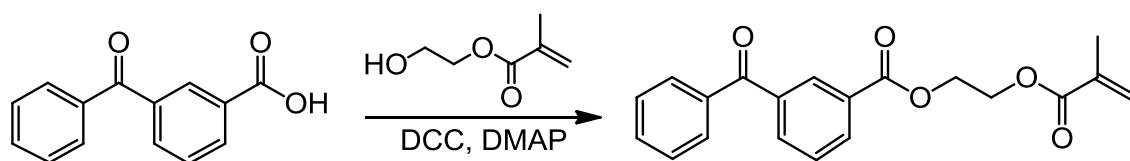
N,N'-Dicyclohexylcarbodiimide (DCC) (1.03 g, 5.04 mmol) was added to a mixture of 3-benzoylbenzoic acid (0.95 g, 4.2 mmol), 4-(dimethylamino)pyridine (DMAP) (97.0 mg), and 2.18 g 2-hydroxyethyl methacrylate (16.8 mmol, 2.04 mL) in 60 mL of CH_2Cl_2 at 0 °C. After 1h the ice bath was removed and the mixture was allowed to stir for additional 16h. The white precipitate was separated by filtration and the organic layer was diluted with 5% hydrochloric acid, neutralized with saturated $NaHCO_3$ solution and dried over sodium sulfate. After the solvent was evaporated under reduced pressure the crude product was purified by flash column chromatography (silica gel, cyclohexane / ethyl acetate = 8:1) to obtain the title compound as a colorless oil.

Yield: 0.83 g (49.0%)

^{1}H-NMR: (δ, 400 MHz, 25°C, CDCl$_3$):
8.46 (s, 1H, AR); 8.28 (d, 1H, AR); 8.0 (d, 1H, AR), 7.83 (d, 2H, AR); 7.62 (q, 2H, AR); 7.52 (t, 2H, AR); 6.14 (s, 1H, $H_2C=C$-); 5.60 (s, 1H, $H_2C=C$-); 4.62 (q, 2H, CH_2); 4.51 (q, 2H, CH_2); 1.96 (s, 3H, CH_3); ppm

^{13}C-NMR: (δ, 100 MHz, 25°C, CDCl$_3$):
195.52 (1C, C=O); 168.09 (1C, C=O); 164.81 (1C, C=O); 138.56 (1C, AR); 136.66 (1C, AR); 137.28 (1C, AR); 134.64(1C, AR); 133.94 (1C, AR); 132.91 (1C, AR); 131.01 (1C, AR); 130.42 (3C, AR); 128,29 (3C, AR); 125.82 (1C, $=CH_2$); 62.68 (1C, CH_2); 62.15 (1C, CH_2); 18.32 (1C, CH_3) ppm

3.4.2.10 2-(Acryloyloxy)ethyl 3-benzoylbenzoate (1b)
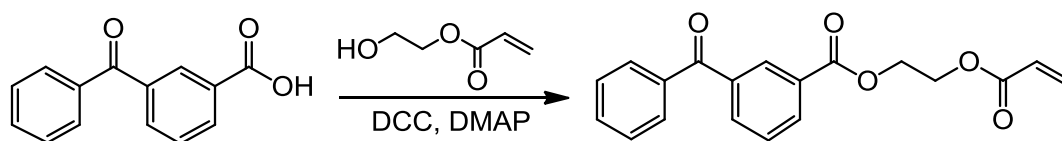
N,N'-Dicyclohexylcarbodiimide (DCC) (1.03 g, 5.04 mmol) was added to a mixture of 3-benzoylbenzoic acid (0.95 g, 4.2 mmol), 4-(dimethylamino)pyridine (DMAP) (97.0 mg), and 1.95 g 2-hydroxyethyl acrylate (16.8 mmol, 2.04 mL) in 60 mL of CH_2Cl_2 at 0 °C. After 1h the ice bath was removed and the mixture was allowed to stir for additional 16h. The white precipitate was separated by filtration and the organic layer was diluted with 5% hydrochloric acid, neutralized with saturated $NaHCO_3$ solution and dried over sodium sulfate. After the solvent was evaporated under reduced pressure the crude product was purified by flash column chromatography (silica gel, cyclohexane / ethyl acetate = 8:1) to obtain the title compound as a white solid.

Yield: 1 g (73.52%)

^{1}H-NMR: (δ, 400 MHz, 25°C, CDCl$_3$):
8.44 (s, 1H, AR); 8.27 (d, 1H, AR); 7.99 (d, 1H, AR), 7.79 (d, 2H, AR); 7.58 (q, 2H, AR); 7.50 (t, 2H, AR); 6.40 (d, 1H, $H_2C=C$-); 6.14 (q, 1H, $H_2C=C$-); 5.88 (d, 1H, $H_2C=C$-); 4.57 (q, 2H, CH_2); 4.51 (q, 2H, CH_2); ppm

^{13}C-NMR: (δ, 100 MHz, 25°C, CDCl$_3$):
195.63 (1C, C=O); 165.83 (1C, C=O); 165.51 (1C, C=O); 138.01 (1C, AR); 136.96 (1C, AR); 134.25 (1C, AR); 133.23(1C, AR); 132.82 (1C, AR); 131.44 (1C, CH=); 131.04 (1C, AR); 130.03 (3C, AR); 128.62 (3C, AR); 127.90 (1C, $=CH_2$); 62.99 (1C, CH_2); 62.12 (1C, CH_2) ppm

3.4.3 Synthesis of Hydroxy ketone derivatives

3.4.3.1 2-Hydroxy-1-(4-hydroxyphenyl)-2-methylpropan-1-one
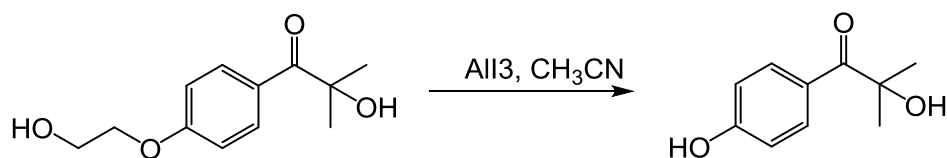
The in acetonitrile dissolved photoinitiator Irgacure 2959 (4 g, 17.84 mmol, 1 Eq.) was added dropwise to 7.3 g AlI$_3$ (17.84 mmol, 1 Eq.) suspended in 100 mL CH$_3$CN. The mixture was heated to reflux overnight and quenched by the addition of water on the next day. Afterwards the dark brown solution was extracted by diethyl ether three times and the combined organic layers were dried over Na$_2$SO$_4$. Subsequently, the solvent was evaporated under reduced pressure and the residue was purified by flash chromatography (silica gel, cyclohexane / ethyl acetate=4:1), to obtain the title compound as a white solid.

Yield: 1.7 g (52.9%)

^{1}H-NMR: (δ, 400 MHz, 25°C, CDCl$_3$):
8.04 (d, 2H, AR); 6.90 (d, 2H, AR); 5.56 (s, 1H, OH); 4.30 (s, 1H, OH); 1.64 (s, 6H, CH$_3$) ppm

^{13}C-NMR: (δ, 100 MHz, 25°C, CDCl$_3$):
198.59 (1C, AR); 162.54 (1C, AR); 132.69 (2C, AR); 126.8 (1C, AR); 115.25 (2C, AR); 81.00 (1C, C); 28.70 (2C, CH$_3$) ppm

3.4.3.2 Phenylisobutyrate
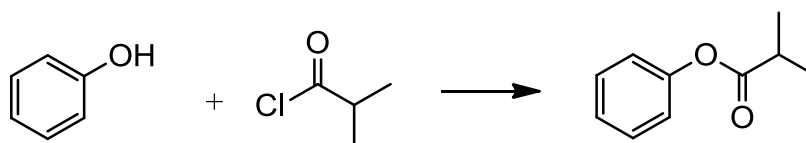
50.00 g (1 Eq., 0.531 mol) phenol were cooled in a flask to 0°C and 70.73 g (1.25 Eq, 0.664 mol) isobutyl acid chloride were added dropwise. The mixture was hold on 0°C for one hour, until it was allowed to warm to room temperature. After two additional hours reaction time, the excess of isobutyl acid chloride was removed under reduced pressure to obtain the pure product as a yellow liquid.

Yield: 85.00 g (97.4%)

^{1}H-NMR: (δ, 400 MHz, 25°C, CDCl$_3$):
7.28 (d, 2H, AR); 7.22 (d, 1H, AR); 7.09 (d, 1H, AR); 2.81 (d, 1H, CH); 1.33 (s, 6H, -CH$_3$) ppm

^{13}C-NMR (δ, 100 MHz, CDCl$_3$, 25 °C):
175.51 (1C, C=O); 150.94 (1C, AR); 129.35 (2C, AR); 125.63 (1C, AR); 121.51 (2C, AR); 34.17 (1C, C); 18.93 (2C, CH$_3$) ppm

3.4.3.3 1-(4-Hydroxyphenyl)-2-methylpropan-1-one
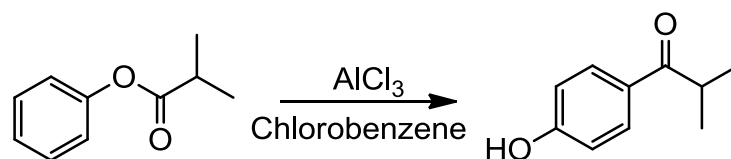
38.98 g (2.4 Eq, 0.292 mol) $AlCl_3$ were suspended in chlorobenzene at 0°C and was stirred at room temperature for 45 min. Next 20.00 g (1 Eq., 0.292) of phenyl isobutyrate were added dropwise and was allowed to react for two days. The reaction was quenched by the addition of ice and HCl and was extracted with toluene.

In the next step the combined organic layers were extracted with saturated NaCl and the solvent was removed under reduced pressure. The residue was suspended in 300 mL H_2O and the pH was adjusted, by the addition of 30% NaOH, to 14. The mixture was extracted with ethyl acetate and the water phase was acidulated to a pH of 0 by the addition of HCl. After an additional extraction step with ethyl acetate the combined organic layers were dried over Na_2SO_4 and the solvent was removed under reduced pressure to obtain the product as a white solid.

Yield: 16.5 g (82.5%)

^{1}H-NMR: (δ, 400 MHz, 25°C, CDCl$_3$):

8.1 (d, 2H, AR); 6.7 (d, 2H, AR); 5.35 (d, 1H, OH) 2.81 (d, 1H, CH); 1.33 (s, 6H, -CH$_3$) ppm

^{13}C-NMR (δ, 100 MHz, CDCl$_3$, 25 °C):

202.20 (1C, C=O); 162.54 (1C, AR); 130.29 (2C, AR); 129.4 (1C, AR); 115.8 (2C, AR); 35.00 (1C, C); 18.01 (2C, CH$_3$) ppm

3.4.3.4 2-Hydroxy-1-(4-hydroxyphenyl)-2-methylpropan-1-one
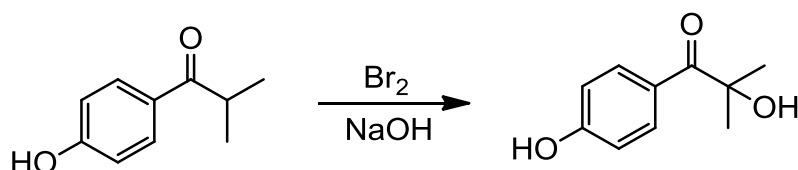
21 g (1 Eq., 0.127 mol) 1-(4-hydroxyphenyl)-2-methylpropan-1-one were dissolved in dioxane and cooled to 0°C. 22.48 g (1.1 Eq., 0.140 mol) Br_2 were added and the mixture was stirred for 2h at room temperature. The reaction was poured on 500 mL water and extracted two times with ethyl acetate. In the next step the solvent was removed under reduced pressure and the brownish oil was suspended in 400 mL water and a pH of 14 was adjusted by the addition of 20 mL 30% NaOH. The mixture was stirred at room temperature for 3h and subsequently neutralized by the addition of HCl. The slightly yellow crystals were filtered of and recrystallized from toluene to obtain the pure product as white crystals.

Yield: 14.0 g (60.8%)

^{1}H-NMR: (δ, 400 MHz, 25°C, CDCl$_3$):
8.1 (d, 2H, AR); 6.7 (d, 2H, AR); 5.35 (s, 1H, OH) 3.28 (s, 1H, OH); 1.33 (s, 6H, -CH$_3$) ppm

^{13}C-NMR: (δ, 100 MHz, 25°C, CDCl$_3$):
198.59 (1C, C=O); 162.54 (1C, AR); 132.69 (2C, AR); 126.8 (1C, AR); 115.25 (2C, AR); 81.00 (1C, C); 28.70 (2C, CH$_3$) ppm

3.4.3.5 2-Hydroxy-2-methyl-1-(4-(prop-2-yn-1-yloxy)phenyl)propan-1-one (3a)
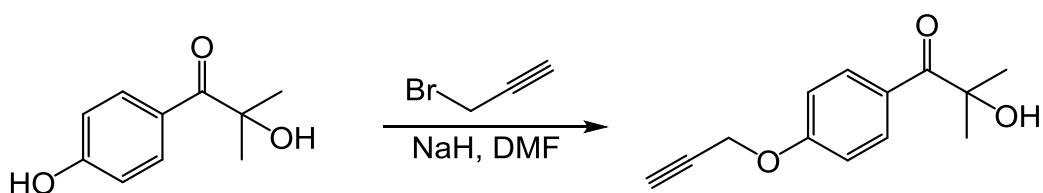
0.21 g (23.99 mmol, 2 Eq.) NaH were added to a three necked round bottom flask and washed three times with dry THF to remove the mineral oil. Afterwards the NaH was suspended in DMF and the reaction was cooled to -40 °C. The dissolved hydroxy-1-(4-hydroxyphenyl)-2-methylpropan-1-one (4.03 mmol, 1.1 Eq.) was added drop wise and the mixture was stirred for one additional hour during the temperature was hold between -40°C and -10°C. Propargyl bromide (80% in Toluene) (0.68 g, 1 Eq.) was added, the cooling bath was removed and the reaction was quenched after 5h by the addition of ice cubes. Subsequently the solvent was evaporated under reduced pressure and the residue was redissolved in water and extracted three times with CH_2Cl_2. The combined organic layers were dried over Na_2SO_4, to obtain the title compound as a white solid, after purification by flash chromatography (silica gel, cyclohexane / ethyl acetate=3:1).

Yield: 600 mg (68.1%)

^{1}H-NMR: (δ, 400 MHz, 25°C, CDCl$_3$):
8.08 (d, 2H, AR); 7.04 (d, 2H, AR); 4.77 (s, 2H, CH$_2$); 4.18 (s, 1H, OH); 2.56 (s, 1H, CH); 1.64 (s, 6H, CH$_3$) ppm

^{13}C-NMR: (δ, 100 MHz, 25°C, CDCl$_3$):
202.60 (1C, C=O); 161.19 (1C, AR); 132.27 (2C, AR); 126.68 (1C, AR); 114.48 (2C, AR); 77.63 (1C, C); 76.30 (1C, ≡C); 75.93 (1C, ≡CH); 28.61 (2C, CH$_3$) ppm

3.4.3.6 4-(2-Hydroxy-2-methylpropanoyl)phenyl vinyl carbonate (3b)
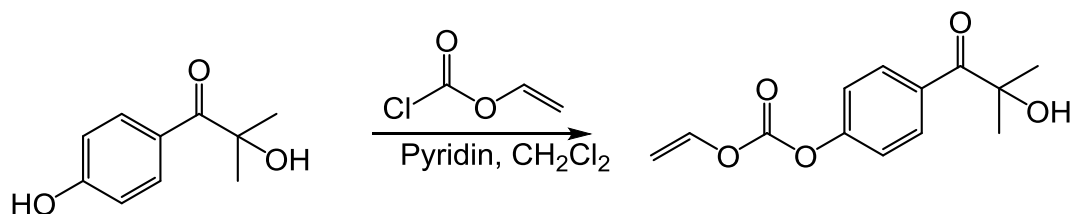
0.5 g Hydroxy-1-(4-hydroxyphenyl)-2-methylpropan-1-one (2.23 mmol) and pyridine (0.54 mL, 6.69 mmol) were dissolved in CH_2Cl_2 and cooled to 0 °C. Vinyl chloroformate (0.2 mL, 2.23 mmol) was added dropwise and after one hour the reaction was warmed to RT and stirred overnight. The product was extracted three times with 5% HCl and the combined organic layers were dried over Na_2SO_4. Subsequently the solvent was evaporated under reduced pressure and the residue was purified by flash chromatography (silica gel, cyclohexane / ethyl acetate=5:1), to obtain the title compound as a colorless viscous oil.

Yield: 0.42 g (75.27%)

^{1}H-NMR: (δ, 400 MHz, 25°C, CDCl$_3$):
8.13 (d, 2H, AR); 7.34 (d, 2H, AR); 7.13 (q, 1H, CH=CH2); 5.07 (q, 1H, CH=CH2); 4.74 (q, 1H, CH=CH2); 3.78 (s, 1H, OH); 1.63 (s, 6H, CH$_3$) ppm

^{13}C-NMR: (δ, 100 MHz, 25°C, CDCl$_3$):
203.04 (1C, C=O); 153.80 (1C, AR); 150.54 (1C, C=O); 142.4 (1C, CH=); 131.78 (1C, AR); 131.68 (2C, AR); 120.80 (2C, AR); 99.00 (1C, =CH$_2$); 28.33 (2C, CH$_3$) ppm

3.4.4 Synthesis of Phosphine oxide derivatives

3.4.4.1 Sodium phenyl(2,4,6-trimethylbenzoyl)phosphinate
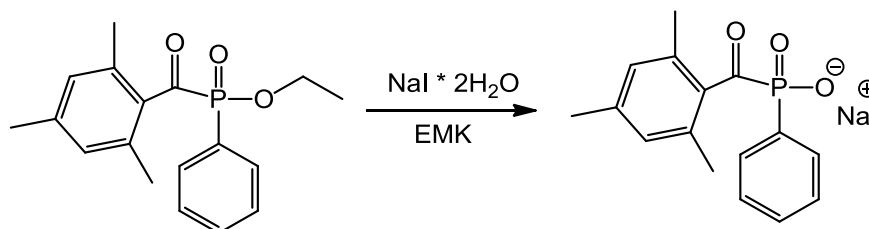
10 g Irgacure TPO-L (31.61 mmol) were dissolved in methyl ethyl ketone and NaI*2H$_2$O (5.9 g, 31.61mmol) were added over a period of 15 minutes. The mixture was stirred overnight at 65°C and the yellow precipitate was filtered off on the next day. It was washed twice with 10 mL n- hexane and dried under vacuum at 60°C for 24h.

Yield: 7.26 g (90.1%)

3.4.4.2 Phenyl(2,4,6-trimethylbenzoyl)phosphine acid
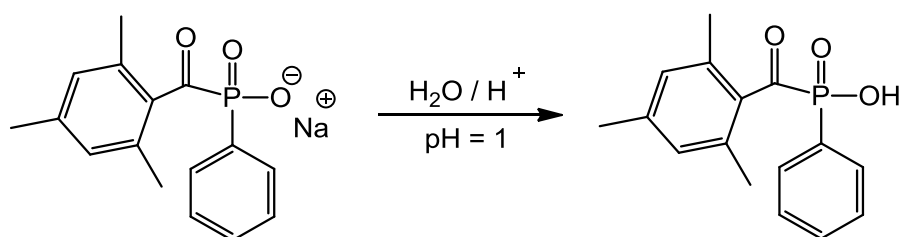
Sodium phenyl(2,4,6-trimethylbenzoyl)phosphinate (7.26 g, 23.3 mmol) was dissolved in H_2O and acidulated with 0.5 M H_2SO_4 to pH = 1. After reaction time of 1h white crystals were filtered off and washed twice with H_2O. The precipitate was dissolved in toluene and dried by azeotropic distillation, the remaining toluene was evaporated under reduced pressure and the residue was recrystallized in ethyl acetate. Subsequently the pale yellow crystals were dried under vacuum at 60°C for 16h.

Yield: 5.18 g (78.1%)

^{1}H-NMR: (δ, 400 MHz, 25°C, CDCl$_3$):
7.71 (m, 2H, AR); 7.63 (m, 1H, AR); 7.52 (m, 2H, AR), 6.85 (m, 2H, AR), 2.24 (s, 3H, CH$_3$), 2.07 (s, 6H, CH$_3$) ppm

^{13}C-NMR: (δ, 100 MHz, 25°C, CDCl$_3$):
215.74 (1C, C=O); 139.61 (1C, AR); 136.20 (1C, AR); 134.30 (2C, AR); 132.96 (1C, AR); 132.7 (1C, AR); 128.28 (4C, AR); 21.02 (1C, CH$_3$); 19.13 (2C, CH$_3$) ppm

3.4.4.3 Phenyl(2,4,6-trimethylbenzoyl)phosphine acid chloride

Phenyl (2,4,6-trimethylbenzoyl)phosphine acid (1.73 mmol, 1 Eq.) was dissolved in 5 mL toluene and 5 µl DMF and 2.5 mL $SOCl_2$ (4.13 g, 34.69 mmol) were added. The mixture was heated to 110°C for 16h and the reaction progress was monitored by ^{1}H-NMR. After complete conversion of phenyl (2,4,6-trimethylbenzoyl)phosphine acid the solvent and the excess of $SOCl_2$ were removed under reduced pressure.
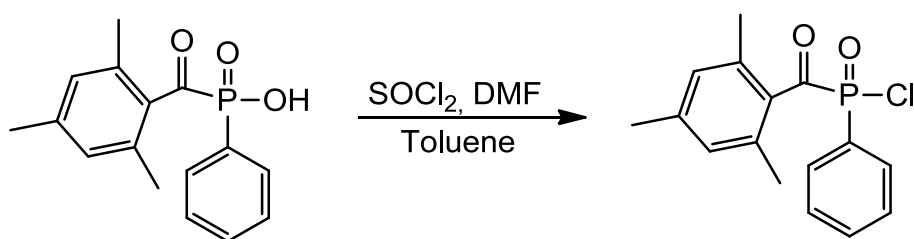
Yield: ~95%

^{1}H-NMR: (δ, 400 MHz, 25°C, CDCl₃):
7.79 (m, 2H, AR); 7.47 (m, 1H, AR); 7.37 (m, 2H, AR), 6.69 (m, 2H, AR), 2.11 (s, 3H, CH₃), 1.99 (s, 6H, CH₃) ppm

3.4.4.4 Prop-2-yn-1-yl phenyl(2,4,6-trimethylbenzoyl)phosphinate (4a)
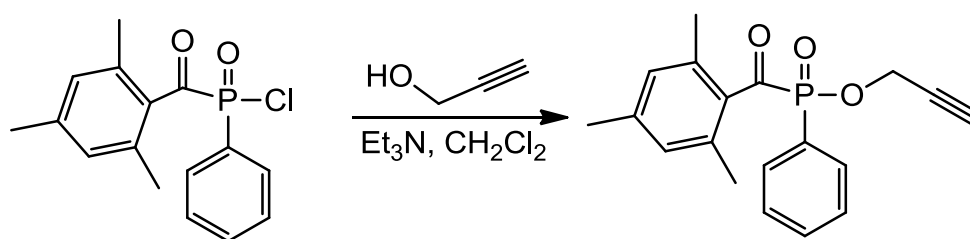
Phenyl (2,4,6-trimethylbenzoyl)phosphine acid chloride (1.38 mmol, 1 Eq.) and propargyl alcohol (80 µl, 1.38 mmol, 1 Eq.) were dissolved in 20 mL CH_2Cl_2 cooled to 0°C. 190 µl (0.140 g, 1.38 mmol, 1 Eq.) triethylamine were added to mixture which was allowed to warm to room temperature after 1h additional reaction time. On the next day the reaction was quenched by addition of water, extracted three times with CH_2Cl_2 and dried over Na_2SO_4. Subsequently the solvent was evaporated under reduced pressure and the residue was purified by flash chromatography (silica gel, cyclohexane / ethyl acetate=4:1), to obtain the title compound as a brownish viscous oil.

Yield: 282 mg (62.5%)

^{1}H-NMR: (δ, 400 MHz, 25°C, CDCl$_3$):
7.85 (m, 2H, AR); 7.59 (m, 1H, AR); 7.48 (m, 2H, AR), 6.81 (m, 2H, AR), 4.69 (d, 2H, CH$_2$), 2.49 (s, 1H, CH), 2.26 (s, 3H, CH$_3$), 2.15 (s, 6H, CH$_3$) ppm

^{13}C-NMR: (δ, 100 MHz, 25°C, CDCl$_3$):
214.89 (1C, C=O); 140.29 (1C, AR); 134.66 (1C, AR); 133.66 (2C, AR); 133.10 (1C, AR); 128.81 (4C, AR); 76.44 (1C, ≡CH); 53.39 (1C, CH$_2$); 21.29 (1C, CH$_3$); 19.56 (2C, CH$_3$) ppm

^{31}P-NMR: (δ, 121.4 MHz, 25°C, CDCl$_3$):
18.52 (s, P) ppm

3.4.4.5 2-Hydroxyethylvinylcarbonate
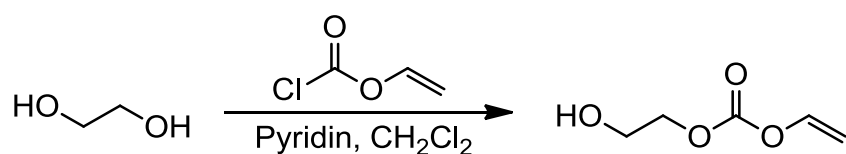
Ethylene glycol (11.19 g, 180.26 mmol, 6.4 Eq.) and pyridine (2.27 mL, 28.17 mmol, 1 Eq.) were dissolved in CH_2Cl_2 and cooled to 0 °C. Vinyl chloroformate (3.0 g, 28.17 mmol, 1 Eq.) was added to the mixture dropwise which was allowed to warm to room temperature after one additional hour reaction time. On the next day the product was extracted three times with 5% HCl and the combined organic layers were dried over Na_2SO_4. Subsequently the solvent was evaporated under reduced pressure and the residue was purified by flash chromatography (silica gel, cyclohexane / ethyl acetate=4:1), to obtain the title compound as a colorless viscous oil.

Yield: 2.0 g (54%)

^{1}H-NMR: (δ, 400 MHz, 25°C, CDCl₃):
7.07 (m, 1H, CH_2); 4.94 (m, 1H, CH_2); 4.58 (m, 1H, CH_2); 4.51 (s, 1H, OH); 4.32 (m, 2H, CH_2), 3.87 (m, 2H, CH_2) ppm

^{13}C-NMR: (δ, 100 MHz, 25°C, CDCl₃):
152.82 (1C, C=O); 142.49 (1C, CH=); 98.02 (1C, =CH_2); 69.78 (1C, CH_2); 60.50 (1C, CH_2) ppm

3.4.4.6 2-((Phenyl(2,4,6-trimethylbenzoyl)phosphoryl)oxy)ethyl-vinylcarbonate (4b)
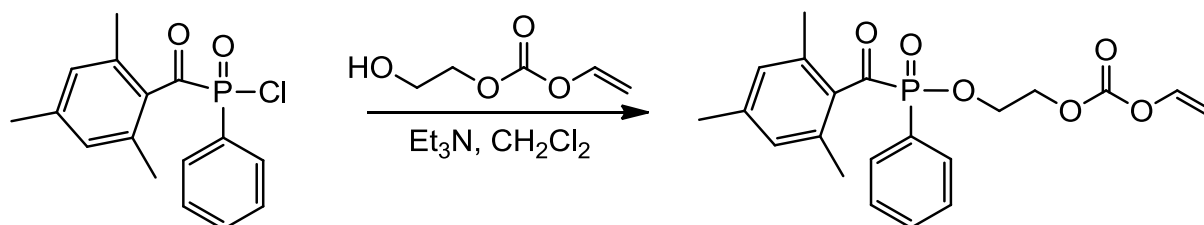
Phenyl (2,4,6-trimethylbenzoyl)phosphinacid chloride (6.85 mmol, 1 Eq.) and 2-hydroxyethylvinylcarbonate (6.85 mmol, 1 Eq.) were dissolved in 40 mL CH_2Cl_2 and cooled to 0°C. 950 µl (0.693 g, 6.85 mmol, 1 Eq.) triethylamine were added to mixture which was allowed to warm to room temperature after 1h additional reaction time. On the next day the reaction was quenched by addition of water, extracted three times with CH_2Cl_2 and dried over Na_2SO_4. Subsequently the solvent was evaporated under reduced pressure and the residue was purified by flash chromatography (silica gel, cyclohexane/cthyl acetate 4:1), to obtain the title compound as a white viscous oil.

Yield: 1.38 g (50%)

^{1}H-NMR: (δ, 400 MHz, 25°C, CDCl$_3$):
7.84 (m, 2H, AR); 7.61 (m, 1H, AR); 7.5 (m, 2H, AR), 7.0 (m, 1H, CH$_2$), 6.81 (m, 2H, AR), 4.96 (d, 1H, CH$_2$); 4.60 (d, 1H, CH$_2$); 4.37 (d, 2H, CH$_2$), 4.30 (d, 2H, CH$_2$), 2.26 (s, 3H, CH$_3$), 2.14 (s, 6H, CH$_3$) ppm

^{13}C-NMR: (δ, 100 MHz, 25°C, CDCl$_3$):
214.89 (1C, C=O); 142.50 (1C, AR); 134.40 (1C, AR); 133.54 (2C, AR); 132.85 (1C, AR); 128.63 (4C, AR); 98.16 (1C, =CH$_2$); 66.97 (1C, CH$_2$); 63.09 (1C, CH$_2$); 20.02 (1C, CH$_3$); 19.32 (2C, CH$_3$) ppm

^{31}P-NMR: (δ, 121.4 MHz, 25°C, CDCl$_3$):
18.80 (s, P) ppm

4 <u>Water soluble Photoinitiators</u>

4.1 <u>Introduction</u>

In the last years the field of water based, photocurable coatings gained increasing importance due to environmental and legislative constraints.[119,120]

The unique solvent properties, especially the low price, the easy availability and the non - toxic characteristics make water an interesting alternative to substitute volatile organic solvents. Furthermore, the easily adjustable viscosity, non flammability and odorlessness are crucial advantages for industrial applications and accentuate the superiority compared to conventional systems.[121–123] Nevertheless, these eco-friendly alternatives also bear some non-negligible drawbacks, which have to be discussed critically. The increased energy consumption for the solvent elimination and the corresponding expenditure of time and space are disadvantages from an economic point of view. Furthermore, a lower gloss of the obtained films and an increased content of amines, as consequence of the neutralization of the carboxylic functionalities of the applied pre-polymer in polyurethane dispersion based resins are reported in the literature.[43]

Another challenging issue is the lack of compatibility of the conventional additives and photoinitiators with water based systems. Most of the agents were developed for organic or organic solvent based formulations[119] and the supply of water soluble photoinitiators is still low. Currently, there are only a few different substances commercially available, which provide explicit compatibility with aqueous systems. These are for instants Irgacure 819 DW, which is a dispersion of a phosphine oxide initiator, and Irgacure 2959, which is a water soluble substance. In fact, there is considerable room for improvement attributed to the reduced amount of available photoinitiators and the unsatisfying material properties. Irgacure 819 DW suffers from the formation of agglomerates of the dispersed photoinitiator, which limits the applicability in the field of inkjet inks, due to the associated reduction of storage stability. The solubility of the Irgacure 2959 is rather low with 1.7g/100mL.[124] Furthermore the undesirable migration of these photoinitiators diminishes the range of applications in the field of food packaging materials and increases the demand for low migration water soluble photoinitiators.

In general, water solubility can be achieved by the introduction of hydrophilic moieties. For instance long-chain ethoxyether and ionic groups fulfill this requirement. Their appropriate reactivity and hydrophilic properties are well reported in the literature.[119,122,125,126] However, the corrosive character of ionic substances, especially of the chloride ions is

frequently ignored, although it is the major drawback of this substance group.[127] Furthermore their ability to interfere with the ionic balance of the investigated formulation and additionally the influence on the colloidal stability have to be taken into consideration.[128]

To circumvent these unwanted interactions there are recent efforts to realize water soluble photoinitiators without ionic functionalities. For example, Liska [128] proposed photoreactive species based on different carbohydrates which are suitable for water based applications. These substances exhibit high polymerization velocities (t_{max}) but suffer from low conversion rates. This effect was attributed to the elevated molecular weight of the modified photoinitiators, because they were applied weight-related and not in equimolar ratio. Thus, a reduced amount of photoactive species was added to the resin and the diminished conversion was therefore expectable. Nevertheless, modified carbohydrates provide an interesting concept for further investigations, to realize highly reactive and water soluble PIs.

To overcome this limiting drawback, which were mentioned before, the focus was set on strategies to increase the concentration of photoreactive residues on carbohydrate molecules. Therefore new concepts were developed for the synthesis of multifunctional photoinitiators to find the perfect balance between acceptable solubility and high conversion rates.

Recently, a paper has been published about the initiation mechanism of difunctional photoinitiators[129], which gives possible explanations for the superiority of this class of photoinitiators. In general, it was proposed that difunctional photoinitiators cannot be seen as two isolated initiator units. The enhanced reactivity is a consequence of the increased extinction coefficients which is attributed to the delocalization of the π orbitals along the conjugated system of the molecule. If two reactive chromophores are separated by an aliphatic spacer, synergy effects regarding the absorption of the molecule can be explained by through-space hyperconjugations.[129] Referring to this findings the elevated reactivity of multifunctional initiators is not only a consequence of the amount of photoreactive moieties, coupled to the molecular backbone, but also a result of interactions of the related orbitals which lead to an increased UV-light absorption. This implicates that the photochemical performance of an oligomeric PI is not equivalent to the same amount of a low molecular photoreactive residues.

Another important aspect was the migration behavior of the photoreactive species. According to the elucidated strategies in chapter 3.1 it was aspired to find a substances with a molecular weight of approximately 1000 g/mol or at least doubled to conventional photoinitiating systems to minimize the expected migration. Furthermore a cheap, easily available and non bioactive carbohydrate backbone is essential and an easy

functionalizable photoinitiating moiety had to be chosen. With regards to these requirements the focus was set on two different carbohydrates (erythritol and glucose) and the precursor material **3** (see Figure 19, chapter 3.2.1) was utilized for the development of the novel photoinitiators.

After the successful synthesis of the new photoreactive compounds, they were characterized by UV-Vis spectroscopy and evaluated by Photo-DSC measurements regarding their photoreactivity. Additionally, the migration behavior of the novel compounds was investigated by HPLC measurements.

4.2 Carbohydrate based photoinitiators

4.2.1 Results and Discussion

4.2.1.1 Synthesis of carbohydrate based photoinitiators

The difunctional erythritol based photoinitiator was obtained in a straightforward synthetic pathway. In the first step (I) the sugar alcohol was reacted with 1,1'-carbonyldiimidazol (CDI) with an catalytic amount of KOH to yield a bicyclic carbonate (88%).[130,131] The reaction of CDI with alcohols and amines was first published in 1957[132] and found a broad field of applications in peptide chemistry.[133] The exact mechanism of this reaction has not been completely clarified, but two presumably possibilities are proposed in the literature.[133,134] In the subsequent reaction step (II), the cyclic carbonate was coupled with the phenolic species of the hydroxy ketone under alkaline conditions (K_2CO_3) to obtain a mixture of isomers of the photoinitiator **5a**. During the reaction, which is performed at 110°C, the nucleophilic attack at either alkylene carbon is followed by evolution of carbon dioxide.[135] After the purification by column chromatography a moderate yield of 20% could be reached. An enhancement might be possible by further optimization of the reaction conditions.
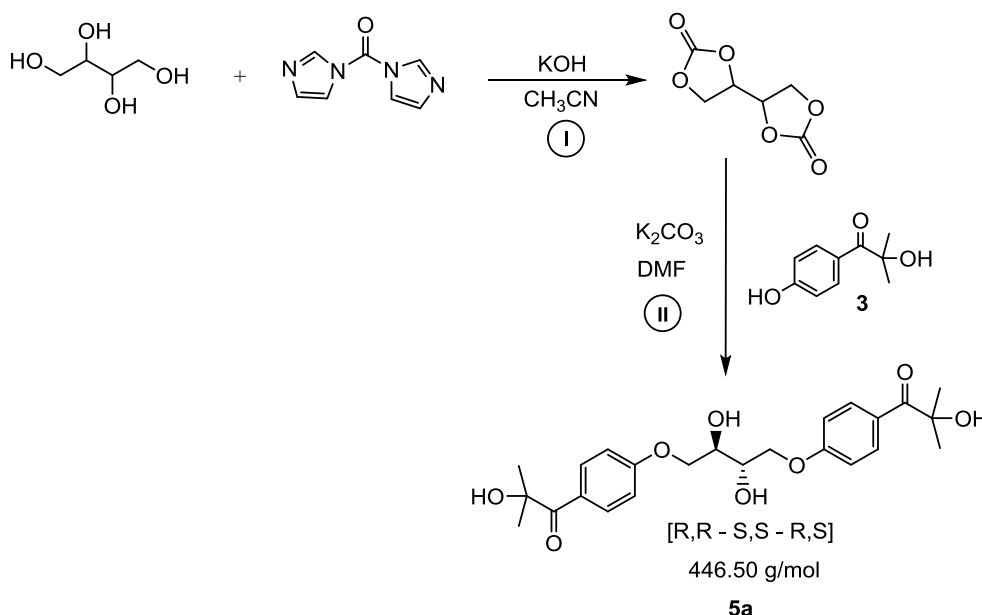

Figure 37: Synthetic pathway of the erythritol based difunctional photoinitiator (5a)

The second multifunctional photoinitiator is based on glucose and was realized in a three step synthetic pathway. Initially, the carbohydrate was etherified (I) by an SN$_2$ reaction with allyl bromide in presence of sodium hydride to obtain the corresponding alkoxide of the glucose.[136] The crude product was purified by column chromatography upon aqueous workup to obtain the allyl glucose in appropriate yields (85%) and purity. The ene modified substance was subsequently epoxidized (II) by the Prilezhaev reaction to the oxirane modified glucose derivative.[137] This molecule was finally coupled with the phenolic hydroxy ketone initiator **3** by a nucleophilic ring opening reaction (III). The mechanism of the epoxidation as well as the ring opening reaction are well reported in the literature.[138,139] The final product **5b** could be obtained in high yields of 73% as a crystalline powder.

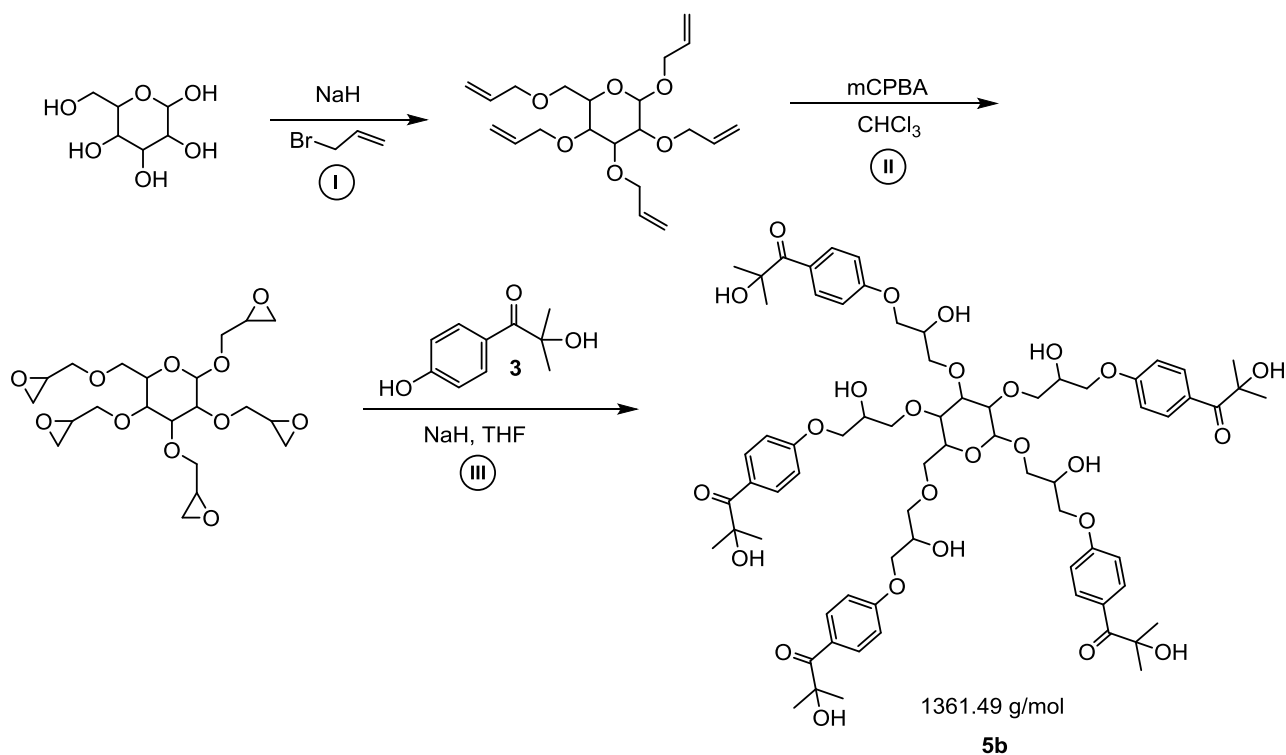**Figure 38: Synthetic pathway of the glucose based multifunctional photoinitiator (5b)**

4.2.1.2 Evaluation of the water solubility

After the successful synthesis of the novel photoinitiators their water solubility was investigated. It could be shown that the erythritol based substance **5a** possess a high water solubility of 10 w% (103.30 ± 3.65 mg/ml), whereas the glucose based substance **5b** was completely insoluble.

Referring to structural properties of the molecule and the huge amount of hydroxy groups the insolubility was not expectable.

To enable a reliable comparison of the novel photoreactive species and a commercially available photoinitiator (Irgacure 2959) the initiation performance of the substances was evaluated in the mono functional tetrahydrofurfuryl acrylate (THFA).

4.2.1.3 Photoreactivity of carbohydrate based photoinitiators

The photoreactivity of the carbohydrate based photoinitiators was characterized by photo-DSC measurements. Due to the lack of solubility of substance **5b** in water, the novel photoreactive species were evaluated within an acrylate resin to compare the photochemical performance. These investigations were performed analogously to the measurements in chapter 3.2.2 and 3.2.3. For the DBC calculation the literature[108] value for acrylates $\Delta H0,p$ of 73.90 J/g was used. All experiments were carried out with different initiator concentrations to observe the related influence on the initiation activity.

The investigated resins included 5 mol% of the reference substance Irgacure 2959 and an equimolar amount of the synthesized photoinitiators **5a** and **5b**. Additionally resins with lower concentrations than 5 mol% were investigated which are summarized in Table 12 and Table 13. Although it was reported by C. Dietlin et al.[129] that a multifunctional PI cannot be treated as separated initiator units, their contents in the resins were reduced to investigate the effect on the photochemical performance.

The difunctional photoinitiator reached the maximum heat of polymerization approximately 0.8 s slower than the reference substance whereas the DBC with a concentration of 2.5 mol% was performed equally. For the formulation which included 5 mol% of **5a**, a noticeable decrease of the conversion could be observed. This effect might be explained by the observable increase of the viscosity, from 2.8 mPas to 5.5 mPas for the resin containing 5 mol% **5a** (see Table 12).[56]

Table 12: Photoreactivity of the synthesized photoinitiator 5a in a THFA resin

Substance	t_{max} [s]	Peak$_{max}$ [mW/mg]	Hp [J/g]	H$_0$p [J/g]	DBC [%]
5 mol% Irgacure 2959	4.68	38.55	353	473.17	75
2.5 mol% Difunc.-PI (5a)	5.46	32.25	354	473.17	75
5 mol% Difunc. PI (5a)	5.46	26.20	331	473.17	70

The same phenomenon became apparent for the glucose based photoinitiator (Table 13). The DBC decreased inverse proportional to the initiator concentration, whereas the resin with 1 mol% of the novel photoinitiator exhibited excellent reactivity. The t_{max} was just 0.3 s higher than for the reference substance and the observed DBC even outperformed the

Irgacure 2959. The considerable increase of the viscosity of the resin was observable for all formulations which included the glucose based photoinitiator. In the case of the formulation with 2.5 mol% glucose-PI an increase of the resin viscosity by 130% (2.8 mPas - (pure THFA) to 6.4 mPas (THFA + 2.5 mol% PI) could be determined. Compared to the liquid resin with 1 mol% photoinitiator, a reduced mobility of the reactive radicals in the tough mixture with 5 mol% of **5b** was expectable.[56]

Table 13: Photoreactivity of the synthesized photoinitiator 5b in a THFA resin

Substance	t_{max} [s]	Peak$_{max}$ [mW/mg]	Hp [J/g]	H$_0$p [J/g]	DBC [%]
5 mol% Irgacure 2959	4.68	38.55	353	473.17	75
1 mol% Glucose-PI (5b)	4.92	37.28	362	473.17	77
3 mol% Glucose-PI (5b)	4.92	33.18	317	473.17	67
5 mol% Glucose-PI (5b)	4.86	29.02	289	473.17	61

To sum it up, it can be said that the novel photoinitiators exhibit the highest activities with the lowest tested concentrations. In particular, the glucose based photoinitiator outperformed the reference substance in terms of DBC, which is remarkable, taking into account that a low migration behavior of this substance is obvious due to its high molecular weight.

In all experiments the photoinitiator concentration was stated in mol% although for industrial applications the effective mass or w% are relevant. In the case of the glucose based initiator and the Irgacure 2959 the mass ratio of 1 mol% **5b** to 5 mol% reference substance (Irgacure 2959) is 1:0.82. This means that low migration behavior as well as satisfying curing performance can be obtained with a slightly increased addition of the novel photoinitiator.

In Table 14 and Figure 39 the results of the best performing resin formulations are summarized which illustrates the outstanding reactivity of substance **5b**. The synthesis of a novel photoinitiator, based on the concept of carbohydrate based photoreactive species, which features additionally a decent water solubility, might be an interesting topic for further research activities.

Table 14: Comparison of the photochemical performance of the photoinitiators 5a and 5b

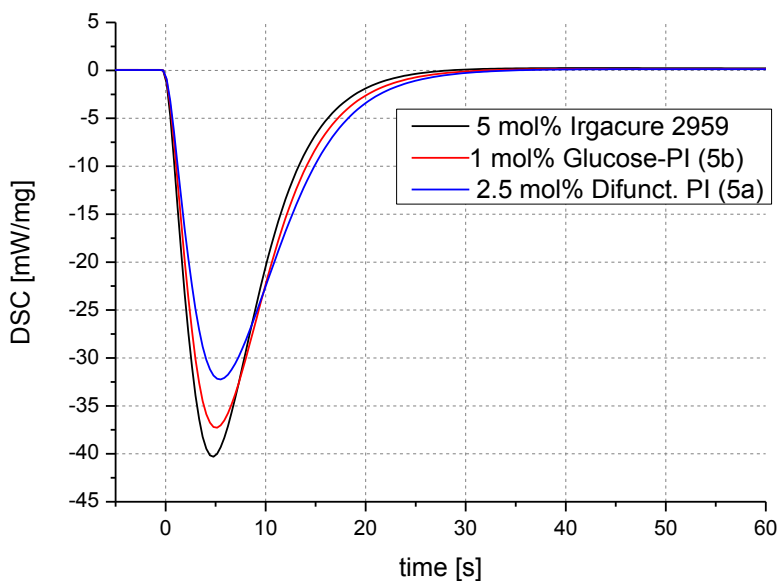|	t_{max} [s]	Peak$_{max}$ [mW/mg]	Hp [J/g]	H$_0$p [J/g]	DBC [%]
5 mol% Irgacure 2959	4.68	38.55	353	473.17	75
1 mol% Glucose-PI (5b)	4.92	37.28	362	473.17	77
2.5 mol% Difunc. PI (5a)	5.46	32.25	354	473.17	75

Figure 39: Comparison of the photoreactivity of the synthesized photoinitiators 5a and 5b

4.2.1.4 Characterization of carbohydrate based photoinitiators by UV-Vis spectroscopy

The synthesized photoinitiators were characterized by UV-Vis spectroscopy to determine their absorption maxima (λ_{max}) (see 6.3).

The π-π* transition band occurs at 275 nm for the substance **5a** and the Irgacure 2959 whereas it is slightly red-shifted for the difunctional photoinitiator **5a** (~3 nm). The extinction coefficient of the absorption maximum (ε_{max}) of the multifunctional photoinitiator is significantly increased compared to the other photoinitiators. It is approximately 13-times higher than the Irgacure 2959, respectively 10-times higher than the difunctional species. These observations are in accordance with the results of Dietlin et al.[129] who proposed that multifunctional initiators cannot be seen as separated initiator units. Otherwise the expected ε_{max} of substance **5b** should be proportional to the amount of photoreactive moieties, which is in accordance with the present results. The observed bathochromic shift of the difunctional photoinitiator might be explained by interactions of the two chromophores which are coupled to the carbohydrate backbone. For the glucose based initiator these effects are more unlikely due the increased spatial extension of the molecule.
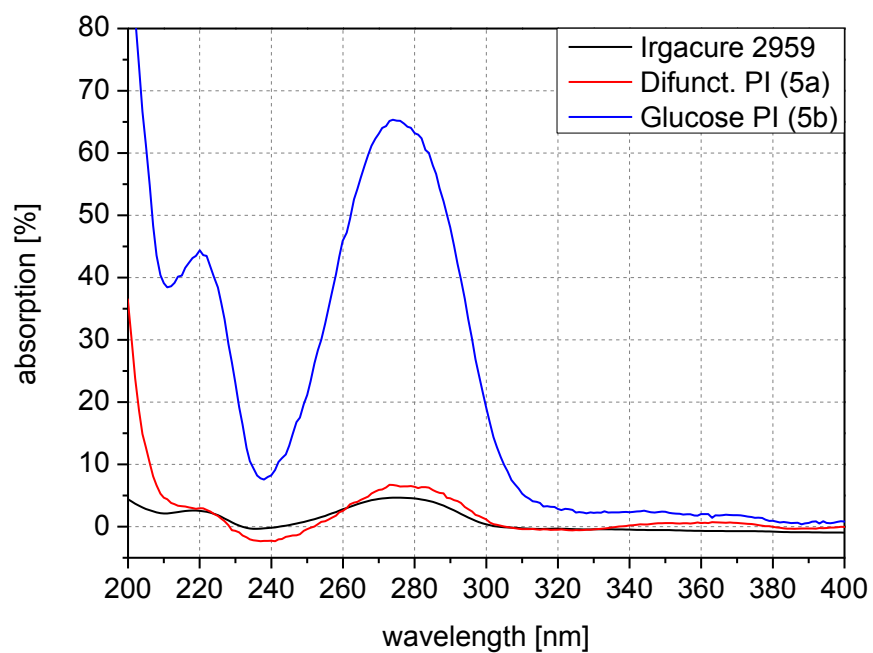
Figure 40: UV-Vis spectra of carbohydrate based photoinitiators 5a and 5b compared with Irgacure 2959 (0.01 M)

4.2.1.5 Migration studies of carbohydrate based photoinitiators

Analogously to the migration studies in chapter 3.2.6, the carbohydrate based photoinitiators were characterized regarding their migration behavior. In this context, the focus was set on the difunctional photoinitiator **5a** and the Irgacure 2959 which was utilized as a reference substance. The migration of the glucose based species was not investigated due to the high molecular weight of 1361.49 g/mol which indicates that no migration is expectable (see Figure 41).[52]
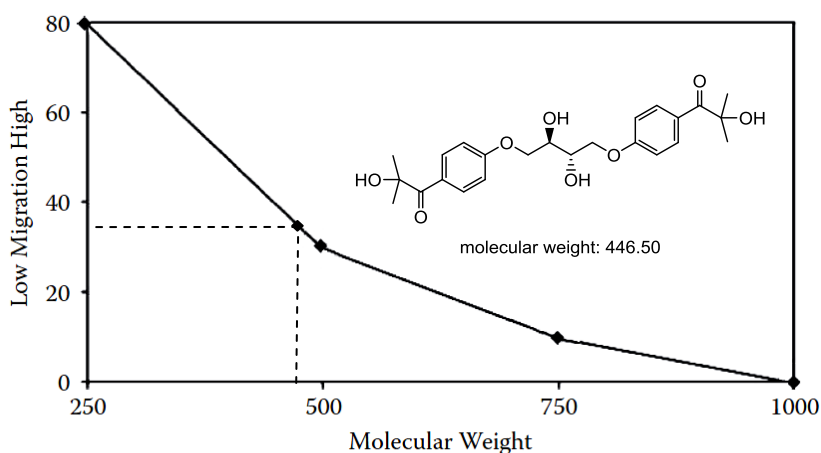

Figure 41: Migration behavior in dependency of the molecular weight [52]

Even in the case of a complete photochemical fragmentation (α-cleavage of all photoreactive moieties) and subsequent hydrogen abstraction, the molecular weight of the remaining compound will be above the limit of 1000 g/mol (see Figure 42).
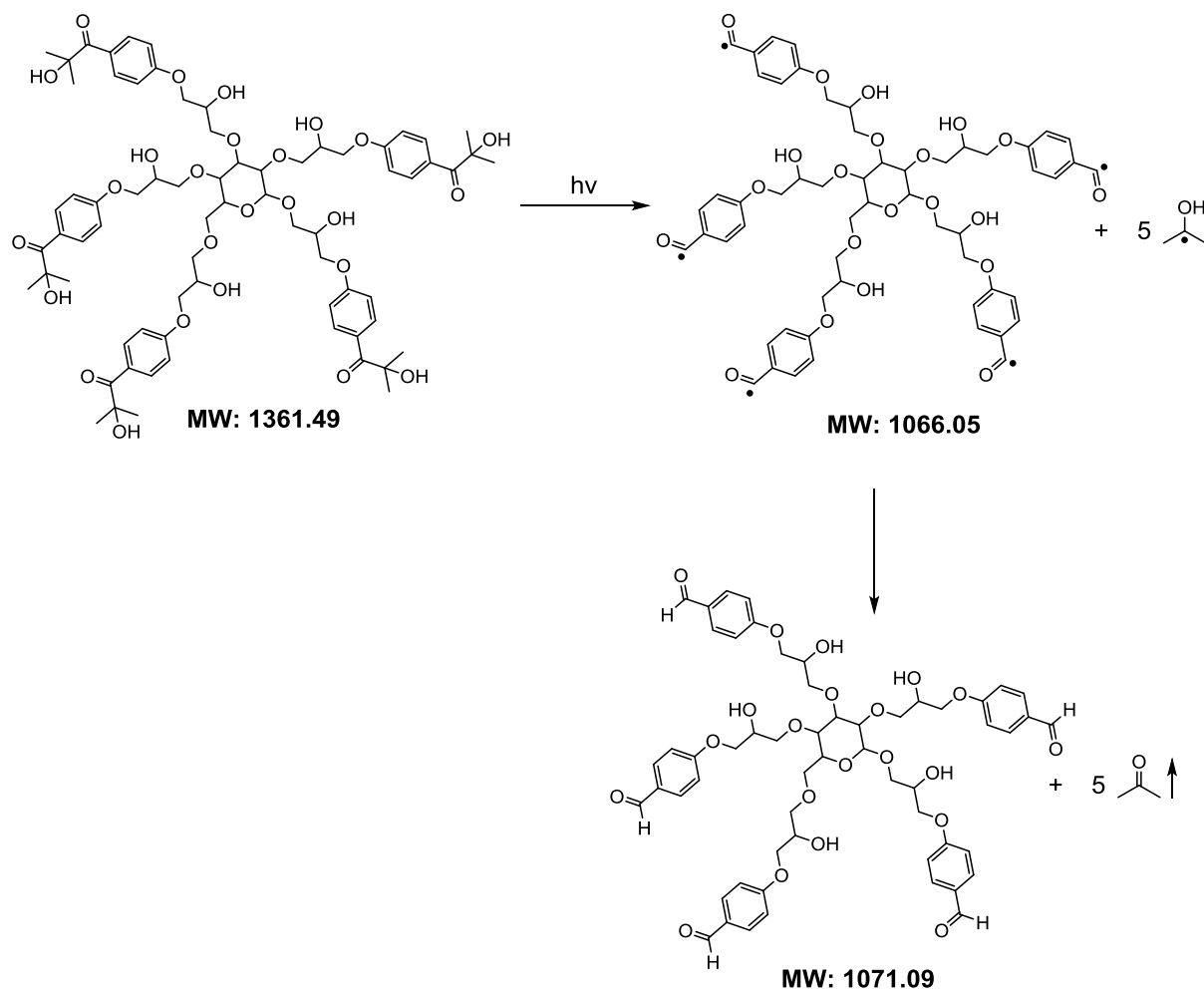
Figure 42: Maximal possible fragmentation of the glucose based photoinitiator (5b)

The sample preparation and the extraction procedure were described comprehensively in chapter 3.2.6. Accordingly, the difunctional acrylate monomer dipropylene glycol diacrylate (DPGAC) was applied to obtain sufficient photoinitiator solubility and adequate crosslinked polymer samples. Based on the results of the photochemical characterization (chapter 4.2.1.3), an initiator content of 5 mol% Irgacure 2959 and 2.5 mol% **5a**, respectively, were applied. Different amounts of photoinitiator were chosen, due to the fact that similar DBCs could be observed for these compositions in chapter 4.2.1.3.

The ethanolic extracts of the polymer samples were characterized by high performance liquid chromatography (HPLC) measurements. The details of the applied method are summarized in Table 35, chapter 6.9.

For the quantification of the investigated photoinitiators two different calibrations were performed. The corresponding detection limits and the coefficients of determination are provided in Table 15.

Table 15: Detection limits of the difunctional photoinitiator (5a) and Irgacure 2959 and the coefficients of determination of the calibrations

Photoinitiator	detection limit [µg/mL]	R² -calibration
Irgacure 2959	2.20	0.9949
Difunc. PI (5a)	0.80	0.9993

In the ethanolic extracts considerable amounts of both photoinitiators could be detected, whereas the reference photoinitiator (Irgacure 2959) exceeded the concentration of substance **5a**. These results are in accordance with the literature which propose that the migration behavior is dependent on the molecular weight of the investigated molecule.[52,53] Accordingly, it could be demonstrated that the percentage of the detected Irgacure 2959, referred to the applied content, is 7.6-fold higher than **5a**.

Table 16: Results of the migration studies of the Irgacure 2959 and the difunctional photoinitiator (5a)

Photoinitiator	applied PI content [mg]	conc. [µg/mL]	± SD [µg/mL]	migration [%]
Irgacure 2959	1.40 (5 mol%)	34.03	11.72	2.42
Difunc. PI (5a)	0.74 (2.5 mol%)	2.38	1.25	0.32

Although the measured migration values of the difunctional photoinitiator **5a** are rather low, higher migration rates for pigmented, thin-film application are expectable. This delimitates the applicability for inkjet inks, suitable for food packaging materials, not least because of the mandatory certification of compounds lower than 1000 g/mol.

Nevertheless, the utilization for other industrial applications, which require high photoinitiator contents in aqueous systems are imaginable.

Furthermore feasible resin optimizations regarding monomer selection, light dose adjustment and photoinitiator content, might lead to improved migration performances.

4.2.2 Experimental

Unless otherwise stated, all reagents were purchased from Sigma–Aldrich, TCI, VWR, Acros, Bruno-Bock and Roth and were used without further purification.

4.2.2.1 Synthesis of Difunctional Photoinitiator

4.2.2.1.1 [4,4'-bi(1,3-dioxolan)]-2,2'-dion
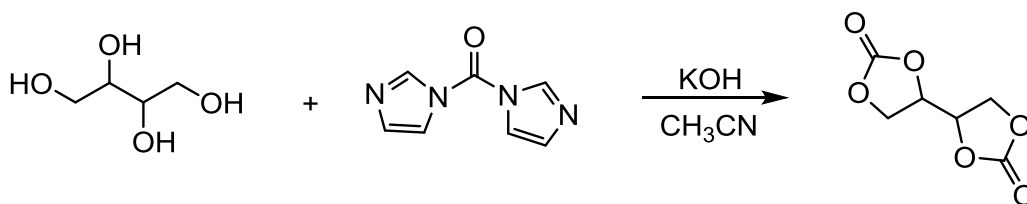
2.00 g (1 Eq., 16.38 mmol) meso-erythritol, 6.37 g (2.4 Eq, 39.31) carbonyldiimidazole (CDI) and a catalytic amount of KOH were suspended in THF and heated to 60°C. The mixture was stirred under constant temperature for 16h and the excess of solvent was removed under reduced pressure. The white residue was suspended 100 mL of water and filtered of after a stirring time of one 1h. Subsequently the precipitate was washed with water to obtain the product as white solid.

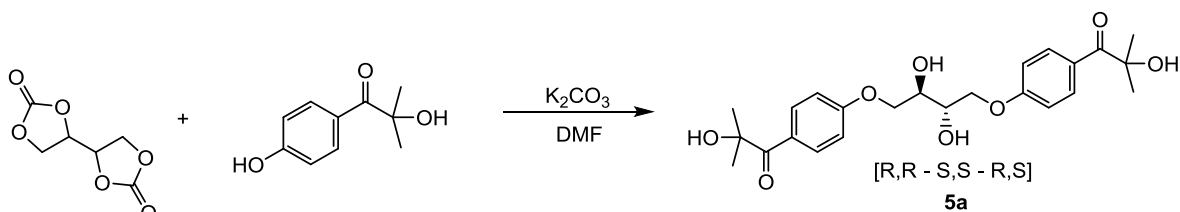**Yield:** 2.5 g (87.67%)

^{1}H-NMR: (δ, 400 MHz, 25°C, DMSO):
5.14 (m, 2H, CH); 4.61 (m, 2H, CH$_2$); 4.40 (m, 2H, CH$_2$) ppm

^{13}C-NMR: (δ, 100 MHz, 25°C, DMSO):
154.55 (2C, C=O); 76.11 (2C, CH); 65.09 (1C, CH$_2$); 63.55 (1C, CH$_2$) ppm

4.2.2.1.2 1,1'-(((2,3-dihydroxybutan-1,4-diyl)bis(oxy))bis(4,1 phenylen))bis(2-hydroxy-2-methylpropan-1-on) (5a)

0.4 g (1 Eq., 2.3 mmol) [4,4'-bi(1,3-dioxolan)]-2,2'-dion, 1.03 g (2.5 Eq., 2.74 mmol) 2-hydroxy-1-(4-hydroxyphenyl)-2-methylpropan-1-one, 0.79 g K_2CO_3 (2.5 Eq., 5.74 mmol) were dissolved in 40 mL DMF and stirred for 16h at 110°C. The solvent was removed under reduced pressure and the residue was dissolved in water which was extracted with ethyl acetate until the product couldn't be found anymore on the TLC ($CHCl_3$/MeOH 5:1) of the water phase. The combined organic layers were dried over Na_2SO_4 and the solvent was removed under reduced pressure. The crude product was purified by flash chromatography (silica gel, $CHCl_3$/MeOH 5:1), to obtain the title compound as a slightly yellow oil

Yield: 0.26 g (20.28%)

¹H-NMR: (δ, 400 MHz, 25°C, DMSO):
8.19 (d, 4H, AR); 6.99 (m, 4H, AR); 4.99 (d, 1H, CH_2); 4.79 (d, 1H, CH_2); 4.72 (d, 1H, CH_2); 4.58 (d, 1H, CH_2); 4.40 (t, 1H, CH); 4.40 (t, 1H, CH); 4.19 – 3.3 (m, 4H, OH); 1.38 (s, 12H, CH_3) ppm
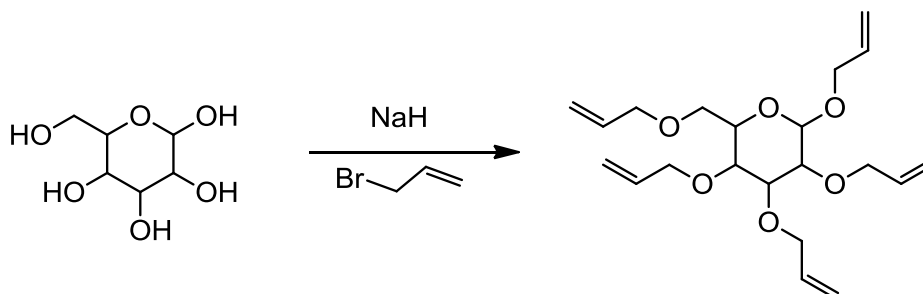
¹³C-APT-NMR (δ, 100 MHz, D_2O, 25 °C):
206.37 (2C, C=O); 162.28 (2C, AR-O); 132.28 (8C, CH_{Ar}); 127.30 (2C, Ar) 114.17 (8C, CH_{Ar}); 77.52 (2C, O=C-C); 76.09 (1C, CH); 72.71 (1C, CH_2); 71.60 (2C, CH); 69.54 (2C, CH); 69.10 (1C, CH_2); 62.57 (1C, CH_2) ppm

ESI MS - positive:
MS calc. $C_{71}H_{92}O_{26}$: [2M+Na]: 916.84; found: 917.13

4.2.2.2 Synthesis of Glucose based Photoinitiator

4.2.2.2.1 2,3,4,5-Tetrakis(allyloxy)-6-((allyloxy)methyl)tetrahydro-2H-pyran

1.49 g (8 Eq., 44.4 mmol) NaH was washed with THF and suspended in DMF. Next 1 g (1 Eq., 5.5 mmol) glucose was added at 0°C and stirred for 45 minutes at room temperature. The mixture was cooled to -20°C and 1.39 g (8 Eq., 44.4 mmol) allyl bromide was added. The reaction was stirred for 15h at room temperature and it was quenched by the addition of 20 mL H_2O. Subsequently the solvents were evaporated under reduced pressure and the product was dissolved in CH_2Cl_2 and extracted with H_2O. The crude product was purified by flash chromatography (silica gel, cyclohexane/ ethyl acetate 2:1), to obtain the title compound as a slightly yellow oil.

Yield: 1.8 g (85.2%)

^{1}H-NMR: (δ, 400 MHz, 25°C, CDCl$_3$):
5.91 (5H, CH_2=CH); 5.28 (10H, CH_2=CH); 4.31 (12H, CH+CH_2); 3.67 (3H, CH); 3.33 (2H, CH); 3.21 (1H, CH) ppm

^{13}C-NMR (δ, 100 MHz, CDCl$_3$, 25 °C):
134.81 (5C, C=C); 116.90 (5C, C=C); 102.48 (1C, CH); 84.17 (1C, CH); 81.62 (1C, CH); 79.39 (1C, CH); 77.53 (1C, CH); 74.39 (1C, CH_2); 73.77 (1C, CH_2); 73.61 (1C, CH_2); 72.43 (1C, CH_2); 70.10 (1C, CH_2); 68.95 (1C, CH_2) ppm

4.2.2.2.2 2,3,4,5-Tetrakis(oxiran-2-ylmethoxy)-6-((oxiran-2-ylmethoxy)methyl) tetrahydro-2H-pyran
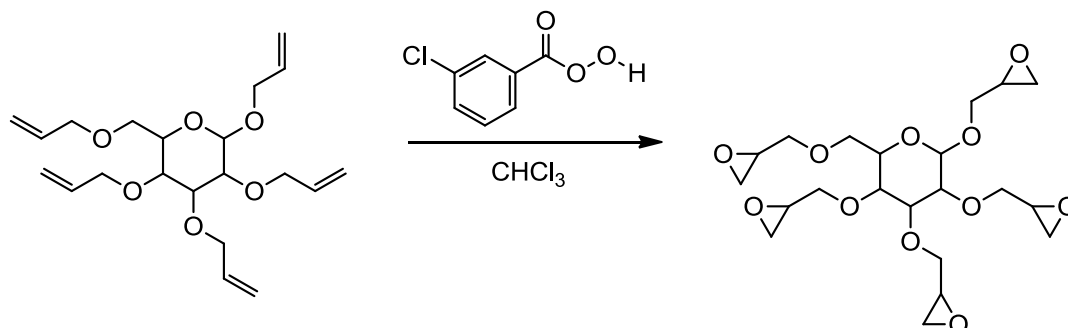
1 g (1 Eq., 2.63 mmol) 2,3,4,5-tetrakis(allyloxy)-6-((allyloxy)methyl)tetrahydro-2H-pyrane and 2.27 (5 Eq., 1.31 mmol) *meta*-chloroperoxybenzoic acid (mCPBA) were dissolved in chloroform and stirred at 60°C for 16h. After the reaction time an additional portion of 1.18 g (2.6 Eq., 6.83 mmol) mCPBA was added and the mixture was stirred for 2h. Next the white precipitate was filtered off and the organic layer was extracted with saturated $NaHCO_3$ and NaCl solution. The solvent was evaporated under reduced pressure and the crude product was purified by flash chromatography (silica gel, cyclohexane / ethyl acetate 1:1), to obtain the title compound as a colorless viscous liquid.
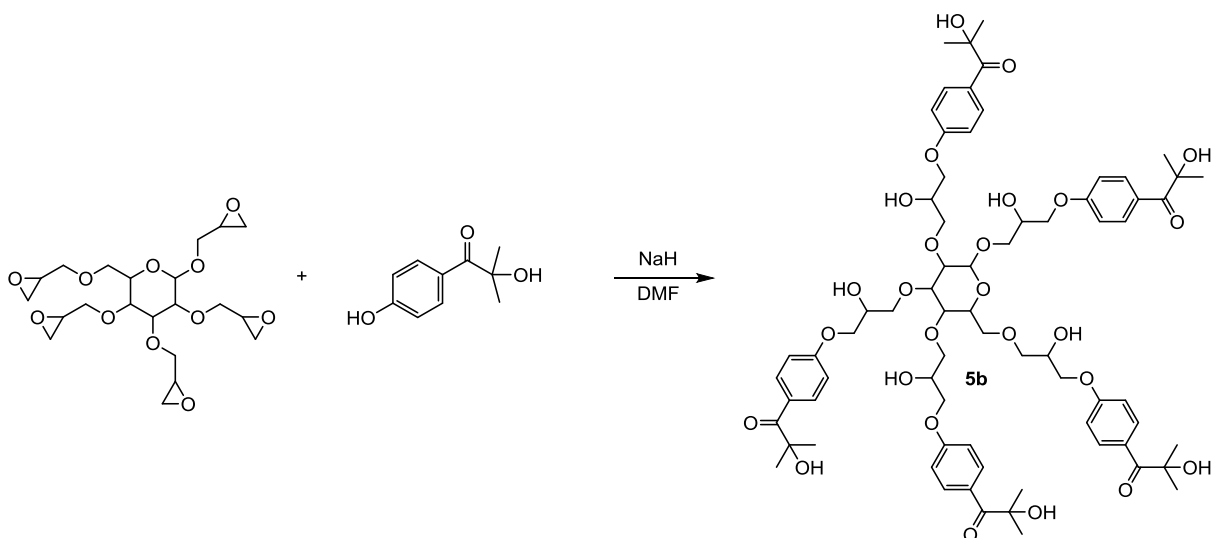
Yield: 1.6 g (80%)

^{1}H-NMR: (δ, 400 MHz, 25°C, CDCl$_3$):
4.28 - 4.23 (m, 1H, CH); 4.06 – 3.11 (m, 21H, CH); 2.72 (m, 5H); 2.53 (m, 5H) ppm

^{13}C-NMR (δ, 100 MHz, CDCl$_3$, 25 °C):
103.20 (1C, O-CH-O); 84.85 (1C, CH); 84.70 (1C, CH); 74.54 (1C, CH); 71.93 (1C, CH); 72.43 (4C, CH$_2$); 70.10 (1C, CH$_2$); 50.79 (5C, CH, epoxide); 44.40 (5C, CH$_2$, epoxide) ppm

4.2.2.2.3 Hydroxy ketone modified glucose derivative (5b)

0.14 g (5.1 Eq., 5.63 mmol) NaH were washed with THF and suspended in DMF. The reaction was cooled to 0°C and 0.97 g (5.1 Eq., 5.63 mmol) 2-hydroxy-1-(4-hydroxyphenyl)-2-methylpropan-1-one were added. After a reaction time of 45 min at room temperature, the mixture was cooled again to -20°C and 0.42 g (1 Eq., 1.10 mmol) glucose epoxide were added drop wise. After a reaction time of 15h the reaction was quenched by addition of 20 mL water. Subsequently the solvents were evaporated under reduced pressure and the product was dissolved in CH_2Cl_2 and extracted with H_2O. The crude product was purified by flash chromatography (silica gel, $CHCl_3$/MeOH 5:1), to obtain the title as white crystals.

Yield: 1.1 g (73.19%)

^{1}H-NMR: (δ, 400 MHz, 25°C, CDCl$_3$):
7.9 (10H, AR); 6.8 (10H, AR); 4.22 - 3.08 (m, 41H); 1.53 (30H, -CH$_3$) ppm

^{13}C-NMR (δ, 100 MHz, CDCl$_3$, 25 °C):
202.58 (5C, C=O); 163.58 (5C, AR); 132.35 (10C, AR); 126.68 (5C, AR); 114.52 (10C, AR); 103.20 (1C, O-CH-O); 84.85 (1C, CH); 84.70 (1C, CH); 75.87 (5C, C); 74.54 (1C, CH); 72.93 (4C, CH); 72.43 (4C, CH$_2$); 71.93 (1C, CH); 70.10 (5C, CH$_2$); 69.5 (5C, C-OH); 68.2 (1C, CH$_2$); 28.58 (10C, CH$_3$) ppm

ESI MS negative:
MS calc. $C_{71}H_{92}O_{26}$: [M+Cl]:1395.43; found: 1395.34

4.3 *Polymeric Photoinitiators*

Attributed to the water insolubility of the glucose based photoinitiator, the subsequent investigations focused on polymeric photoinitiators, to realize photoreactive species with a molecular weight higher than 1000 g/mol.

In consideration of the elucidated drawbacks of these materials (see chapter 3.1), it was aspired to develop novel water soluble and, in particular, low migration PIs for polyurethane dispersion based resins.

In the literature a huge amount of different polymeric systems are reported[140], whereas the number of publications, which deal with water soluble materials, is rather low.[141,142] Nevertheless, all of these papers have in common that they emphasize the migration properties[141–143] of the polymeric initiator species and they offer several strategies to adjust the solubility and reactivity of the macromolecular photoinitiators.[144]

Ensuing from these studies promising monomer candidates were chosen to realize the synthesis of water soluble photoreactive copolymers. As a photoinitiating monomer a water insoluble, acrylate modified Irgacure 2959 (**PI**) was utilized, which was polymerized with a hydrophilic co-monomer. For that purpose sodium-4-vinylbenzensulfonat (**mono1**) and acrylic acid (**mono2**) were selected to obtain polymers suitable for aqueous formulations (see Figure 43). At this point, especially the photoinitiator loading had to be taken into consideration, which is essential for an acceptable reactivity.[52] The initiator loading implicates the mass ratio of the photoreactive moieties to the overall molecule and is proportional to the initiator performance.[52] Thus, it was the aim to copolymerize the insoluble photoinitiator monomer **PI** with **mono1** and **mono2**, to form a water soluble backbone of the polymer, despite a maximal content of photoinitiator. Consequently, co-monomers with a low molecular weight were favored to enable higher initiator loadings, provided that an appropriate solubility could be obtained.
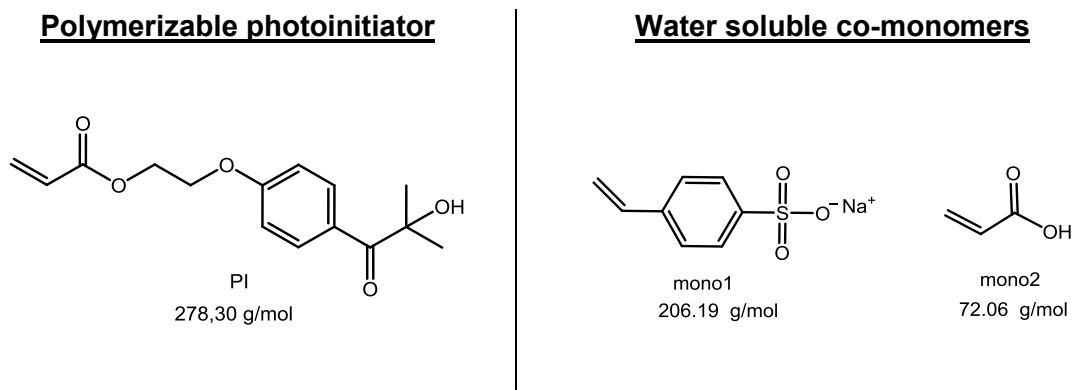

| **Polymerizable photoinitiator** | **Water soluble co-monomers** |

PI
278,30 g/mol

mono1
206.19 g/mol

mono2
72.06 g/mol

Figure 43: Applied monomers for the synthesis of polymeric photoinitiators

Beside the challenge to find the ideal monomer ratio it was essential to determine the appropriate content of thermal Initiator (AIBN) for the polymerization. It is well known, that the average molecular weight (M_n) of a polymer is the crucial parameter for the solubility of a macromolecule. [144] It is proportional to the square root of the applied amount of thermal initiator azobisisobutyronitrile (AIBN)[145] and the monomer concentration in the reactive mixture. Unfortunately, it is not possible to generalize the reaction conditions for radical polymerizations, especially for the case of alternating co-monomers.[146] Therefore several AIBN concentrations as well as monomer ratios were, in consideration of the water solubility of the polymers, investigated in the present study.

4.3.1 Results and Discussion

4.3.1.1 System 1 - Poly(PI-co-mono1)*stat.*

4.3.1.1.1 Synthesis and characterization of Poly(PI-co-mono1)*stat.*

The photoreactive monomer was synthesized in a one step reaction. The commercially available Irgacure 2959 was esterified with acryloyl chloride under alkaline conditions, to obtain the modified photoinitiator. After the purification by column chromatography, the pure monomer could be isolated in appropriate yields of 73%. (see Figure 44)

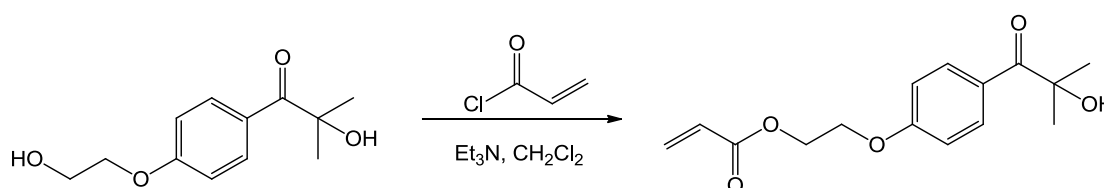**Figure 44: Synthesis of the photoreactive Monomer (PI - Monomer)**

The radical polymerizations were performed in anhydrous methanol, with AIBN as thermal initiator and a monomer concentration of 4 M. All reactions were carried out at 60°C, for a period of 24 h before the polymerization was stopped and precipitated in cold diethyl ether. (see Figure 45)
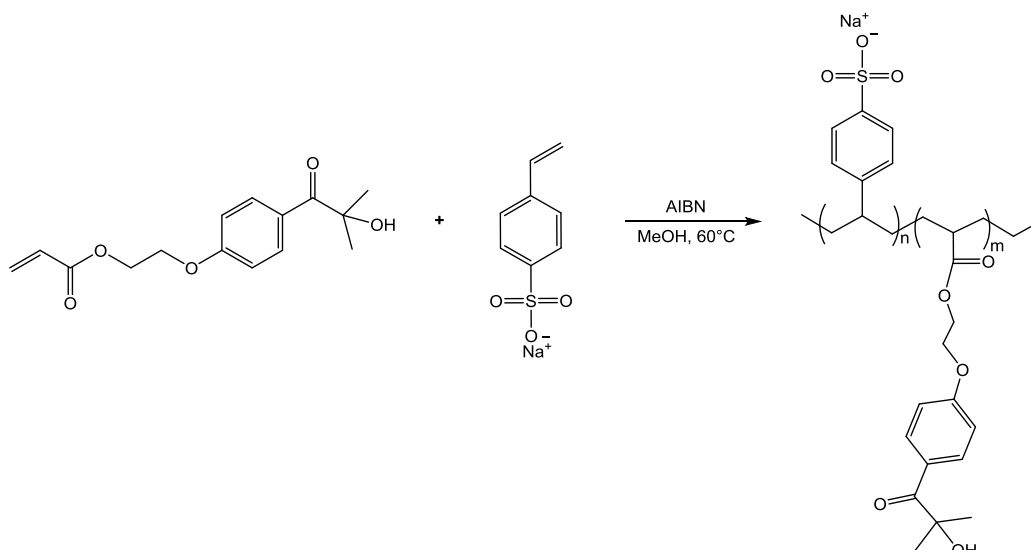

Figure 45: Synthesis of water soluble polymers

To ascertain the maximal photoinitiator loading, in consideration of an acceptable water solubility, five polymers with different monomer ratios and a constant amount of thermal initiator (7.5 mol% AIBN) were synthesized.

Table 17: Polymers with different monomer ratios to evaluate the water solubility referring to the maximal initiator loading (green: soluble, red: insoluble)

Polymer	sodium-4-vinylbenzensulfonate	PI-monomer	Mn [g/mol]	PDI	theo. PI-loading [w%]
Poly1A	30	70	/	/	75.90
Poly1B	40	60	/	/	66.93
Poly1C	50	50	71200	1.26	57.44
Poly1D	60	40	79300	1.34	47.36
Poly1E	70	30	76000	1.35	36.50

It turned out that the polymers are water soluble until a photoinitiator concentration of 57.44 w%, which is proportional to 50 mol% of photoreactive groups (see Table 17). Furthermore, the average molecular weight (M_n) of the three water soluble photoinitiators and the corresponding polydispersity indices (PDI) were determined by gel permeation chromatography (GPC). These measurements were carried out at the Polymer Standard Service GmbH in Mainz.

Surprisingly, the M_n increased with higher ratios of mono1, although the molecular weight of the sulfonate was approximately 70 g/mol lower. Obviously, an elevated degree of polymerization can be obtained with a reduced amount of the photoreactive monomer, which subsequently leads to higher M_n. Nevertheless, all polymers which were synthesized with 7.5 mol% AIBN, exhibit significantly too high molecular weights in consideration of the defined limit of 1000 g/mol. Therefore, additional experiments were performed to adjust the M_n toward lower values, which was essential to optimize the expected water solubility (see 4.3.1.1.2), as well as the photochemical performance. It is well documented in the literature that photochemical activity of a macromolecular initiator is inverse proportional to the molecular weight of the polymer which is obviously a result of the enhanced mobility of the smaller polymer fragments.[52,53]

To confirm that the practical polymer composition is in accordance with the theoretical monomer ratio, the synthesized macromolecular photoinitiators (Poly1C, 1D, 1E) were characterized by elementary analysis. Therefore, the focus was set on the elements carbon, hydrogen, nitrogen and sulfur to determine the specific concentration of these elements and to calculate the correlated ratio of the incorporated monomers. These analysis were carried out at the University of Vienna by Mag. Theiner.

Table 18: Elementary analysis of Poly(PI-co-mono1)$_{stat.}$ with different monomer ratios

Sample		C%	H%	N%	S%	observed Sulfonate [w%]	observed Initiator [w%]	theoretical Sulfonate [w%]	theoretical Initiator [w%]
Poly1C	**1.**	52.28	4.99	0.43	6.91	44.44	55.56		
50/50	**2.**	52.37	5.29	0.42	6.22	40.00	60.00		
7.5% AIBN	**3.**	52.20	5.34	0.43	6.89	44.31	55.69	**43**	**57**
	averaged monomer ratio					**42.92**	**57.08**		
Poly1D	**1.**	50.47	4.95	0.43	8.11	52.16	47.84		
60/40	**2.**	50.41	4.82	0.52	7.90	50.81	49.19		
7.5% AIBN	**3.**	50.73	4.98	0.48	8.16	52.48	47.52	**53**	**47**
	averaged monomer ratio					**51.82**	**48.18**		
Poly1E	**1.**	47.48	4.50	0.34	9.30	59.81	40.19		
70/30	**2.**	47.35	4.76	0.41	9.69	62.32	37.68		
7.5% AIBN	**3.**	48.17	4.85	0.40	9.77	62.83	37.17	**63**	**37**
	averaged monomer ratio					**61.66**	**38.34**		

According to the results in Table 18, the measured monomer ratios are in good accordance with the theoretical calculation. In other words the composition of the statistical polymer was analogous to the applied monomer ratios.

To characterize the copolymerization behavior of the PI and mono1, it was the aim to determine the copolymerization parameters which are the ratio of the homo- and copolymerization rate. Presupposition for the validity of this method is the irreversibility of the polymeric chain growth as well as a low degree of polymerization (<5%).[147–149] The latter one is essential to guarantee a constant monomer concentration ratio in the reactive mixture which is decisive for the copolymerization behavior of the applied monomers. Unfortunately, it turned out that Poly(PI-co-mono1)$_{stat.}$ exhibit poor precipitation properties at low monomer conversion which hampered a representative determination of the copolymerization parameters. Alternatively the polymerization was characterized by ^{1}H-NMR measurements.

The reaction was carried out, according to the description in the experimental part of the work in chapter 4.3.3, whereas the characteristic ^{1}H-NMR signals of the reactive double bonds were integrated after defined time intervals. Thus, it was possible to observe the progress of the polymerization and the correlating conversion of the monomers (50/50). For the integration, the hydrogen signal at 6.0 ppm of the acrylate (PI) and the hydrogen

signal at 5.3 ppm for the vinyl functionality (mono1) were chosen and compared over the whole time period (see Figure 46).
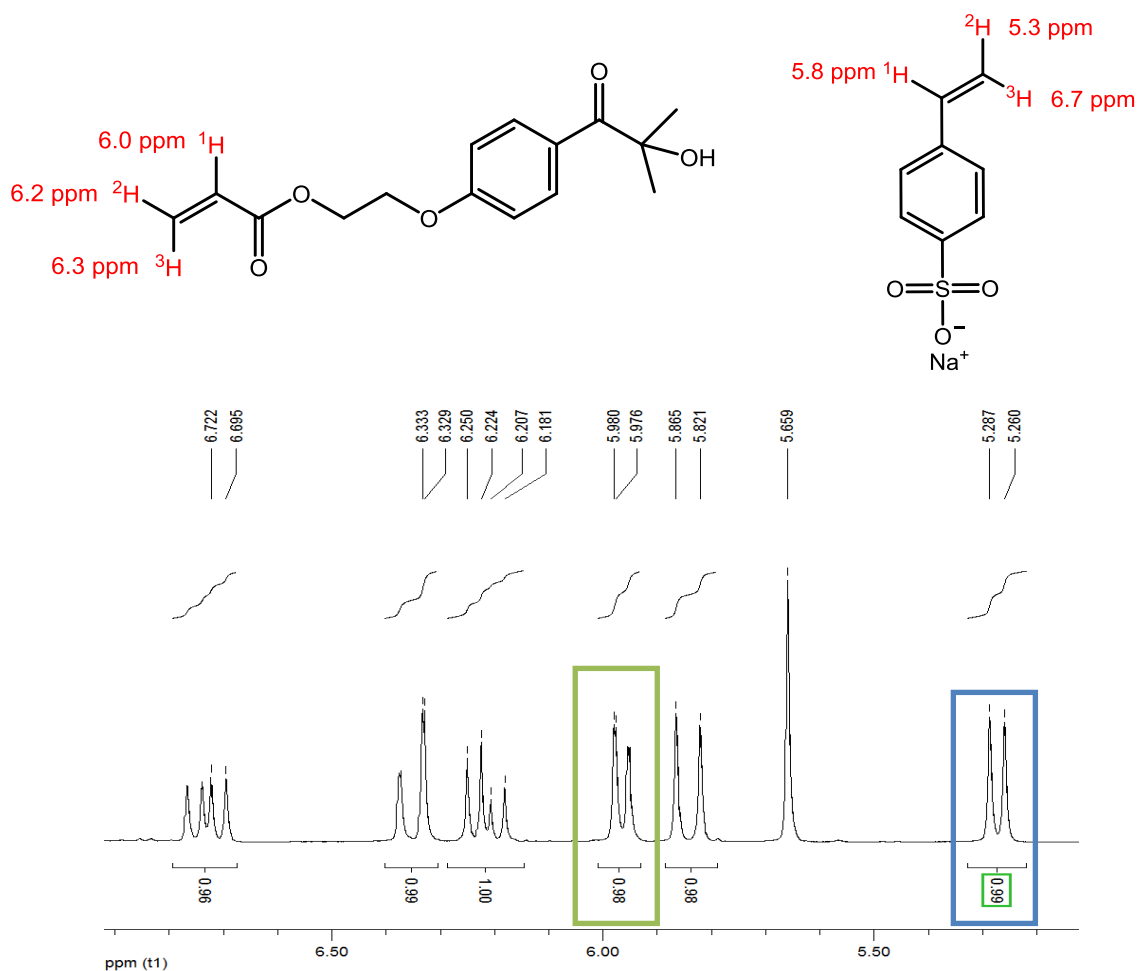

Figure 46: ^{1}H-NMR spectrum of the monomer mixture and the related signals of the reactive functionalities of the applied monomers

According to the integral ratios in Table 19 the monomer ratio stays constant over the whole observed period. Thus, it can be stated that the functional groups of the monomers exhibit similar reactivities which favors the formation of a statistical polymer with a monomer ratio which is in accordance with the composition of the feed. This assumption could be confirmed by the elementary analysis. For that reason it was desisted to perform an exact quantification of the monomer conversion as it was performed for system 2 (see chapter 4.3.1.2.1).In consideration of these findings, we were able to design tailor-made photoinitiators with defined monomer ratios for water based resins.

Table 19: Monomer ratios during the polymerization for 120 minutes

time [min]	ratio integrals of NMR Signals Vinyl benzene sulfonate (5.2 ppm) : PI-Acrylate (5.9 ppm)
0	1 : 1.00
5	1 : 0.98
10	1 : 1.02
15	1 : 1.02
30	1 : 0.99
45	1 : 0.95
60	1 : 1.04
90	1 : 1.03
120	1 : 1.00

4.3.1.1.2 Adjustment of the molecular weight and determination of the water solubility of Poly(PI-co-mono1)$_{stat.}$

As it was already described in chapter 4.3.1.1.1 further experiments for the adjustment of the M_n were performed. Consequently, the focus was set on the composition with the highest ratio of photoreactive moieties (50 mol% PI-Monomer / 50 mol% monomer 1) and the content of thermal Initiator (AIBN) was increased. The obtained macromolecular photoinitiators were characterized by GPC to investigate the influence of the AIBN concentration on the molecular weight.

Table 20: Results of GPC measurements of the polymers which were synthesized with different AIBN concentrations

Polymer	Initiator [w%]	Sulfonate [w%]	M_n [g/mol]	PDI
Poly1C 50/50 - 7.5%	57.1	42.9	71200	1.26
Poly1C 50/50 - 10%	57.1	42.9	71000	1.18
Poly1C 50/50 - 15%	57.1	42.9	67900	1.19

According to the results in Table 20, the M_n of the polymer decreases inverse proportional to $[I]^{1/2}$ (AIBN). Unfortunately, only a slight change in the molecular weight could be observed, although a high influence of the applied amount of the thermal initiator was expected. Furthermore, a significant decrease of the polymer yield became apparent, which hampered an additional increase of the AIBN, for a subsequent M_n reduction. It was assumed, that the lack of appropriate yields can be attributed to the precipitation process

which was the limiting factor of the synthesis. Especially, the separation of the dispersed polymer was hardly achievable despite centrifugation and precipitation at -40°C. Additional experiments to optimize this synthetic step might be essential to provide sufficient polymer purity and acceptable processability of the photoreactive materials.

The maximal water solubility of the obtained photoinitiators was evaluated for all monomer and thermal initiator (AIBN) ratios.

Figure 47: Clear aqueous solutions of the polymers 1C (50/50), 1D (40/60) and 1E (30/70)

To obtain representative results, saturated polymer solutions were prepared and the polymer residue of a defined volume was determined gravimetrically after solvent evaporation. The water solubility increases dependent to the moleculare weight and the content of the sodium 4-vinylbenzenesulfonate co-monomer. Deviations from the expected solubility are explainable by the lack of reproducibility regarding the determination of the saturation point of the polymer solution.With the gradually addition of the macromolecular material, only an appearing cloudiness was detectable, whereas no polymer sedimentation could be observed. Thus, an exact quantification was not possible, although the expected tendencies could be determined. (see Figure 48)
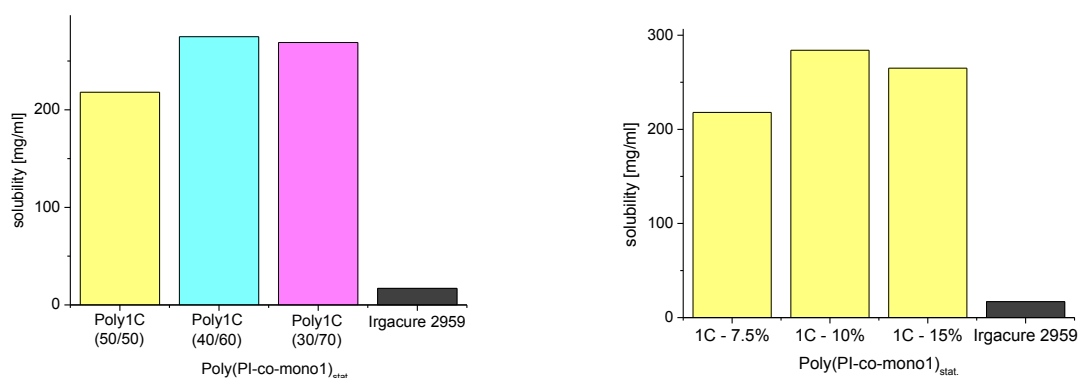

Figure 48: left: Solubility of Poly(PI-co-mono1)$_{stat.}$ with increasing content of mono1; right: Solubility of Poly1C (50/50) with increasing content of AIBN; both: Reference photoinitiator Irgacure 2959

4.3.1.1.3 Photoreactivity of Poly(PI-co-mono1)$_{stat.}$

The synthesized polymeric photoinitiators were also characterized regarding their photoreactivity. These analysis were carried out by Photo-DSC measurements (see 6.4) with a water based resin. The investigated formulations consisted of a mixture of polyurethane and polyacrylate dispersions, as well as propylene glycol and the investigated macromolecular photoinitiators (see Table 21).

Table 21: Composition of the investigated resin (viscosity=4.00 mPas)

Components	ratio [w%]
pigments	0.00
LUX 399	18.00
AC2523	12.00
water	50.00
PG	20.00

All of them included 5 w% photoinitiating units whereas the mass of the added polymer was related to the specific amount photoreactive moieties in the macromolecular material. In other words, every resin formulation included the same amount of photoreactive groups, which leaded to an enhanced addition of the photoinitiators (referring to the mass) which exhibit a lower content photoreactive residues. For a better understanding the calculation in Table 22 illustrates the applied amounts of photoinitiators for 1g of the resin.

Table 22: Calculation of the applied photoinitiator referring to the amount of photoreactive moieties for 1g of the resin formulation

Subtance	Sulfonate w%	Initiator w%	Applied mass [mg]
Irgacure 2959	/	100	50
Poly1C (50/50)	42.92	57.08	71.46
Poly1D (60/40)	51.82	48.18	75.91
Poly1E (70/30)	61.66	38.34	80.83

All synthesized polymeric photoinitiators exhibit a significant reduced t_{max}, whereas the reaction enthalpy is in the range of the reference photoinitiator Irgacure 2959 (see Figure 49). Within the polymers which were polymerized with 7.5%, 10% and 15% of AIBN, the reaction speed of the polymerization decreases proportional to the ratio of the photoreactive monomer, whereas the conversion remains unaffected on a constant value (see Table 23). Possible explanations for this effect might be the significant increase of the resin viscosity (from 4.00 mPas (without PI) to 8.9 mPas for Poly1E), which is a

consequence of the weight related addition of the photoinitiators. As described before, it was the aim to hold a constant concentration of photoinitiating units (5 w%), to enable a representative comparison of the photoinitiator performance.

Furthermore, significant tendencies referring to the amount of applied AIBN of the three different groups of photoinitiators could be identified. Photoinitiators synthesized with a higher content of thermal initiator exhibit lower t_{max} values. A correlation of the expected average molecular weight and photoinitiator mobility might be conceivable however to give a reliable explanation further experiments are necessary.

Table 23: Results of the Photo-DSC measurements for the system 1 photoinitiators

AIBN	Initiator	t_{max} [s]	ΔH [J/g]
/	Irgacure 2959	1.56	14
7.5%	Poly1C (50/50)	2.76	14
	Poly1D (60/40)	3.54	14
	Poly1E (70/30)	5.22	15
10%	Poly1C (50/50)	2.46	15
	Poly1D (60/40)	3.12	15
	Poly1E (70/30)	5.16	17
15%	Poly1C (50/50)	2.22	14
	Poly1D (60/40)	3.12	14
	Poly1E (70/30)	4.02	14
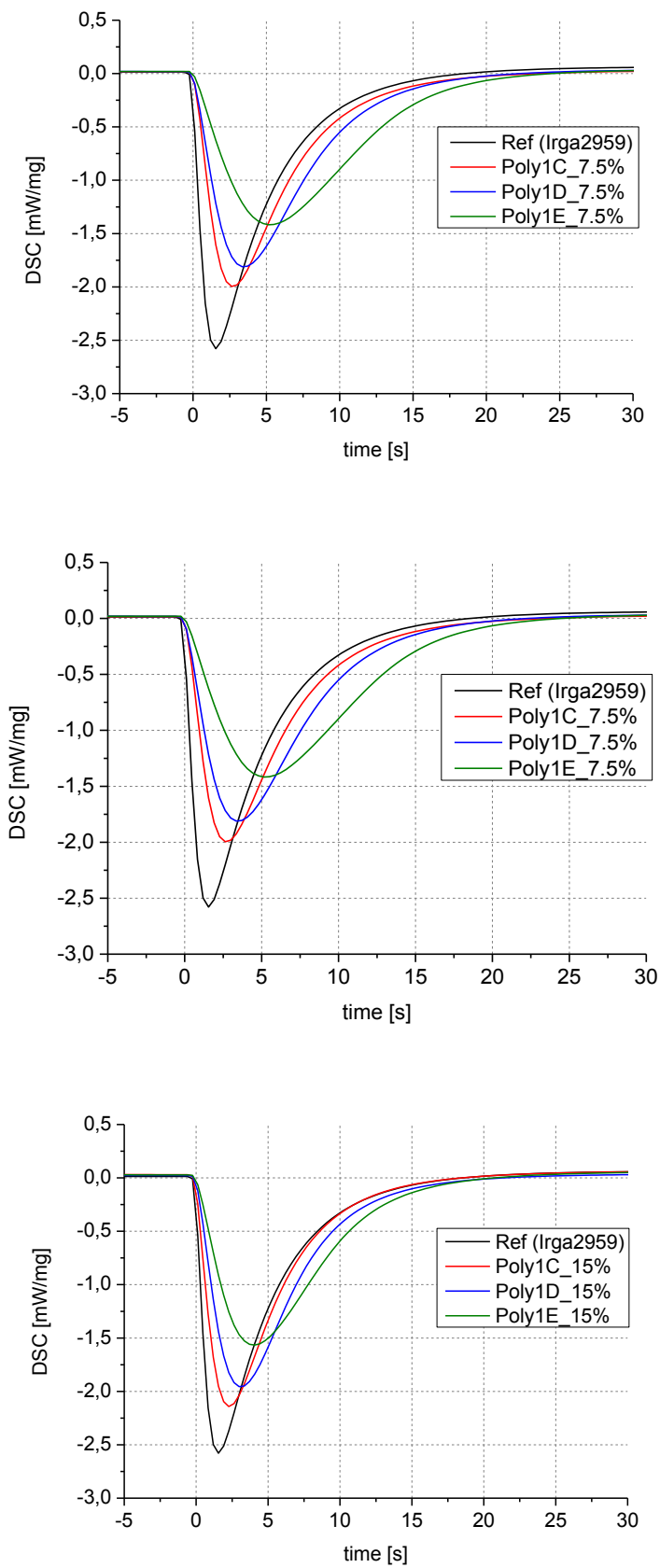
Figure 49: Results of the Photo-DSC measurements of polymer system 1

4.3.1.2 System 2 - Poly (PI-co-Mono2)_stat.

4.3.1.2.1 Synthesis and characterization of Poly(PI-co-mono2)_stat.

For the synthesis of the Poly(PI-co-mono2)_stat, the PI-monomer and acrylic acid (mono2) were copolymerized under the same conditions as Poly(PI-co-mono1)_stat.. Additionally the macromolecular photoinitiators were dissolved in 25% NH_3 solution, to convert the precursor materials into the water soluble, photoreactive anionic polyelectrolyte (see Figure 50).
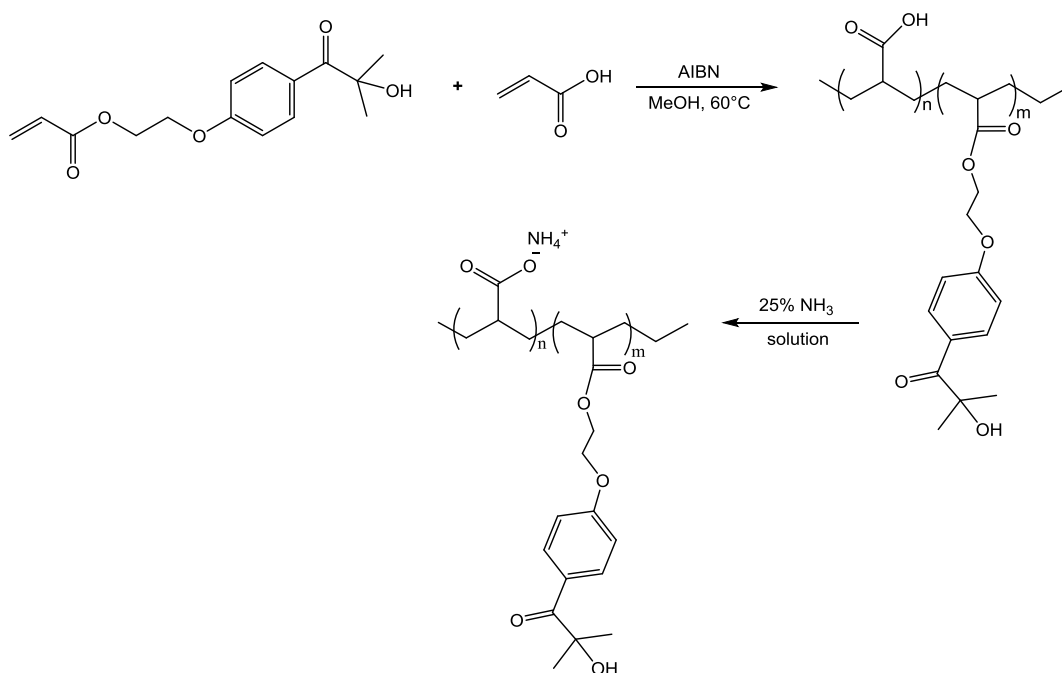
Figure 50: Synthesis of Poly (PI-co-Mono2)_stat. - system 2

First, the maximal possible initiator loading was determined to find the perfect balance between maximal concentration of photoreactive units and acceptable polymer solubility. Furthermore, the ideal content of thermal initiator (AIBN) was evaluated to obtain molecular weights higher than 1000 g/mol. Concerning the photoinitiator loading, it was found that the polymers with an initiator content higher than 50 mol% were not soluble in ammonia, which prevented the required post modification. All photoinitiators which were polymerized with 7.5% AIBN exceed the specified limit of 1000 g/mol, whereas they were in an acceptable range that high reactivities could be expected (see Table 24).

The molecular weight of the polymers was determined by GPC measurements before the carboxylic acid functionalities of precursor material were neutralized.

Table 24 Polymers with different monomer ratios to evaluate the water solubility referring to the maximal initiator loading (green: soluble, red: insoluble)

Polymer	PI - Monomer	Acrylic acid	Mn [g/mol]	PDI	theo. PI-Loading [w%]
Poly2A	10	90	1265	2.1	30.0
Poly2B	20	80	9137	2.7	49.1
Poly2C	30	70	7067	2.7	62.3
Poly2D	40	60	2828	3.6	72.0
Poly2E	50	50	3924	3.2	79.4
Poly2F	60	40	39610	4.1	85.2
Poly2G	70	30	76104	2.5	90.0

To confirm that the actual polymer composition is in accordance with the theoretical monomer ratio, the synthesized macromolecular photoinitiators (Poly2C, 2D, 2E) were characterized by elementary analysis. The focus was set on the elements carbon, hydrogen, nitrogen and sulfur to determine the specific concentration of these elements and to calculate the correlated ratio of the incorporated monomers. These analyses were carried out at the University of Vienna by Mag. Theiner.

Table 25: Elementary analysis of three different polymers (MR - monomer ratio)

Sample		C%	H%	N%	S%	observed Acrylic acid [w%]	observed Initiator [w%]	theoretical Acrylic acid [w%]	theoretical Initiator [w%]
		Elements							
Poly2E 50/50	1.	56.63	6.83	2.85	0.02	16.23	83.77		
	2.	56.88	6.84	2.88	0.02	16.4	83.60		
	3.	56.67	7.07	2.91	0.02	16.57	83.43	**21**	**79**
		averaged monomer ratio				**16.4**	**83.6**		
Poly2D 40/60	1.	56.70	6.80	3.13	0.047	17.82	82.18		
	2.	56.29	7.26	3.06	0.046	17.42	82.58		
	3.	56.35	7.07	3.12	0.054	17.77	82.23	**28**	**72**
		averaged monomer ratio				**17.67**	**82.33**		
Poly2C 30/70	1.	52.37	7.12	5.16	0.023	29.38	70.62		
	2.	52.26	7.25	5.26	0.023	29.95	70.05		
	3.	51.92	7.32	5.38	0.024	30.64	69.36	**38**	**62**
		averaged monomer ratio				**29.99**	**70.01**		

The elementary analysis (see Table 25) showed that the theoretical and practical monomer ratio of the polymer differ significantly. The amount of photoreactive units is enhanced compared to theoretical calculation, which can be a consequence of the different reactivities of the applied monomers. Compared to the results in chapter 4.3.1.1.1 the actual photoinitiator loading was approximately 5-10% higher, for all polymer compositions (Poly2E, 2D, 2C).

Due to the apparent differences of the monomer reactivities, the polymerization was characterized by the determination of the copolymerization parameters. According to the described challenges, regarding the precipitation procedure (see 4.3.1.1.1), the polymerization behavior of the applied monomers was investigated by ^{1}H-NMR studies. Therefore the polymerization was performed in CD_3OD (methanol-d_4) and the conversion of the monomers was referenced to a constant solvent peak (DMSO). The ^{1}H-NMR spectra were taken after defined time intervals to observe the progress of the polymerization.
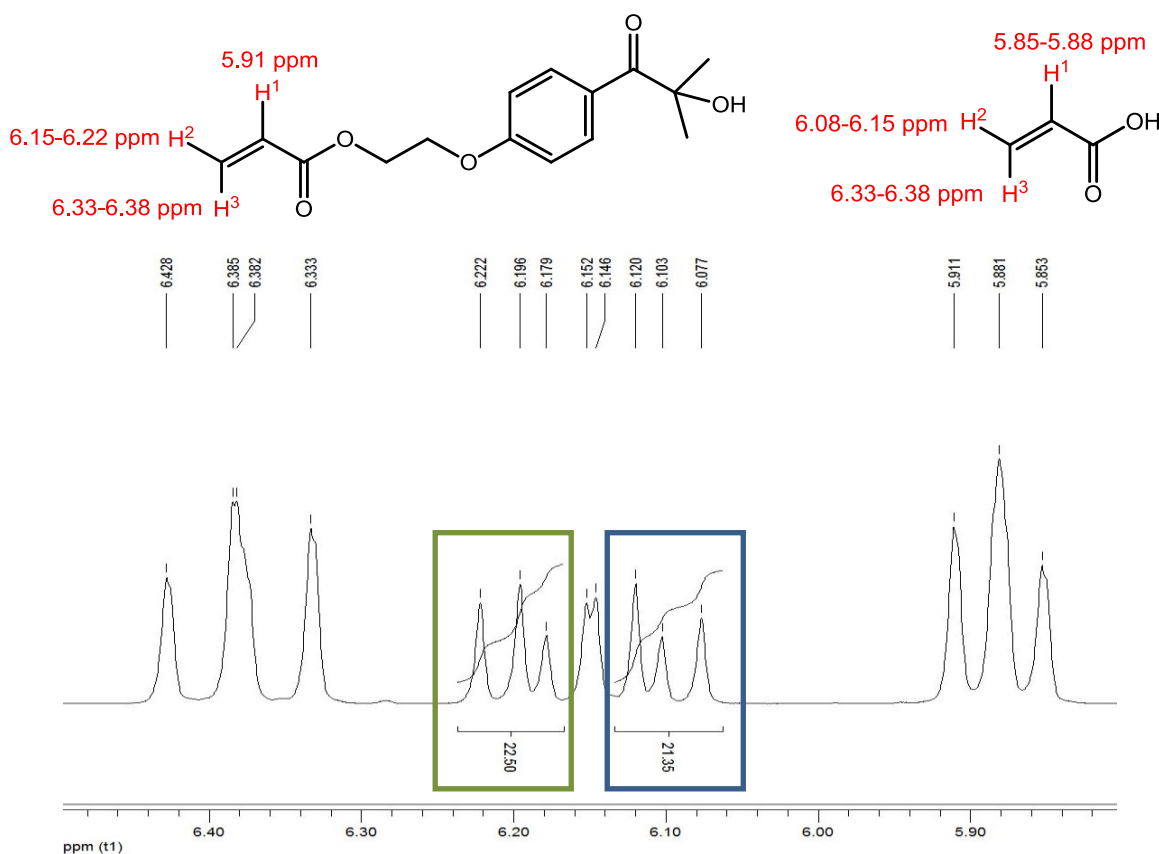
Figure 51: ^{1}H-NMR spectrum of the monomer mixture and the related signals of the reactive functionalities of the applied monomers

Fortunately, an exact quantification was feasible, because of the adequately distinguishable hydrogen signals of the acrylate functionalities of the monomers. Only for one peak of the quadruplet an overlap was detectable (see Figure 51).

The measurements showed that the concentration of the PI-monomer was reduced significantly faster than for the acrylic acid. This indicates a favored addition of the photoreactive monomer, to the polymer chain. After a polymerization time of 22 h, a monomer conversion of 66% acrylic acid and 77% PI-monomer could be observed.
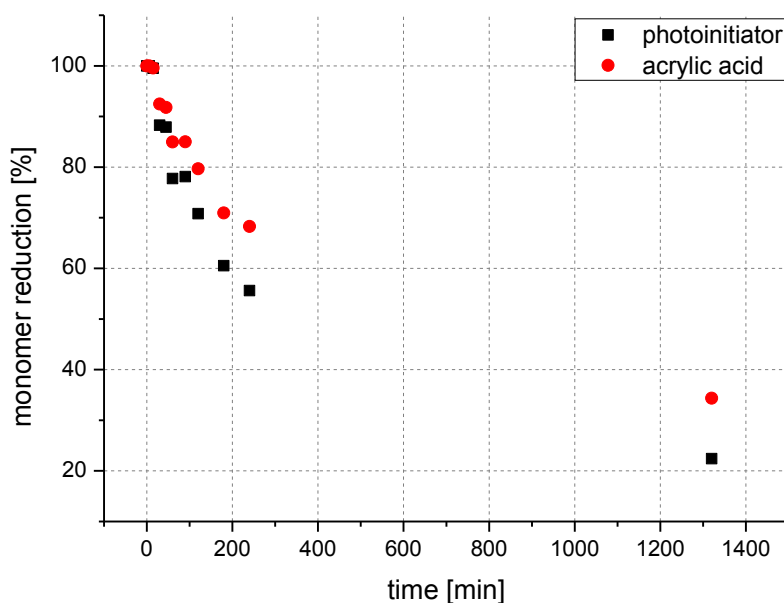
Figure 52: Decrease of the acrylate functionalities of the applied monomers

4.3.1.2.2 Investigation of the water solubility of Poly(PI-co-mono2)stat.

The water solubility of the system 2 polymers was evaluated according to the procedure which was described before (see 4.3.1.2.2). Unfortunately, it was found that only a small amount of the polymers was soluble in water. They were rather dispersible in water (see Figure 53).
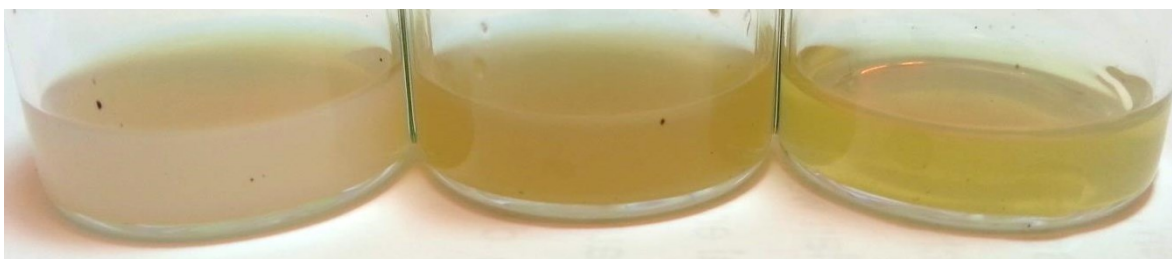
Figure 53: Polymer dispersions of the polymers Poly2E, 2D and 2C

In particular, the solution of the Poly2E is a cloudy dispersion, whereas the solubility (indicated by the reduction of the cloudiness) is increased proportional to the acrylic acid content (see Table 26). Therefore a nearly clear yellow solution could be obtained for Poly2C. The maximal dispersibility was determined by the continuous addition of the polymer until a distinctive sedimentation of the polymeric material could be observed. Furthermore, the storage stability of the dispersions was evalutated optically, after a period of one week no sedimentation was detectable.

Table 26: Dispersibility of the polymers Poly2E, Poly2D and Poly2C

Polymer	Acrylic acid content [w%]	Initiator content [w%]	Max. dispersibility [mg/mL]
Poly2E 50/50 - 7.5%	16.4	83.6	58.6
Poly2D 40/60 - 7.5%	17.7	82.3	122.8
Poly2C 30/70 - 7.5%	30.0	70.0	265.2

4.3.1.2.3 Photoreactivity of Poly(PI-co-mono2)$_{stat.}$

The photoreactivity of the polymers was characterized with the identical resin formulation and under the same conditions as it was described in chapter 4.3.1.1.3. All investigated polymers exhibit a decent photoreactivity and especially the t_{max} was only slightly reduced (see Table 27). The conversion decreased inverse proportional to the content of photoreactive monomers. This effect might be explained by a change of the resin viscosity. As it was elucidated in chapter 4.3.1.2.2, the water solubility increased with the content of acrylic acid. Due to the fact that all formulations were investigated with a constant amount of photoinitiating moieties, the highest mass of polymeric material was applied for Poly2C. This substance contained the highest content of acrylic acid, which was accompanied by the highest solubility and therefore increased viscosity of the formulation (6.9 mPas).

Table 27: Results of the Photo-DSC measurements for the system 2 photoinitiators

Initiator	t_{max} [s]	ΔH [J/g]
Irgacure 2959	1.56	14
Poly2E	1.80	12
Poly2D	1.86	14
Poly2C	1.86	12
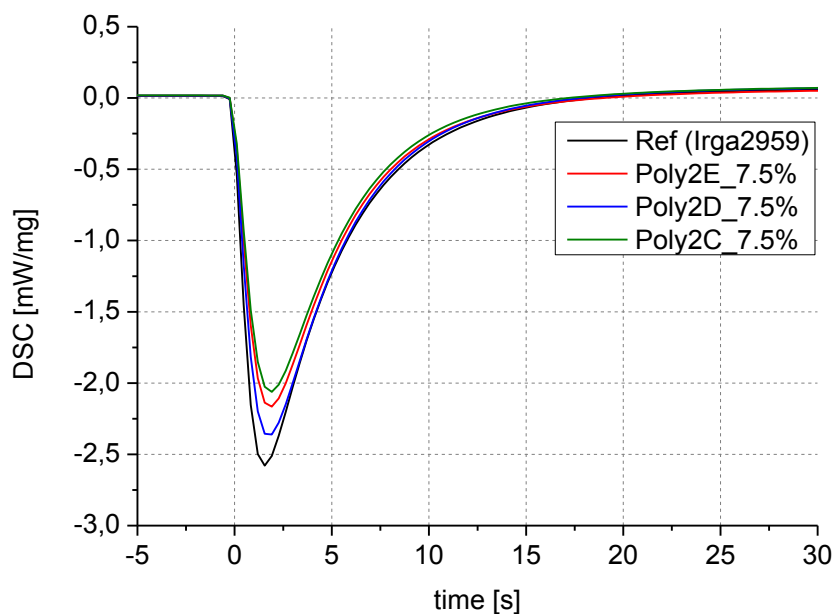
Figure 54: Results of the Photo-DSC measurements of polymer system 2

4.3.1.3 Curing behavior of the polymeric photoinitiators after solvent evaporation

As it was described in chapter 2.2.3 the hardening of UV curable polyurethane dispersions films is usually a thermal drying process which can be support by additional photochemical curing steps. By the illumination with UV-light, acrylate functionalities which are coupled to the polyurethane backbone, lead to a crosslinking reaction which subsequently improves the scratch resistance of the applied polymer films.[51]

Therefore the photochemical performance of the synthesized macromolecular photoinitiators was characterized before (see chapter 4.3.1.1.3 and chapter 4.3.1.2.3) and after the evaporation of the solvents which were included in the resin formulation. The drying process was performed at 40°C in the vacuum oven before the formulations were characterized by Photo-DSC measurements.

It could be demonstrated that the synthesized photoinitiators deteriorated their photochemical performance drastically in absence of a resin diluent. This observation supports the assumption that the reactivity of the polymeric photoinitiators is strongly influenced by the mobility of the polymer chain in the resin formulation. In high viscous media or the absence of suitable solvents, the reactivity of the polymeric photoinitiators is neglectable low (see Table 28).

Table 28: Comparison of the photoreactivity of polymeric photoinitiators before and after (blue) a thermal drying step

Initiator	t_{max} [s]	t_{max} [s]	ΔH [J/g]	ΔH [J/g]
Irgacure 2959	1.56	2.22	14	7
Poly 2E	1.80	4.32	12	4
Poly 1E_7.5% AIBN	2.22	5.76	14	3
Poly 1E_10% AIBN	3.12	5.22	14	3
Poly 1E_15% AIBN	4.02	5.82	14	3

4.3.2 Conclusion

In chapter 4 the synthesis and characterization of water soluble photoinitiators was discussed extensively.

Two different strategies carbohydrate based and polymeric photoinitiators to realize water solubility were investigated, whereas the focus was set on substances with a molecular weight higher than 1000 g/mol, to guarantee low migration behavior.

In the first part of this chapter, carbohydrate based photoinitiators were introduced, as a promising alternative to the rather small number of water soluble, commercially available systems. Altogether two multifunctional, sugar based photoinitiators were successfully synthesized and characterized by UV-Vis spectroscopy and Photo-DSC measurements. Additionally the migration behavior of these novel substances was investigated and compared to the commercially available photoinitiator (Irgacure 2959).

It could be demonstrated that reasonable water solubility of an erythritol based photoinitiator (**5a**) could be realized, whereas low migration behavior, as a consequence of the enhanced molecular weight, could be observed. In contrast to this difunctional photoinitiator the glucose based photoreactive species exhibited no solubility in aqueous media although an excellent curing performance in acrylate based systems could be observed. This makes the novel glucose based photoinitiator an interesting candidate for conventional photoreactive resins due to its high molecular weight and the therefore expected low migration behavior (MW>1000 g/mol) (see Chapter 4.2.1.3).

Attributed to legislative constraints substances with a molecular weight lower than 1000 g/mol have to be classified regarding their toxicological properties and migration behavior. Due to the fact that the approval procedure involves excessive costs and requires a disproportionate amount of time, the focus was set on two different anionic polymer systems, which were investigated systematically, considering both, their photoinitiator loading and the molecular weight. Furthermore, the copolymerization behavior was characterized by ^{1}H-NMR studies and the water solubility was evaluated for all synthesized materials. The photoreactivity of the polymers was tested in a polyurethane/polyacrylate dispersion based resin formulations, suitable for low migration applications. For all measurements the amount of photoinitiator units was kept on a constant value to make reliable statements regarding the initiation behavior of the novel substances. It turned out, that the photochemical performance of all photoinitiators was appreciably reduced, in terms of reaction speed (t_{max}) as well as conversion rates (see Table 29). Furthermore, a significant increase of the resin viscosity (from 4.00 mPas to 8.9

mPas for Poly1E) could be observed, which might be responsible for the lack of sufficient reactivity.[109]

Table 29: Comparison of the photoreactivity of polymeric photoinitiators without an additional drying step

Initiator	t_{max} [s]	ΔH [J/g]
Irgacure 2959	1.56	14
Poly 2E	1.80	12
Poly 1E_7.5% AIBN	2.22	14
Poly 1E_10% AIBN	3.12	14
Poly 2E_15% AIBN	4.02	14

This theory is supported by additional experiments considering the post curing efficiency of the polymeric photoinitiators. These investigations included a thermal drying step, previous to the photochemical curing process. A significant reduction of the photochemical performance could be observed, which might be attributed to the absence of an appropriate solvent, to enable an adequate mobility of the attached photoinitiating moieties. The bound photoinitiators are drastically limited in their initiation behavior, which might be illustrated by a significant breakdown of the polymerization speed (t_{max}) as well as the monomer conversion (ΔH) (see table 4.3.1.3).

Beside this negative post curing behavior, the purification of the reactive polymers with a molecular weight in the range of 1000 to 10000 g/mol is problematically. Repetitive precipitation processes are on the expense of the polymerization yield, dialysis techniques are time consuming and inapplicable for industrial processes.

To summaries, it can be stated that the discussed polymeric materials are inappropriate as a water soluble alternative for low migration applications. Further investigations considering oligomeric photoinitiators, based on ionic backbones might be a promising class of photoinitiators to realize highly reactive, water soluble photoinitiators.

4.3.3 Experimental

Unless otherwise stated, all reagents were purchased from Sigma–Aldrich, TCI, VWR, Acros, Bruno-Bock and Roth and were used without further purification.

4.3.3.1 2-(4-(2-Hydroxy-2-methylpropanoyl)phenoxy)ethylacrylate
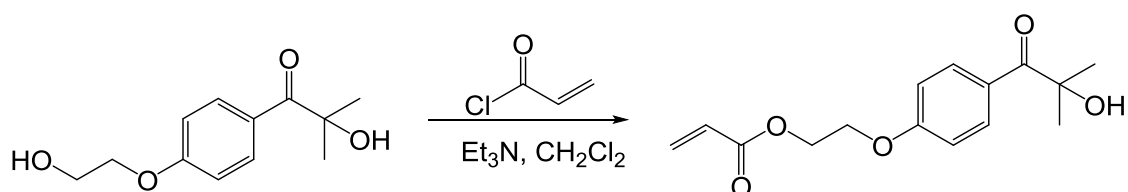
Irgacure 2959 (10.0 g, 44.59 mmol, 1 Eq.) and Et$_3$N (4.6 mL, 44.59 mmol, 1 Eq.) were dissolved in CH$_2$Cl$_2$ and cooled to 0 °C. Acryloyl chloride (4.0 g, 40.13 mmol, 0.9 Eq.) was added over a period of 2 minutes under inert atmosphere and continuous stirring. After 30 minutes the ice bath was removed and the reaction was warmed to room temperature. After a reaction time of 20h the mixture was extracted with 5% HCl (3x50 mL) and dried over Na$_2$SO$_4$. Finally, the crude product was purified by flash chromatography (silica gel, cyclohexane/ ethyl acetate=4:1), to obtain the title compound as a white solid.

Yield: 8.15 g (73%)

^{1}H-NMR: (δ, 400 MHz, 25°C, CDCl$_3$):
8.03 (d, 2H, AR); 6.94 (d, 2H, AR); 6.39 (q, 1H, CH=CH$_2$); 6.13 (q, 1H, CH=CH$_2$); 5.85 (q, 1H, CH=CH$_2$); 4.50 (m, 2H, CH$_2$); 4.26 (m, 2H, CH$_2$); 1.59 (s, 6H, CH$_3$) ppm.

^{13}C-NMR (δ, 100 MHz, CDCl$_3$, 25 °C):
202.60 (1C, C=O); 166.19 (1C, C=O); 162.31 (1C, AR) 132.27 (2C, AR); 131.59 (1C, C=C); 127.93 (1C, C=C) 126.68 (1C, AR); 114.48 (2C, AR); 75.87 (1C, C); 66.08 (1C, CH$_2$); 62.54 (1C, CH$_2$); 28.61 (2C, CH$_3$) ppm.

4.3.3.2 Synthesis of Poly(PI-co-mono1)_{stat.}
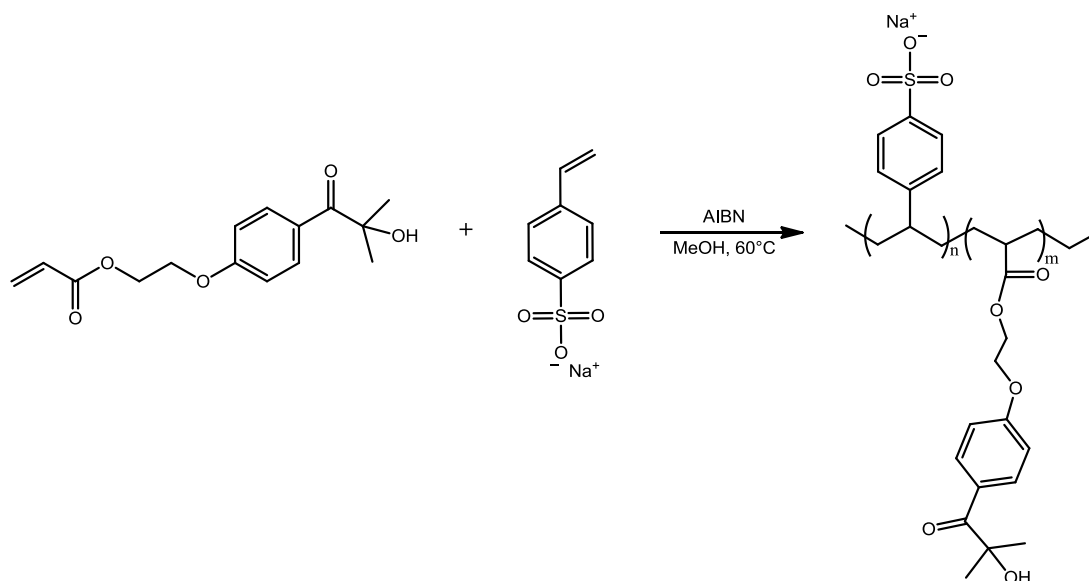
The photoreactive monomer (PI) and sodium-4-vinylbenzensulfonat (mono1) were weigh in to a dried Schlenk tube and dissolved anhydrous methanol (monomer conc. 4 M) under nitrogen atmosphere. The mixture was heated to 50°C. The thermal initiator (AIBN) was dissolved in the same solvent in a separate Schlenk tube and added to reaction. After the reaction time of 24h the mixture was cooled to room temperature and the 75% of the solvent were evaporated under reduced pressure. The polymer was precipitated in cold diethyl ether and the solvent excess was decanted after sedimentation. The product was dried in the vacuum drying oven at 40 °C.

Table 30: Synthesized polymers system 1

Polymer	PI- Monomer	sodium-4-vinylbenzensulfonat	Mn [g/mol]	PDI
Poly1A	70 Eq. - 9.05 mM	30 Eq. - 3.88 mM	insoluble	
Poly1B	60 Eq. - 5.82 mM	40 Eq. - 3.88 mM	insoluble	
Poly1C	50 Eq. - 3.88 mM	50 Eq. - 3.88 mM	71200	1.26
Poly1D	40 Eq. - 2.59 mM	60 Eq. - 3.88 mM	79300	1.34
Poly1E	30 Eq. - 1.66 mM	70 Eq. - 3.88 mM	76000	1.35

^{1}H-NMR: (δ, 400 MHz, 25°C, CDCl$_3$):

8.2 - 7.9 (AR, PI-M); 7.7-7.4 (AR, Sulf.); 7.1-6.3 (AR, PI-M); 4.4-3.5 (CH$_2$, PI-M); 2.6-0.8 (CH$_2$+CH$_3$, both) ppm.

4.3.3.3 Synthesis of Poly(PI-co-mono2)*stat.*
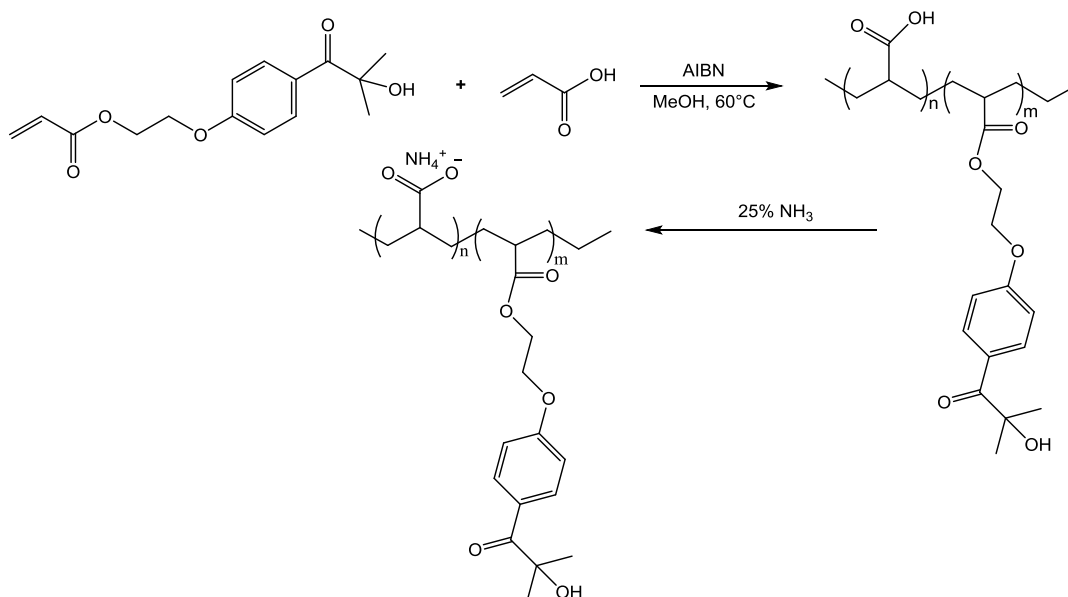
The photoreactive monomer (PI) and acrylic acid (mono2) were weigh in to a dried Schlenk tube and dissolved anhydrous methanol (monomer conc. 4 M) under nitrogen atmosphere. The mixture was heated to 50°C. The thermal initiator (AIBN) was dissolved in the same solvent in a separate Schlenk tube and added to reaction. After the reaction time of 24h the mixture was cooled to room temperature and the 75% of the solvent were evaporated under reduced pressure. The polymer was precipitated in cold diethyl ether and filtrated over celite (Diatomaceous earth). Afterwards the product was redissolved in THF and the excess of solvent was removed under reduced pressure to obtain the precursor polymer. The obtained material was dissolved in 25% NH_3 solution and dried in the vacuum drying oven at 40 °C.

Table 31 Synthesized polymers system 2

Polymer	PI - Monomer	Acrylic acid	Mn [g/mol]	PDI
Poly2A	10 Eq. - 0.22 mM	90 Eq. - 2.64 mM	1265	2.1
Poly2B	20 Eq. - 0.66 mM	80 Eq. - 2.64 mM	9137	2.7
Poly2C	30 Eq. - 1.13 mM	70 Eq. - 2.64 mM	7067	2.7
Poly2D	40 Eq. - 1.76 mM	60 Eq. - 2.64 mM	2828	3.6
Poly2E	50 Eq. - 2.64 mM	50 Eq. - 2.64 mM	3924	3.2
Poly2F	60 Eq. - 3.96 mM	40 Eq. - 2.64 mM	39610	4.1
Poly2G	70 Eq. - 6.15 mM	30 Eq. - 2.64 mM	76104	2.5

^{1}H-NMR: (δ, 400 MHz, 25°C, CDCl$_3$):

8.2 - 7.9 (AR, PI-M); 7.1-6.3 (AR, PI-M); 4.4-3.5 (CH$_2$, PI-M); 2.9-2.4 (CH; Acrylic acid) 2.6-0.8 (CH$_2$+CH$_3$, both) ppm

4.3.3.4 ^{1}H-NMR studies of the polymerization of system 1 and system 2

4.3.3.4.1 System 1 - Poly(PI-co-mono1)stat.

The 3.88 mM photoreactive monomer (PI) and 3.88 mM sodium-4-vinylbenzensulfonat (mono1) were weigh in to a dried Schlenk tube and dissolved anhydrous methanol (monomer conc. 4 M) under nitrogen atmosphere. The mixture was heated to 50°C. The thermal initiator (AIBN) was dissolved in the same solvent in a separate Schlenk tube and added to reaction. After 0, 5, 10, 15, 30, 45, 60, 90, 120 min a sample of 1 ml was taken, dried in a separate Schlenk tube and dissolved in DMSO-d6 for ^{1}H-NMR analysis.

4.3.3.4.2 System 2 - Poly(PI-co-mono2)stat.

The 2.64 mM photoreactive monomer (PI) and 2.64 mM acrylic acid (mono2) were weigh in to a dried Schlenk tube and dissolved anhydrous methanol-d4 (monomer conc. 4 M) under nitrogen atmosphere. The mixture was heated to 50°C. The thermal initiator (AIBN) was dissolved in the same solvent in a separate Schlenk tube and added to reaction. Additional 10 µl DMSO were added to the reactive mixture to enable a quantification of the monomer conversion. After 0, 5, 10, 15, 30, 45, 60, 90, 120, 180, 240, 1320 min a sample of 1 ml was taken and analyzed by ^{1}H-NMR.

5 Silicon Based Mercaptans for Thiol-ene Photopolymerization

5.1 Motivation

In contrast to the homopolymerization of acrylates, thiol-ene formulations lead to homogenous networks and high monomer conversions.[33] These are crucial advantages to realize novel polymeric materials and to overcome the extensively discussed migration problems of resin components. In order to enlarge the number of potential applications for thiol-ene formulations, there is a huge demand for novel mercaptans as reactive monomers. In this context key requirements are high reactivity, low viscosity and a molecular shape which is not susceptible towards hydrolyzation reactions and water absorption. Especially the latter one is an essential drawback of conventional thiols, due to the significant deterioration of the mechanical properties of the resulting polymers after storage in aqueous media. Therefore the focus was set on novel mercaptans avoiding polar ester functionalities in their molecular backbone, which are responsible for the water uptake of cured resins based on commercially available mercaptopropionic esters. [150]

The viscosities of the mercaptans and of the resulting resin formulations as well as the surface tension, are decisive parameters for the processability of the reactive mixture and have to be tuned.[17]

Therefore it was the aim of this work to design novel substances, which pave the way towards new, mechanical stable materials, suitable for 3D printing and biocompatible inkjet inks.

Parts of the work in this chapter have been published previously in *Journal of Polymer Science Part A: Polymer Chemistry*, **2015** - "*Silicon-based mercaptans: High-performance monomers for thiol-ene photopolymerization*"

Andreas Moser (PhD student) - Institute of Material Science and Testing of Polymers - University of Leoben - performed the mechanical characterization of the investigated polymers, Dr. Josef Spreitz (Aglycon) contributed to the upscaling of the thiol synthesis and Andreas Oesterreicher (PhD student) - Chair of Chemistry of Polymeric Materials - University of Leoben - carried out the degradation studies.

5.2 *Introduction*

Although the reaction of thiols with enes has already been observed in 1905, it was not until the beginning of the 1930´s that this reaction was used for the fabrication of polymeric materials.[31,151] Thiol-ene polymers are formed by the stoichiometric reaction of multifunctional enes and thiols via a multiple step radical mechanism after thermal [152] or photochemical initiation.[153] In contrast to acrylate polymerization, the thiol-ene polymerization follows a step growth mechanism bringing unique properties to this interesting class of materials.[154] Polymerization shrinkage is low, and high impact strength materials can be achieved due to the homogenous network structure. However, the most salient feature of thiol-ene photopolymerization is that almost any type of ene can be applied in this photoreaction. Furthermore, it is important to note that oxygen inhibition plays only a minor role due to efficient hydrogen abstraction of peroxy radicals from thiols under the simultaneous formation of highly reactive thiyl radicals.[36] Besides these advantages, two important issues have to be considered for thiol-ene systems. First, the characteristic odor of thiol monomers and second the generally low glass transition temperature (Tg) of thiol-ene based polymers, which can be attributed to the rather flexible thioether linkages.[155] For applications that desire high moduli and high Tgs such as dental restoratives and automotive and aerospace resins, the low Tg of thiol-ene networks is a detriment.

One strategy to overcome this limitation is to use rigid ene structures such as triallyl-1,3,5-triazine-2,4,6(1H,3H,5H)-trione (TATT) or norbornene derivatives.[156,157] Also monomers which are capable to form hydrogen bonds in the thiol-ene network provide reasonable glass transition temperatures together with excellent hardness and impact properties.[158]

Another method for producing thiol-ene networks with high Tgs is to use multifunctional (meth)acrylate (co)monomers which can on the one hand copolymerize with the thiol (step growth thiyl addition) but also homopolymerize (chain growth mechanism).[31] However, the corresponding high temperature glass transition regions of these systems are broad compared to thiol-ene networks obtained by pure step growth polymerization.

Besides the mechanical properties, other limitations of the thiol-ene photopolymerization can mainly be attributed to specific characteristics of the used multifunctional thiols. The predominatly applied and studied thiols for thiol-ene curing are esters of mercapto propionic acid (MPA), e.g. trimethylolpropane tri(3-mercaptopropionate) and pentaerythritol tetra-3-mercaptopropionate (PETMP), and thioglycolates which are commercially available and offer superior reactivity compared to alkylthiols. [38]

The hydrolytic sensitivity of the ester groups reduces the resistance of the cured polymeric materials towards acidic and basic media which is detrimental for high performance applications such as dental restoratives and automotive resins. The hydrolysis process deteriorates the mechanical properties over time and ultimately leads to mechanical failure.[159,160] Further, the polarity of the ester group and its affinity to water favor water absorption which decreases the mechanical performance by lowering the modulus, glass transition and strength.[150] In principle, the formed thioether groups in thiol-ene polymers are rather stable and, therefore, it can be expected that formulations that contain persistent monomers, i.e. enes and thiols without hydrolytic sensitive groups, lead to stable polymeric materials similar to cationic cured epoxy resins.

While there is a vast number of studies describing the effect of different enes on the physico-chemical properties of thiol-ene polymers [161–163] there are only a few reports, which deal with alternative thiol compounds and their impact on the polymeric properties.[164,165] Very recently, the group of Bowman successfully demonstrated the beneficial behavior of ester-free thiols based on the example of tetra(2-mercaptoethyl)silane.[150]

In the present article, we studied several ester-free silane and siloxane based thiol monomers for thiol-ene photopolymerization. A particular focus was set on the synthesis and application of a multifunctional monomer bearing secondary thiol groups. It is well reported that resins prepared from such steric hindered mercaptans show improved shelf life stability.[164] In this context, the photoreactivity and storage stability of these monomers, in combination with TATT as ene component were investigated and compared with those of PETMP/TATT formulations. Moreover, also the mechanical properties as well as the degradation behavior of the cured formulations were determined revealing the versatility of this class of monomers.

5.3 *Results and Discussion*

5.3.1 Synthesis of silicon based mercapto compounds

For the preparation of functional thiol compounds several reaction strategies are described in the literature.[166–168] One elegant and straightforward procedure exploits the radical induced thiol-ene reaction of thioacetic acid with functional alkenes to give thioester derivatives that can be hydrolyzed under alkaline or acidic conditions yielding to the corresponding thiol compounds.
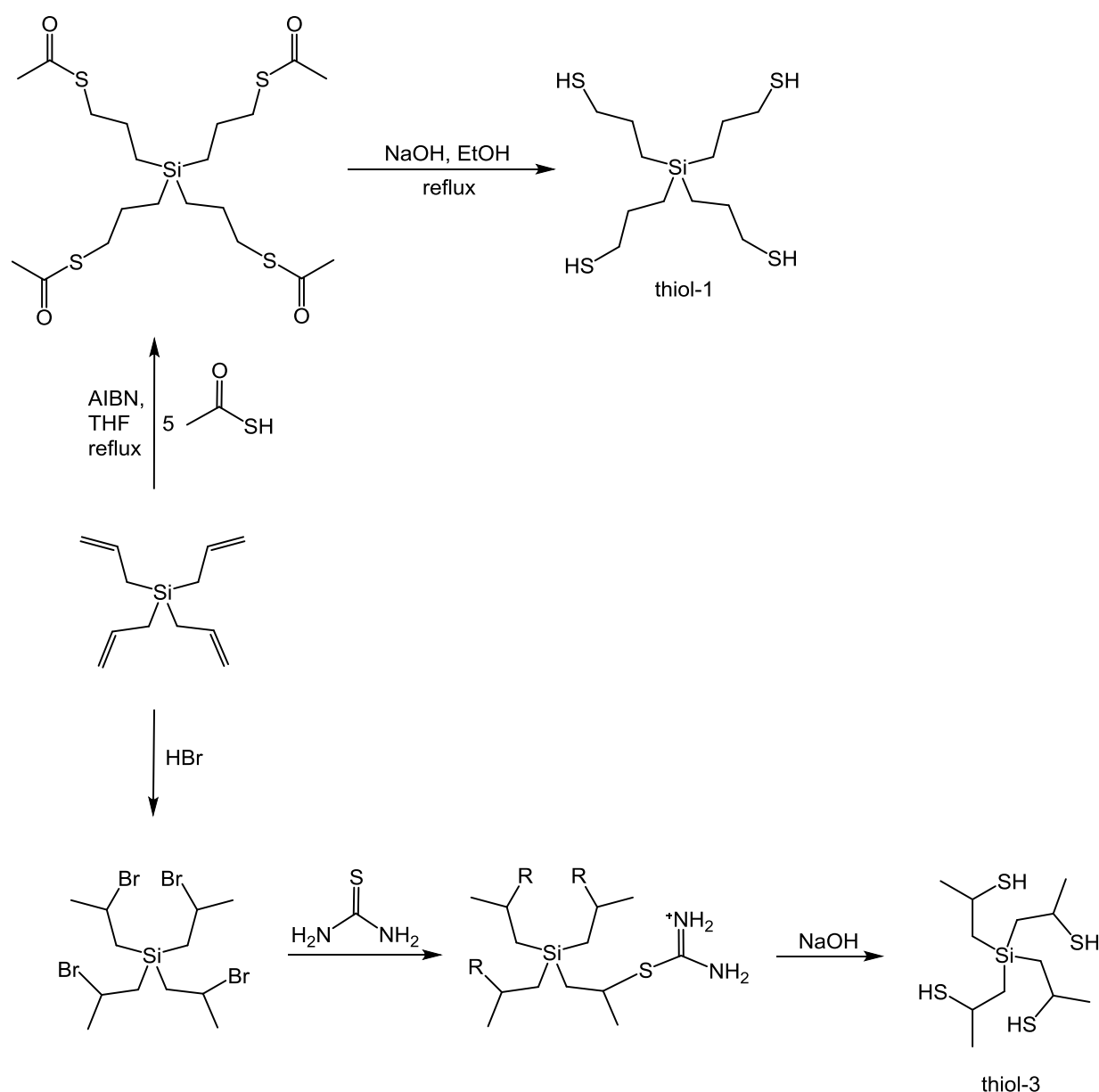
Figure 55: Synthetic pathway of thiol-1 and thiol-3

This method has been applied for the preparation of thiol-**1** and thiol-**2** (Figure 55, Figure 56) starting from tetraallylsilane and 2,4,6,8-tetravinyl-2,4,6,8-tetramethylcyclotetracyclosiloxane, which gives reasonable yields of 75% and 45%, respectively. This reaction procedure is not suitable for the synthesis of secondary thiol compounds due to the anti-markovnikov behavior of the radical induced addition of thioacetic acid.

Consequently, a multistep reaction route has to be chosen for the synthesis of thiol-**3**. In the first step the ionic addition reaction of hydrogen bromide to tetraallylsilane was exploited to give tetrakis(2-bromopropyl)silane in a good yield of 84%. Subsequently, this intermediate was converted with thiourea to the corresponding isothiouronium salt, which can be hydrolyzed with aqueous sodium hydroxide to give thiol-3 in a moderate yield of 10%. The conversion of alkylhalogenides to thiols by the aid of thiourea is well known and represents a versatile alternative to the thioacetic based reaction route.[168]
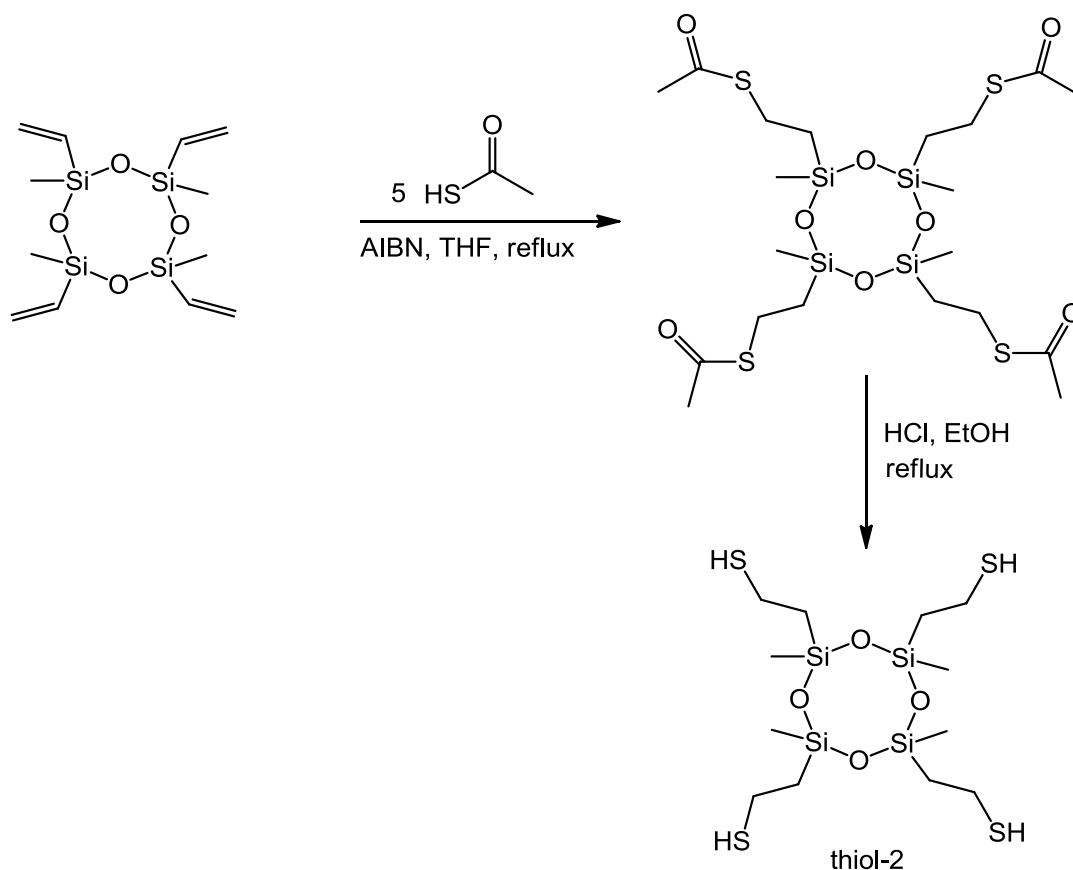
Figure 56: Synthetic pathway of thiol-2

The synthesized thiol were characterized by ^{1}H, ^{13}C and ^{29}Si NMR spectroscopy. The obtained data are in good agreement with the proposed structures. The chemo-physical properties of these compounds compared with PETMP are depicted in Table 32. The silicon based mercaptans exhibit much lower viscosities as the commercially available

PETMP making these monomers interesting candidates for the formulation of UV curable thiol-ene resins for low viscosity applications in the printing and coating industry (e.g. ink-jet printing). Although, thiol-**2** shows a significant lower surface tension (σ=27 mN m-1) than the other measured mercaptans, which is mainly explained by the apolar siloxane ring, no negative effect on the miscibility with the utilized ene components, i.e. TATT and triethylenglycol divinylether (TEGDVE) was observed. Furthermore, it has to be mentioned that the secondary thiol-3 had only little odor compared to the other mercapto compounds.

5.3.2 Photoreactivity of the silicon based mercapto compounds

It is well reported that thiols based on propionate esters and glycolate esters result in higher reaction rates than conventional alkyl thiols because of a weakening of the sulfur-hydrogen bond by hydrogen bonding of the thiol hydrogen group with the ester carbonyl. Rates of addition almost 6 times greater have been found for the free radical addition of methyl mercaptopropionate to 1-heptene than for pentanethiol to 1-heptene.[31]

The reactivity of the synthesized thiol monomers (in combination with TATT) towards polymerization after photo initiation has been investigated by photo-DSC, which represents a unique method for the fast and accurate evaluation of the curing behaviour of UV polymerizable resins.[107] Using photo-DSC, various important parameters can be obtained with one single measurement. The reaction time tmax is the time to reach the maximum of polymerization enthalpy and reveals information about the curing speed of the investigated system. Furthermore, the double bond conversion (DBC) can be calculated from the overall reaction enthalpy ΔH (peak area) providing that the theoretical heat of polymerization (ΔH0,p) is known. A straightforward method to obtain ΔH0,p is to determine the DBC of photo-DSC cured samples by means of ATR-IR and correlated this value to the heat released during the photo-DSC experiment.[41] In general, the determination of the DBC by means of photo-DSC is restricted to enes that show no homopolymerization, which can be observed in (meth)acrylate based thiol-ene formulations.

Due to overlapping IR signals and the fact that the reaction enthalpy for thiol-ene systems strongly depends on the structure of the ene (electron density), monofunctional model thiol compounds, i.e. octane thiol and butyl-mercaptopropionate, were used to estimate ☐H0,p of the thiol addition to TATT. In these experiments, the DBC was determined by means of NMR spectroscopy after dissolving the non-crosslinked thiol-ene adducts in CDCl3. For the photoinduced addition of octanethiol and butyl-mercaptopropionate to TATT the theoretical reaction enthalpy (ΔH0,p) was found to be 203 and 228 kJ/mol. Interestingly, the structure of the thiol compound (alkyl thiol vs. mercaptopropionic ester

derivative) also influences the overall reaction enthalpy. This fact was considered for the calculation of the DBC of the synthesized mercaptans thiol-1, thiol-2 and thiol-3.

It was found that thiol-1 and thiol-2 react almost quantitatively (see Table 32), whereas thiol-3 and PETMP yield conversions of 93% and 90%, respectively. Although, the multifunctional mercapto propionic ester derivative PETMP leads to the lowest measured DBC, it reached the maximum of polymerization heat within 1s. In comparison, the monomers containing primary thiol moieties, i.e. thiol-1 and thiol-2, show t_{max} values of 1.6 s and 1.7 s, respectively, while thiol-3 exhibits the slowest reaction rate (tmax=2.5 s). These measured values are in good accordance with previously described reaction behaviours of thiol derivatives.2 The moderate reaction rate of thiol-3 can be explained by the sterically hindered secondary mercapto groups.

Table 32: Physical and photochemical properties of the thiol resins

Thiol Monomer	P [g cm^{-3}]	σ [mN m^{-1}]	η (25°C) [mPa s]	t_{max} [s]	ΔH [J g^{-1}]	DBC [%]
thiol-1	1.10	43.9	49.7 (300)	1.6	422.2	100
thiol-2	1.02	27.0	37.8 (300)	1.7	353.8	100
thiol-3	1.07	35.6	52.4 (300)	2.5	381.4	93
PETMP	1.28	47.9	450.8 (300)	1.0	331.4	90

One possible explanation for the higher conversions of the silicon based thiols are their comparable low viscosities. While PETMP exhibits a viscosity of 450 mPas, the viscosity of the synthesized mercaptans is in the range between 40-50 mPas. A lower viscosity leads to a higher mobility of the monomers during polymerization, which may explain the superiority in terms of DBC despite lower reactivity.

5.3.3 Storage stability of the thiol-ene resins

One limiting factor of thiol-ene formulations is their poor shelf life stability preventing a broad application in the UV curing and coating industry so far. The limited stability of such resins may be due to a variety of reasons including (1) a base catalyzed addition of thiol to the ene double bond, (2) the decomposition of peroxide impurities and subsequent initiation of a thermal free-radical reaction or (3) the spontaneous initiation of polymerization via the generation of radicals through a ground-state charge-transfer complex formed between the thiol and ene components in the mixture. [31]However, it is well reported that resins prepared from steric hindered mercaptans, e.g. secondary thiols such as thiol-3, are superior in terms of shelf life stability. [158]
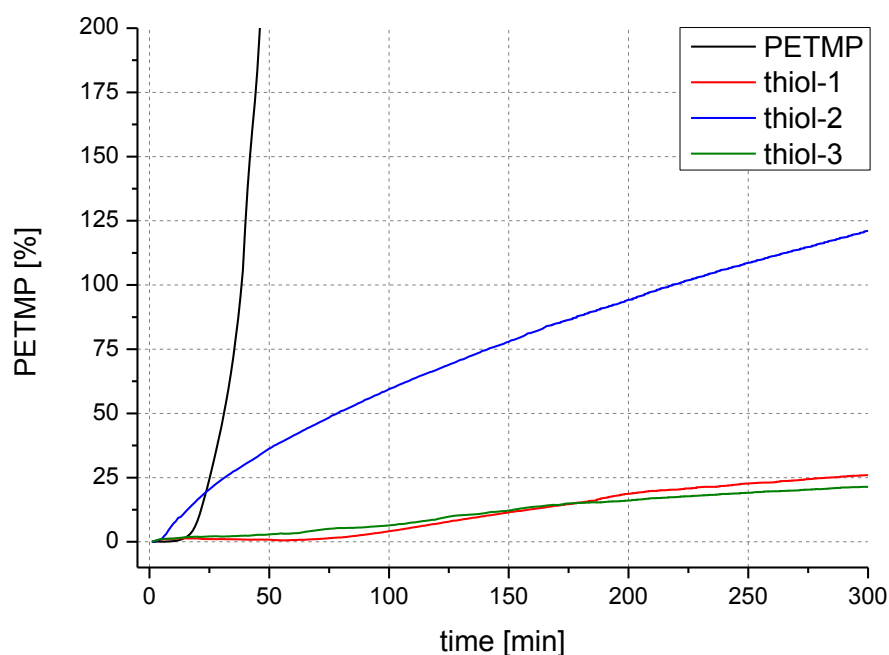
Figure 57: Increase in viscosity of the investigated resins during time of storage (50°C)

Figure 57 shows the viscosity increase of resins containing the synthesized thiols in combination with TATT as a function of time at a storage temperature of 50°C. This accelerated shelf life tests clearly reveal the inferiority of the PETMP/TATT system, in which a viscosity increase of 100% can be observed after 40 min of storage (50°C). Interestingly, the secondary (thiol-3) as well as the primary thiol monomer (thiol-1) exhibit similar good stability under these conditions, which is reflected by a minor viscosity increase of approximately 25% after 300 min of storage time for both thiol compounds. In contrast, formulations containing thiol-2 lead to an increase of 125% after 300 min. Although, the observed stability behavior is –as expected- inversely proportional to the measured reactivities (vide supra) of the investigated thiol monomers, the absolute values clearly indicate the superiority of the silane based thiols, i.e. thiol-1 and thiol-3, over PETMP. While the resin with thiol-1 shows only a slightly lower t_{max} value (only a difference of 0.6 s, see Table 32), the storage stability is far better than the formulation prepared with PETMP.

5.3.4 Mechanical properties of the obtained thiol-ene polymers

The characterization of photocured thiol-ene networks has mainly been focused on the structural parameters related to ene flexibility in the past.[31,154,157] Although there are some reports describing the effect of different thiol monomer on the cured network[150,156,165] most of them deal with mercapto propionic acid derivatives such as PETMP, TMPMP or pentaerythritol tetrakis (mercaptobutylate).[31,154,158] Basically it is well documented that thermal and mechanical properties directly correspond to features inherent to the chemical structure of the ene and thiol monomer. Furthermore, it has been shown that the functionality of both types of monomers influence the crosslink density and glass transition temperature.[31]

For a detailed investigation of the effect of the different mercaptane compounds on the network properties, a DMA analysis of cured resins prepared form TATT and the synthesized thiols (1:1 ratio of molar functional groups) were performed and compared to the network properties of a PETMP/TATT based polymer as shown in Table 2. The corresponding storage moduli and tan delta versus temperature plots are shown in the supplementary information. In general, all cured formulations show rather narrow tan delta peak widths ($Tg_{1/2 \text{ width}}$ ~ 20-40°C) which are characteristic for step-growth systems. [31]

Table 33: Mechanical properties of the resins before and after aqueous storage for 24 h

Thiol Monomer	Tg [°C][a] before	Tg [°C] after	E' [GPa] before	E' [GPa] after
thiol-1	67 (±1)	67 (±1)	1.5	1.3
thiol-2	58 (±1)	60 (±2)	1.5	1.6
thiol-3	67 (±5)	63 (±3)	2.2	2.1
PETMP	61 (±1)	42 (±1)	2.0	1.4

The networks containing thiol-1 and thiol-3 achieved noticeable higher glass transition temperatures of 67 (±1)°C and 67 (±5)°C, respectively, compared to cured PETMP/TATT samples (Tg= 61 (±1)°C). This result is in good accordance with the findings of Podgorski et. al. for a photocured tetra(2-mercaptoethyl)silane/TATT formulation exhibiting also a higher glass transition temperature than the corresponding PETMP/TATT sample. This behavior is explained by the good crosslinking capability of silane based multifunctional thiols as well as the absence of ester moieties in the formulations. [150] Furthermore, thiol-3 provides also the highest storage modulus (thiol-3: 2.2 GPa, PETMP: 2.0 GPa; at 25°C) of the investigated thiols in the glassy state.

The superiority of thiol-3 based networks can be assigned to the hindered rotation of thiol-ether linkages afforded by the additional -methyl group of thiol-3. This behavior has also been reported for secondary mercapto propionic ester based mercaptans previously.[150] It is worth mentioning that this outstanding performance of the investigated networks was achieved without the use of excessively viscous resin mixtures.

For many industrial and medical applications, the mechanical performance of the materials after water storage is of significant importance. Several studies of acrylate based photopolymers have shown a clear dependency between strength, stiffness, hydrophilicity and water uptake of the polymer. In Table 33 the effect of water storage at room temperature of the photocured samples on the moduli and the Tgs is shown. This treatment strongly deteriorates the network properties of the PETMP based polymers, while silane and siloxane based samples are only slightly influenced. The performance of the PETMP/TATT significantly decreased after storage in water. The storage modulus was lowered from 2.0 to 1.4 GPa as well as the glass transition temperature dropped from 61 (±1) to 42 (±1) °C. Very recently, a similar deterioration after water treatment has also been reported for PETMP/TATT based dental composite materials. [156]

5.3.5 Degradation behavior of the thiol-ene polymers

In order to investigate the hydrolytic stability of the synthesized thiol monomers, the degradation behavior of cured polymer samples were evaluated under alkaline conditions (1 M NaOH) at a storage temperature of 37°C and compared with the PETMP based thiol-ene polymer. For that purpose, TATT and TEGDVE were used as ene components. It is expected that the hydrophilic ethylene glycol groups of TEGDVE facilitate a good penetration of water into the polymeric network, which should increase the degradation rate of the thiol component towards reasonable time scales.

In Figure 58 the decrease in weight of the cured polymer samples during the immersion in 1 M NaOH solution (50°C) is depicted. While samples of cured PETMP/TEGDVE fully degrade within 15 h (not shown in Figure 58), owing to the hydrolytic sensitivity of the ester groups in PETMP, both silane based polymers show no significant loss of weight even after a storage time of 15 days. Accordingly, cured PETMP/TATT formulations also show a significant degradation of approximately 80 w% after 50 days of storage, whereas cured blends of TATT with thiol-**1**, thiol-**2** and thiol-**3** remained stable. Interestingly, the thiol-**2**/TEGDVE network also fully degrades under storage in sodium hydroxide solution within four days, which is presumably caused by the hydrolytic sensitivity of the Si-O bond. In general, siloxane based polymers such as PDMS are known to undergo readily degradation reactions under alkaline conditions.[169]
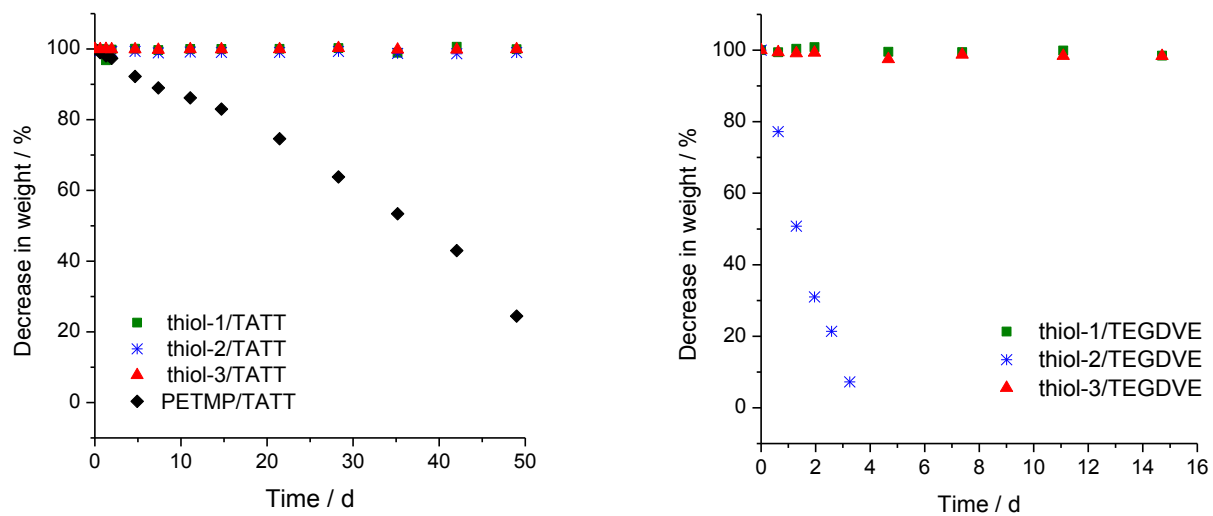
Figure 58: Decrease in weight of the cured polymer samples during the immersion in 1 M NaOH solution (50°C). left: thiol/TATT resins, right: thiol/TEGDVE resins

5.4 Conclusion

In this contribution, several ester-free silane and siloxane based thiol monomers were successfully synthesized and evaluated for an application in thiol-ene resins. Besides the reaction behavior, i.e. reaction rate and yield, of these monomers in combination with TATT as ene component, also the mechanical properties as well as the degradation behavior of photo cured samples were investigated and compared with those of PETMP/TATT formulations. While PETMP and thiol-**2** yield conversions of 90% and 93%, respectively, the silane based thiol monomers, i.e. thiol-**1** and thiol-**2**, react almost quantitatively. Moreover, the synthesized thiols showed also appropriate reaction rates with reaction times (t_{max}) in the range of 1.6 and 2.5 s. The observed storage stability of the thiol/TATT formulations is indirect proportional to the measured reactivities. However, a comparison of the stability with the reaction behavior of the synthesized thiols with PETMP clearly indicates the superiority of the silane based mercaptans. While the resin with thiol-**1** shows only a slightly lower t_{max} value (0.6 s slower), the storage stability is far better than the stability formulation prepared with PETMP. Moreover, photo cured samples containing thiol-**1** and **3** provide higher glass transition temperatures compared to PETMP/TATT resins. Thiol-**3** offers the highest storage modulus of the investigated thiols in the glassy state, which can be assigned to the hindered rotation of thiol-ether linkages afforded by the additional α-methyl group. In addition, ester-free thiol-ene networks were shown to withstand water storage without a significant loss in the network properties and also basic treatment for an extended amount of time. This behavior together with the excellent mechanical properties make silane based thiol/ene formulations interesting candidates for high performance applications such as dental restoratives and automotive resins.

5.5 *Experimental*

5.5.1 Silanetetrayltetrakis(propane-3,1-diyl))tetraethanethioate (1)
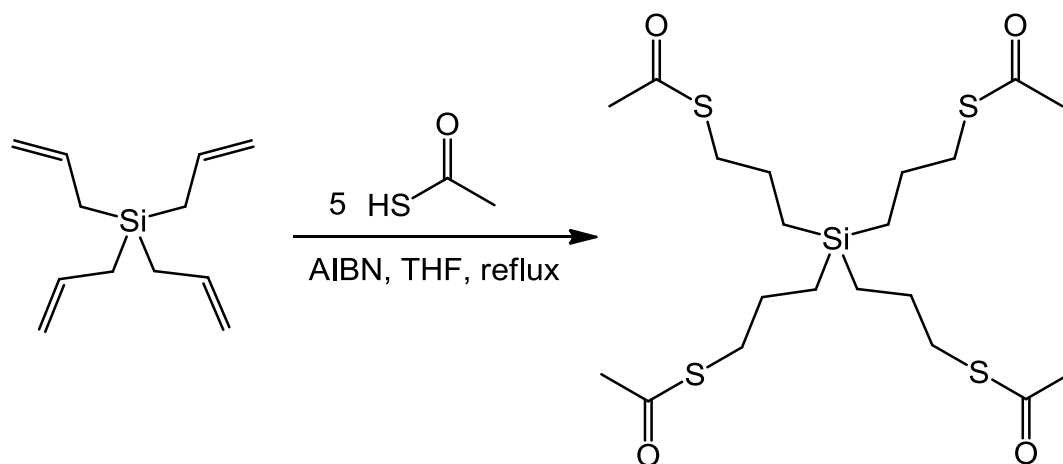
100 g (1314 mmol, 10 Eq.) thioacetic acid and 25.25 g (131.3 mmol) teraallylsilane were dissolved in 200 mL THF. After the addition of 1.08 g (6.6 mmol, 0.05 Eq.) 2,2′-Azobis(2-methylpropionitrile) the mixture was heated to 65°C and stirred overnight. The solvent was evaporated and the residue was dissolved in ethyl acetate and extracted with 200 mL water, sodium hydrogen carbonate and brine. Afterwards the solvent was removed under reduced pressure and the product was dried by azeotropic distillation with toluene. The crude product was used for the next reaction step without further purification.

5.5.2   Silanetetrayltetrakis(propane-1-thiol)
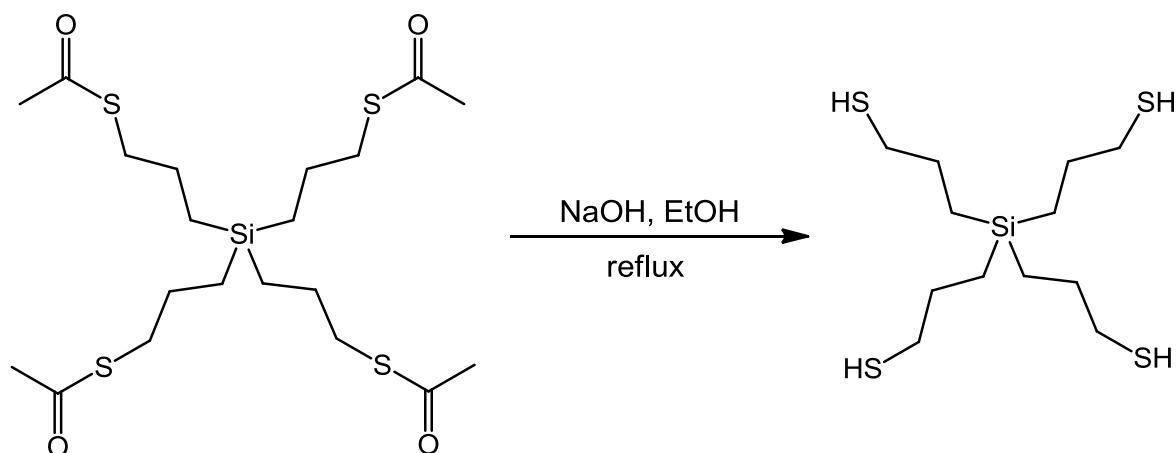
65.28 g (148.1mmol) **1** were dissolved in EtOH and cooled to 0°C. 32 mL of 25% NaOH solution was added and stirred overnight until complete conversion of the educt (reaction progress by TLC ethyl acetate / cyclohexane 1:5). The mixture was neutralized with HCl and extracted three times with 200 mL Toluene. The combined organic layers were washed three times with 200 mL water and dried over Na_2SO_4. The solvent was removed under reduced pressure and the crude product was purified by Kugelrohr – vacuum distillation (300°C, 2 mbar) to obtain the colorless liquid product.

Yield: 24 g (60%)

^{1}H-NMR (δ, 400 MHz, CDCl$_3$, 25 °C):
2.51 (m, 8H, C-SH); 1.58 (m, 8H, C-C-SH); 0.63 (m, 8H, Si-C) ppm

^{13}C-NMR (δ, 100 MHz, CDCl$_3$, 25 °C):
28.65 (d, 4C, C-C-SH); 28.27(s, 4C, C-SH), 11.45 (s, 4C, Si-C) ppm

^{29}Si-NMR (δ, 59.3 MHz CDCl$_3$, 25 °C): 3.64 (s, Si) ppm

5.5.3 (2,4,6,8-Tetramethyl-2,4,6,8-tetrayl)tetrakis(ethane-2,1-diyl))tetraethanethioate (2)
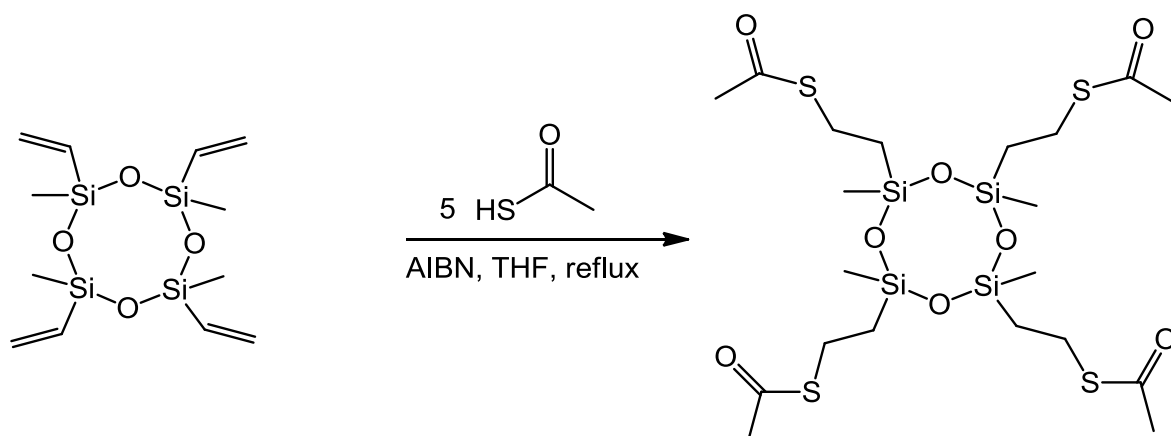
23.7 g (0.069mmol) of 2,4,6,8-tetravinyl-2,4,6,8-tetramethylcyclotetracyclosiloxane, 26.2 g (0.343mol, 5 Eq) thioaceticacid and 1.13 g 2,2′-Azobis(2-methylpropionitrile) (6.88 mmol, 0.1 Eq) were dissolved in 110 mL anhydrous THF. The mixture was refluxed under inert gas for 18h until it was cooled down to room temperature. The excess of solvent and thioacetic acid was removed under reduced pressure.

The crude product was used for the next reaction step without further purification.

^{1}H-NMR: (δ, 400 MHz, 25°C, CDCl$_3$):

2.88 (m, 8H, CH$_2$); 2.26 (m, 12H, - CH$_3$); 0.89 (m, 8H, - CH$_2$); 0.14 (m, 12H, -CH$_3$) ppm

5.5.4 (2,4,6,8-Tetramethyl-2,4,6,8-tetrayl)-tetraethanethiol
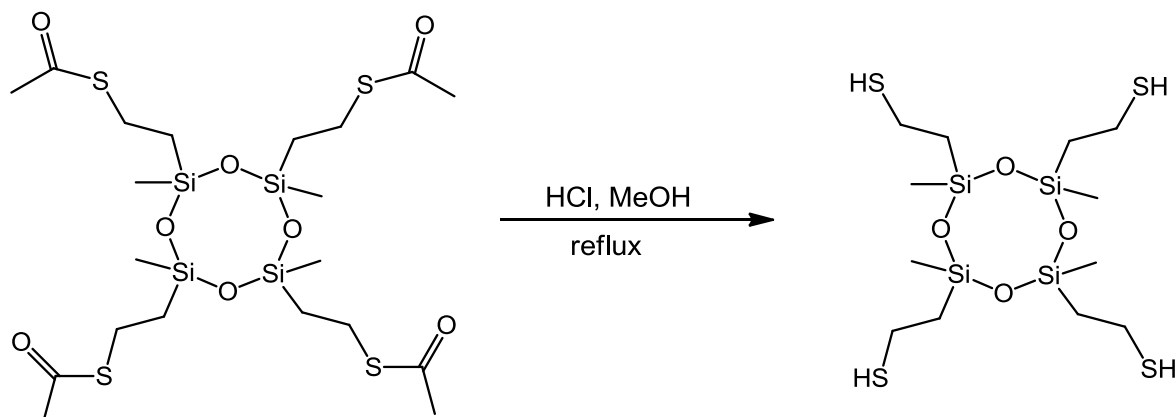
2 was dissolved in 100 mL methanol and mixed with 16 mL concentrated hydrochloric acid, degassed by bubbling with nitrogen for 30 min and hold on 60°C for 10h. In the next step 100 mL of water were added and the mixture was extracted 3 times with CH_2Cl_2. The combined organic layers were washed with saturated $NaHCO_3$ solution and dried over Na_2SO_4. The crude product was purified by column chromatography (Hexane: Diethylether / 3:2) and activated carbon filtration to give a slight yellow liquid. Furthermore a Kugelrohr – vacuum distillation was performed (300°C, 2 mbar) to obtain the slightly yellow liquid product.

Yield: 20 g (60%)

^{1}H-NMR: (δ, 400 MHz, 25°C, CDCl$_3$):
2.62 (m, 8H, CH$_2$); 1.54 (m, 4H, - SH); 0.99 (m, 8H, - CH$_2$); 0.14 (m, 12H, -CH$_3$) ppm

^{13}C-NMR (δ, 100 MHz, CDCl$_3$, 25 °C):
31.05 (d, 4C, C-Br); 27.92 (s, 4C, Si-C), 31.05 (s, 4C, C-CH$_3$) ppm

^{29}Si-NMR (δ, 59.3 MHz, CDCl3, 25 °C): -22.20 (s, Si) ppm

5.5.5 Tetrakis(2-bromopropyl)silane (3)
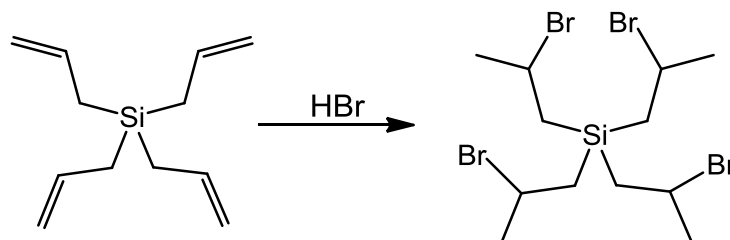
21.5 g (111.8 mmol) tetraallylsilane was dissolved in n-Hexane and cooled to -3°C. Under constant stirring 38.0 g (469.7mmol, 4.2 Eq.) gaseous HBr was introduced into the flask which was tightly sealed for 2h. The excess of solvent was removed under reduced pressure to obtain 54 g of the product as a white solid which was recrystallized from n-hexane. (50 g, 84%)

Yield: 50 g (84%)

¹H-NMR (δ, 400 MHz, CDCl₃, 25 °C):
4.52 (m, 4H, C-Br); 1.82 (m, 12H, C-CH3); 1.66 (m, 8H, Si-C) ppm

¹³C-NMR (δ, 100 MHz, CDCl₃, 25 °C):
31.05 (d, 4C, C-Br); 27.92 (s, 4C, Si-C), 31.05 (s, 4C, C-CH₃) ppm

5.5.6 Silanetetrayltetrakis(propane-2-thiol)
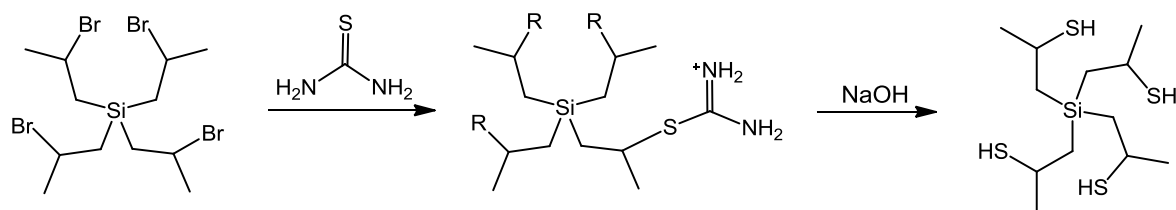
25.0 g (48.4 mmol) **3** and 25.4 g (333.96 mmol, 6.9 Eq.) thiourea were dissolved in 400 mL dry THF and refluxed for 24h. Afterwards the reaction was cooled to room temperature and quenched with 50% NaOH. The mixture was stirred for 1h, neutralized with 5% HCl, extracted with 2-methoxy-2-methylpropane and dried over Na_2SO_4. The crude product was purified by column chromatography (cyclohexane: ethyl acetate / 5:1) to give a colorless liquid (2.5 g, 10%).

Yield: 2.5 g (10%)

^{1}H-NMR (δ, 400 MHz, CDCl$_3$, 25 °C):
 4.52 (m, 4H, C-Br); 1.82 (m, 12H, C-CH3); 1.66 (m, 8H, Si-C) ppm

^{13}C-NMR (δ, 100 MHz, CDCl$_3$, 25 °C):
 31.05 (d, 4C, C-Br); 27.92 (s, 4C, Si-C), 31.05 (s, 4C, C-CH$_3$) ppm

^{29}Si-NMR (δ, 59.3 MHz, CDCl$_3$, 25 °C):
-1.49 (s, Si), 0.18 (s, Si), 1.22 (s, Si) ppm

6 Analytical equipment and methods

6.1 Thin-layer chromatography TLC

Reactions were monitored by TLC (Silica gel 60 F254 on aluminum, Merck). Detection was conducted by UV-light (254 nm and 365 nm for fluorescent/phosphorescent compounds), by staining with potassium permanganate (2% in H_2O dest.) and iodine absorption.

6.2 Fourier transformed infrared spectroscopy (FTIR)

The real-time-FTIR measurements were conducted on a VERTEX 70 (Bruker, Billerica, USA) with the measurement unit A513. 0.5 µl of the investigated resin was applied in between two CaF_2-discs and illuminated with an Omnicure s1000 (Lumen Dynamics, Mississauga, USA). Light intensity was adjusted to an operating level of 20% and 9 cm gap in between the light guide and the sample. 69 IR-spectra per minute were taken.

6.3 UV-Vis – spectroscopy

UV-Vis spectra were recorded in absorbance mode, in the range of 200 nm - 800 nm with a Varian Cary 50 conc.-spectrophotometer. All substances were dissolved in MeOH and measured in Hellma QS 10.00 mm absorption cells with an spectral transmission between 200 nm and 2500 nm. All provided spectra were measured in a concentration of 0.01 M, except the phosphine oxide initiators, which were characterized in a concentration of 0.25 M.

6.4 Photo differential scanning calorimetry (Photo - DSC)

The Photo-DSC experiments were performed on a NETZSCH Photo-DSC 204 F1 Phoenix. All measurements were conducted at 50°C in aluminum crucibles under nitrogen atmosphere. The Omnicure s2000 was used as the light source at 0.5 W/cm^2 and 5 W/cm^2 (for migration studies) respectively. For the determination of the reaction enthalpy and t_{max} the samples (sample quantity: 8 mg and 20 mg) were illuminated twice for 10 min each. For the analysis the second run was subtracted from the first one to give the reaction enthalpy curve.

6.5 Gel permeation chromatography (GPC)

Number average molar mass and mass average molar mass (M_n and M_w) as well as the polydispersity index (PDI) were determined by size exclusion chromatography with the follwing set-up: Merck Hitachi L6000 pump, separation columns from Polymer Standards Service (8 mm*300 mm, STV 5 µm grade size; 106, 104 and 103 pore size), and a refractive index detector (model Optilab DSP Interferometric Refractometer) from Wyatt Technology. Polystyrene standards from Polymer Standard Service were used for calibration. All GPC runs were performed with THF as eluent. The polymers which were exclusively water soluble were characterized by PSS SECcurity 1200 HPLC Pump, pre-column PSS MCX, 10 µm, Guard, ID 8.0 mm x 300 mm, two serial separation columns (PSS MCX, 10 µm, 1.000 Å, ID 8.0 mm x 300 mm; PSS MCX, 10 µm, 10.000 Å, ID 8.0 mm x 300 mm) and a PSS SECcurity 1200 differential refractometer (RID) detector. The eluent was a 0.07 M Na_2HPO_4*$2H_2O$ solution.

6.6 Nuclear magnetic resonance – spectroscopy (NMR)

^{1}H NMR and ^{13}C NMR spectra were recorded with a Varian 400-NMR spectrometer operating at 399.66 MHz and 100.5 MHz, respectively, and were referenced to $Si(CH_3)_4$. A relaxation delay of 10 s and a 45° pulse were used for acquisition of the ^{1}H-NMR spectra. Solvent residual peaks were used for referencing the NMR spectra to the corresponding values given in the literature.[170] ^{29}Si-NMR (59.3 MHz) and ^{31}P-NMR (121.4 MHz) spectra were recorded on a Varian INOVA 300 spectrometer.

6.7 X-ray photoelectron spectroscopy (XPS)

For the XPS measurements photopolymer sample specimens with 2 x 4 x 500 rectangular dimensions were fabricated by curing the corresponding resins (E= 4.5 J cm^{-2}) in glass moulds. To obtain representative results, regarding the distribution of the photoinitiator within the polymeric sample, the polymeric bar was cut into three fragments, whereas the middle piece with 2 x 4 x 5 rectangular dimension, was utilized for the Soxhlet extraction. The extraction was carried out with ethanol at 90°C for 24h and the samples were dried in a vacuum drying oven at 50°C for 12h. Afterwards the polymer fragment was cut in three pieces whereas the middle section was tilted by 90°C and measured by XPS.

XPS analyses were performed with a monochromatic Thermo Fisher K-Alpha spectrometer equipped with an Al X-ray source (1486.6 eV) operating with a base pressure in the range of 10^{-8} to 10^{-10} mbar. Charge compensation for insulator samples

was adjusted with a flood gun. High resolution scans were acquired at a pass energy of 50 eV and a step size (resolution) of 0.1 eV. Survey scans were acquired with a pass energy of 200 eV and a step size of 1.0 eV. The instrument work function was calibrated to give a binding energy (BE) of 83.96 eV for the Au $4f_{7/2}$ line for metallic gold. The analyses were carried out with a defined spatial resolution (300 µm diameter).

6.8 *Gas chromatography mass spectroscopy (GC-MS)*

The migration studies were performed with a Shimadzu QP2010 plus GS-MS with a Optima 5-Accent column (length: 30.0 m; thickness: 0.25 µm; diameter: 0.25 mm). The parameters of the applied method are summarized in Table 34.

Table 34: GC-MS method for the determination of hydroxy ketone and benzophenone derivatives

GC-Method	Column	MS
Oven Temp.: 50.00°C	**Optima 5-Accent**	**Electron energy:** -70 eV
Injection Temp.: 300.0°C	**Length:** 30.0 m	**Ion Source Temp:** 300°C
Heat rate: 10°C/min	**Thickness:** 0.25 µm	**Interface Temp:** 300°
Injection Mode: Split	**Diameter:** 0.25 mm	**Fragment:** see chapter 3.2.6
Injection Vol.: 8 µl		
Carrier Gas: He		
Pressure: 100.0 kPa		
Total Flow: 6.4 mL/min		
Column Flow: 1.69 mL/min		
Linear velocity: 47.2 cm/sec		
Purge flow: 3.0 mL/min		
Split ratio: 1.0		

6.9 *High performance liquid chromatography (HPLC)*

The migration studies were performed with a Thermo Scientific Ultimate HPLC. The parameters of the applied method are summarized in Table 35.

Table 35: LC-MS method for the determination of difunctional photoinitiator (5a) and Irgacure 2959

LC-Method	Column	UV/Vis detection
Column Temp.: 25.00°C **Injection Vol.:** 10 µl **Eluent:** ACN:H2O - 80:20 isocratic **Column Flow:** 0.200 mL/min	**ACE C18 3 µm** **Length:** 100 mm **Diameter:** 2.1 mm **Pre column:** ACE 3 C 18 Guard Cartridge	**Diode Array Detectors DAD-3000(RS) and MWD-3000(RS)** **wavelength:** 272 nm (±1 nm) 272 nm (±2 nm) 274 nm 331 nm

6.10 *Inductively coupled plasma mass spectroscopy (ICP-MS)*

The phosphorus containing samples were characterized by Agilent 8800 Triple-quadrupole-ICP-MS, after acidic digestion. The measurements were performed in MS/MS-modus with oxygen as reactive gas. For external calibration 1000 mg/l CertiPur standards from Merck were diluted with water to the desired concentration.

6.11 *Acidic digestion*

Acidic digestion was performed in a High Pressure Asher (HPA-S, Anton Paar), with concentrated HNO_3 at 240°C and a pressure of 120 bar for 60 minutes to dissolve the phosphorus containing samples in the aqueous medium.

6.12 *Dynamic mechanical analysis (DMA)*

The thermomechanical properties were measured in tension mode using a DMA/SDTA 861 (METTLER TOLEDO) with a heating rate of 2 K/min in the temperature range from -20 to 110°C. The operating frequency was determined at 1 Hz. For comparison of the thiol formulations the storage modulus was evaluated at room temperature (25°C) and the glass transition temperature was determined at the maximum of the tan δ curve for each measurement. For the determination of the thermo-mechanical properties and the

degradation behavior photopolymer sample specimens with 2 x 4 x 19 mm and 2 x 4 x 5 mm rectangular dimensions, respectively, were fabricated by curing the corresponding resins (E= 4.5 J cm^{-2}) in glass moulds.

6.13 *Viscosity*

The viscosity of the formulations was determined using an Anton Paar rheometer (MCR-102, Graz, Austria) in a cone-plate system setup with a Titan cone (MK 22 /60 mm, 0.5°) with an opening angle of 0.5° and a diameter of 60 mm at a shear rate of 300 s^{-1}

7 **Appendix**

7.1 *Abbreviation list*

AIBN	Azobisisobutyronitrile
$AlCl_3$	Aluminium chloride
APT	Attached proton test
BuVc	Butandiol divinylcarbonate
CaF2	Calcium fluoride
CD_3OD	Deuterated methanol
CH_2Cl_2	Dichloromethane
CH_3CN	Acetonitrile
$CHCl_3$	Chloroform
CINDP	Induced dynamic nuclear polarization
CTC	Charge-transfer complex
DBC	Double bond conversion
DCC	N,N'-Dicyclohexylcarbodiimide
DMA	Dynmaic mechanical analysis
DMAP	4-Dimethylaminopyridine
DMF	Dimethylformamide
DMPA	Dimethylol propionic acid
DMSO	Dimethyl sulfoxide
DPGAC	Dipropylene glycol diacrylate
EPHT	electron proton hydrogen transfer
Eq.	Equivalents
EtOH	Ethanol
FTIR	Fourier transformed infrared spectroscopy
GC	Gas chromatography
H_2O	Water
HBr	Hydrogen bromide
HCl	Hydrogen chloride
HDDA	Hexandiol diacrylate
HPLC	High performance liquid chromatography
ICP	Inductive coupled plasma

IPDI	Isophorone diiscocyanate
ITX	Isopropyl thioxanthon
K_2CO_3	Potassium carbonate
KOH	Potassium hydroxide
LATs	Light absorbing transients
mCPBA	meta-Chloroperoxybenzoic acid
MDEA	Methyl diethanolamine
MeOH	Methanol
Mn	Number average molecular weight
MS	Mass spectroscopy
N_a	Number of reacting molecules
Na_2SO_4	Sodium sulfate
NaCl	Sodium chloride
NaH	Sodium hydride
$NaHCO_3$	Sodium bicarbonate
NaOH	Sodium hydroxid
NH_3	Ammonia
NH_4Cl	Ammonium chloride
NMR	Nuclear magnetic resonance
N_Q	Number of absorbed photons
PAD	Polyacrylic dispersion
PDI	Polydispersity index
PETMP	Pentaerythritol tetra-3-mercaptopropionate
PHT	Proton hydrogen transfer
PI	Photoinitiator
PUD	Polyurethane dispersion
RT	Room temperature
RT-FTIR	Real-time - Fourier transformed infrared spectroscopy
SCF	Scientific committee on food
SCN	Thioissocyanate
$SOCl_2$	Thionyl chloride
TATT	Triallyl-1,3,5-triazine-2,4,6(1H,3H,5H)-trione
TBAF	Tetra-n-butylammonium fluoride
TEGDVE	Tetraethylene glycol divinyl ether
T_g	Glass transition temperature
THF	Tetrahydrofurane

THFA	Tetrahydrofurfuryl acrylate
TLC	Thin-layer chromatography
t_{max}	Time of the maxium reaction heat
UV	Ultraviolet
UV-Vis	Ultraviolet-visible
VOCs	volatile organic solvents
XPS	X-ray photoelectron spectroscopy
ε_{max}	Extinction maxium

7.2 *List of figures*

7.3 *List of tables*

7.4 *List of publications*

Patents:

2013 - AT201350557 - **Roth, M.**; Grießer, T.; Oesterreicher, A.; Edler, M.; Mostegel, F.; Gassner, M.; Billiani, J.; - Photoinitiator

under revision:

2014 - GB1406683.1 - Oesterreicher, A.; Grießer, T.; Edler, M.; Mostegel, F.; Gassner, M.; **Roth, M.;** Billiani, J.; - Resin composition suitable for printing and printing method utilizing the same

2015 - WO2015031927 - **Roth, M.;** Grießer, T.; Oesterreicher, A.; Edler, M.; Mostegel, F.; Gassner, M.; Billiani, J.; - Photoinitiator

Journals:

Roth, M.; Oesterreicher, A.; Mostegel, F.; Moser, A.; Pinter, G.; Edler, M.; Piock,R.; Griesser, T.: Silicon Based Mercaptans: High-performance Monomers for Thiol-ene Photopolymerization – Accepted: Journal of Polymer Science, Part A: Polymer Chemistry

Radl, S.; **Roth, M.**; Gassner, M.; Wolfberger, A.; Lang, A.; Hirschmann B.; Trimmel, G.; Kern, W.; Grießer, T.: Photo-induced crosslinking and thermal de-crosslinking in polynorbornenes bearing pendant anthracene groups. - European Polymer Journal 01/2014; 52:98–104

Hauser, L.; Knall, A.-C.; **Roth, M.**; Trimmel, G.; Edler, M.; Grießer, T.; Kern, W.: Reversible photochromism of polynorbornenes bearing spiropyran side groups. - in: Monatshefte für Chemie (Chemical monthly) 143 (2012) , S. 1551 – 1558

Conferences:

Talks:

Roth, M.; Oesterreicher, A.; Mostegel F.; Samusjew A.; Edler, M.; Grießer, T.: Low migration photoinitiators for biocompatible applications – in: ICP 2015 – Jeju /South Korea 30.06.2015

Roth, M.; Grießer, T.; Kern, W.; Edler, M.; Trimmel, G.: Photosensitive Polynorbornenes for Optical Devices. - in: Macro 2014 - Chiang Mai / Thailand 05.07.2014

Poster:

Radl, S. V.; **Roth, M.**; Hirschmann, B.; Grießer, T.; Kern, W.: <u>New Functional Polynorbornenes Bearing Anthracene Groups for Reversible Crosslinked Materials.</u> - in: Photopolymerization Fundementals 2013. Jackson Hole / Wyoming - US 22.09.2013

7.5 *Curriculum Vitae*

Meinhart Roth, M.Sc.

E-Mail: meinhart.roth@gmail.com

Date of birth: 27. Dezember 1985, Klagenfurt

Citizenship: Austria

Education and Qualifications

1992 - 1996   Elementary school in Klagenfurt

1996 - 2004   Secondary school Europagymnasium Klagenfurt

2004 - 2011   Graz University of Technology - Technical Chemistry
Masterthesis under supervision of Assoc. Prof. DI Dr. Gregor Trimmel
Title:"Photosensitive coblockpolymer micelles"

2011 - 2012   Research Associate - Graz University of Technology - Institute for
chemistry and technology of materials (ICTM)
Research Topic: "Synthesis and characterization of semiconducting
polymers for organic photovoltaic applications"

2012 - 2015   University of Leoben - Chair of Chemistry of Polymeric Materials
PhD thesis under supervision of Assoc. Prof. DI Dr. Thomas Grießer
Title: "Low migration Photoinitiators for Thiol-ene and Water Based
Systems"

8 <u>References</u>

[1]   J. V. Crivello, E. Reichmanis, *Chem. Mater.* **2014**, *26*, 533.

[2]   S. V. Murphy, A. Atala, *Nature biotechnology* **2014**, *32*, 773.

[3]   H. N. Chia, B. M. Wu, *Journal of biological engineering* **2015**, *9*, 4.

[4]   S. Pastorelli, A. Sanches-Silva, J. M. Cruz, C. Simoneau, P. P. Losada, *Eur Food Res Technol* **2008**, *227*, 1585.

[5]   A. Gil-Vergara, C. Blasco, Y. Picó, *Analytical and bioanalytical chemistry* **2007**, *389*, 605.

[6]   H. Dreeskamp, *Berichte der Bunsengesellschaft für physikalische Chemie* **1989**, *93*, 827.

[7]   A. Goel, *Wave mechanics*, Discovery Pub. House, New Delhi **2006**.

[8]   https://classconnection.s3.amazonaws.com/255/flashcards/4013255/jpg/electromagneticspectrum-141B490BAC872789434.jpg, *electromagnetic spectrum* **2015**.

[9]   K. K. Rohatgi-Mukherjee, *Fundamentals of photochemistry*, Wiley, New Delhi **1978**.

[10]   http://www.expertsmind.com/CMSImages/810_Jablonski%20Diagram.png, *Jablonski diagram* **2015**.

[11]   P. W. Atkins, J. de Paula, *Physical chemistry*, W.H. Freeman, New York **2010**.

[12]   A. Singh, L. W. Johnson, *Spectrochimica Acta Part A: Molecular and Biomolecular Spectroscopy* **2003**, *59*, 905.

[13]   M. Klessinger, J. Michl, *Excited states and photochemistry of organic molecules*, VCH, New York, NY **1995**.

[14]   D. O. Cowan, R. L. Drisko, *Elements of organic photochemistry: [Tab.]*, Plenum Pr, New York **1978**.

[15]   H. Okabe, *Photochemistry of small molecules*, Wiley, New York **1978**.

[16]   S. E. Braslavsky, *Pure and Applied Chemistry* **2007**, *79*.

[17]   S. Magdassi, S. Magdassi (Eds.), *The chemistry of inkjet jets // The chemistry of inkjet inks: Raw Materials for UV Curable Inks*, World Scientific Pub. Co, World scientific **2009 // 2010**.

[18]   A. F. Senyurt, H. Wei, C. E. Hoyle, S. G. Piland, T. E. Gould, *Macromolecules* **2007**, *40*, 4901.

[19]   J. G. Kloosterboer, *Advanced Polymer Science* **1988**.

[20]   T. Scherzer, S. Müller, R. Mehnert, A. Volland, H. Lucht, *Polymer* **2005**, *46*, 7072.

[21]   B. Husar, R. Liska, B. Husár, *Chem. Soc. Rev* **2012**, *41*, 2395.

References

[22] M. J. Forrest, *Coatings and inks for food contact materials*, Rapra Technology Ltd, Shawbury, Shrewsbury, Shropshire, U.K **2006**.

[23] L. Kanerva, T. Estlander, R. Jolanki, *Contact Dermatitis* **1989**, *20*, 201.

[24] L. S. Andrews, J. J. Clary, *Journal of toxicology and environmental health* **1986**, *19*, 149.

[25] B. Bjorkner, I. Dahlquist, S. Fregert, *Contact Dermatitis* **1980**, *6*, 405.

[26] C. D. Calnan, *Contact Dermatitis* **1980**, *6*, 53.

[27] M. Tucek, J. Tenglerová, B. Kollárová, M. Kvasnicková, K. Maxa, I. Mohyluk, E. Svandová, O. Topolcan, Z. Vlasák, M. Cikrt, *International archives of occupational and environmental health* **2002**, *75 Suppl*, S67-72.

[28] U. Blaschke, K. Eismann, A. Böhme, A. Paschke, G. Schüürmann, *Chemical research in toxicology* **2012**, *25*, 170.

[29] J. G. Kloosterboer, Van de Hei, G. M., H. M. Boots, *Journal of Polymer communication* **1984**.

[30] K. S. Anseth, C. N. Bowman, *J. Polym. Sci. B Polym. Phys.* **1995**, *33*, 1769.

[31] C. E. Hoyle, T. Y. Lee, T. Roper, *J. Polym. Sci. A Polym. Chem* **2004**, *42*, 5301.

[32] M. Roth, A. Oesterreicher, F. H. Mostegel, A. Moser, G. Pinter, M. Edler, R. Piock, T. Griesser, *J. Polym. Sci. Part A: Polym. Chem.* **2015**.

[33] C. E. Hoyle, C. N. Bowman, *Angew. Chem. Int. Ed* **2010**, *49*, 1540.

[34] C. E. Hoyle, A. B. Lowe, C. N. Bowman, *Chemical Society reviews* **2010**, *39*, 1355.

[35] T. Roper, T. Kwee, T. Lee, C. Guymon, C. Hoyle, *Polymer* **2004**, *45*, 2921.

[36] D. P. Gush, A. D. Ketley, *Modern Paint and Coatings* **1978**.

[37] G. Eisele, J. P. Fouassier, R. Reeb, *J. Polym. Sci. A Polym. Chem.* **1997**, *35*, 2333.

[38] N. B. Cramer, C. N. Bowman, *J. Polym. Sci. A Polym. Chem* **2001**, *39*, 3311.

[39] E. Klemm, S. Sensfuß, U. Holfter, J. J. Flammersheim, *Angew. Makromolekulare Chemie* **1993**.

[40] A. Mautner, X. Qin, G. Kapeller, G. Russmüller, T. Koch, J. Stampfl, R. Liska, A. Mautner, X. Qin, B. Kapeller, G. Russmueller, J. Stampfl, *Macromolecules Rapid Communications* **2012**, *33*, 2046.

[41] C. Heller, M. Schwentenwein, G. Russmüller, T. Koch, D. Moser, C. Schopper, F. Varga, J. Stampfl, R. Liska, *J. Polym. Sci. A Polym. Chem* **2011**, *49*, 650.

[42] K. Uhlig, *Polyurethan-Taschenbuch: Mit 34 Tabellen*, Hanser, München **2006**.

[43] P. Glöckner, T. Jung, S. Struck, K. Studer, *Radiation curing: Coatings and printing inks ; technical basics, applications and trouble shooting*, Vincentz Network, Hannover **2008**.

References

[44] A. Bernard, J. P. Renault, B. Michel, H. R. Bosshard, E. Delamarche, *Adv. Mater* **2000**, *12*, 1067.

[45] T. Tawa, S. Ito, *Polym J* **2006**, *38*, 686.

[46] S.-H. Son, H.-J. Lee, J.-H. Kim, *Colloids and Surfaces A: Physicochemical and Engineering Aspects* **1998**, *133*, 295.

[47] Y.-K. Jhon, I.-W. Cheong, J.-H. Kim, *Colloids and Surfaces A: Physicochemical and Engineering Aspects* **2001**, *179*, 71.

[48] A. K. Nanda, D. A. Wicks, *Polymer* **2006**, *47*, 1805.

[49] H.-W. Engels, H.-G. Pirkl, R. Albers, R. W. Albach, J. Krause, A. Hoffmann, H. Casselmann, J. Dormish, *Angewandte Chemie (International ed. in English)* **2013**, *52*, 9422.

[50] H. Casselmann, *drying PUD*, https://de.wikipedia.org/wiki/Polyurethandispersion#/media/File:Trocknung_PUD_1-5_HC1.png.

[51] Q. Gao, H. Li, X. Zeng, *J Coat Technol Res* **2011**, *8*, 61.

[52] W. A. Green, *Industrial photoinitiators: A technical guide*, Taylor & Francis, Boca Raton **2010**.

[53] J. P. Fouassier, J. Lalevée, *Photoinitiators for Polymer Synthesis: Scope, Reactivity and Efficiency*, Wiley, Weinheim **2012**.

[54] V. Lemee, D. Burget, P. Jacques, J. P. Fouassier, *J. Polym. Sci. A Polym. Chem.* **2000**, *38*, 1785.

[55] J. Gersdorf, J. Mattay, H. Goerner, *J. Am. Chem. Soc.* **1987**, *109*, 1203.

[56] J. Lalevée, X. Allonas, S. Jradi, J.-P. Fouassier, *Macromolecules* **2006**, *39*, 1872.

[57] V. Castelvetro, M. Molesti, P. Rolla, *Macromol. Chem. Phys.* **2002**, *203*, 1486.

[58] J. E. Baxter, R. S. Davidson, H. J. Hageman, T. Overeem, *Makromol. Chem., Rapid Commun.* **1987**, *8*, 311.

[59] T. Majima, Y. Konishi, A. Böttcher, K. Kuwata, M. Kamachi, W. Schnabel, *Journal of Photochemistry and Photobiology A: Chemistry* **1991**, *58*, 239.

[60] G. W. Sluggett, C. Turro, M. W. George, I. V. Koptyug, N. J. Turro, *J. Am. Chem. Soc.* **1995**, *117*, 5148.

[61] T. Sumiyoshi, W. Schnabel, A. Henne, P. Lechtken, *Polymer* **1985**, *26*, 141.

[62] S. Jockusch, I. V. Koptyug, P. F. McGarry, G. W. Sluggett, N. J. Turro, D. M. Watkins, *J. Am. Chem. Soc.* **1997**, *119*, 11495.

[63] G. W. Sluggett, P. F. McGarry, I. V. Koptyug, N. J. Turro, *J. Am. Chem. Soc.* **1996**, *118*, 7367.

[64] U. Kolczak, G. Rist, K. Dietliker, J. Wirz, *J. Am. Chem. Soc.* **1996**, *118*, 6477.

References

[65] J. P. Fouassier (Ed.), *Photochemistry and UV curing: New trends*, Research Signpost, Trivandrum **2006**.

[66] D. Rehm, A. Weller, *Israel Journal of Chemistry* **1970**.

[67] H. Block, A. Ledwith, A. R. Taylor, *Polymer* **1971**, *12*, 271.

[68] A. D. Scully, M. A. Horsham, P. Aguas, J. K. Murphy, *Journal of Photochemistry and Photobiology A: Chemistry* **2008**, *197*, 132.

[69] V. Le Fol, S. Aït-Aïssa, N. Cabaton, L. Dolo, M. Grimaldi, P. Balaguer, E. Perdu, L. Debrauwer, F. Brion, D. Zalko, *Environmental science & technology* **2015**, *49*, 3860.

[70] A. S. Silva, R. S. García, I. Cooper, R. Franz, P. P. Losada, *Trends in Food Science & Technology* **2006**, *17*, 535.

[71] C. Heller, M. Schwentenwein, G. Russmüller, T. Koch, D. Moser, C. Schopper, F. Varga, J. Stampfl, R. Liska, *J. Polym. Sci. A Polym. Chem* **2011**, *49*, 650.

[72] B. Jasurek, N. Bendakova, J. Valis, *Scientific Papers of the University of Pardubice, Series A: Faculty of Chemical Technology* **2011**.

[73] H. Gallart-Ayala, O. Núñez, P. Lucci, *TrAC Trends in Analytical Chemistry* **2013**, *42*, 99.

[74] Hubergroup.

[75] O. Piringer, R. Franz, M. Huber, T. H. Begley, T. P. McNeal, *J. Agric. Food Chem.* **1998**, *46*, 1532.

[76] G. L. Robertson (Ed.), *Food packaging: Principles and practice*, CRC Press, Boca Raton, Fla. **2013**.

[77] J. P. Fouassier, X. Allonas, J.-P. Fouassier (Eds.), *Basics and applications of photopolymerization reactions: Cationic initiators in photocuring applications*, Research Signpost, Kerala, India **2010**.

[78] J.-P. Fouassier, X. Allonas (Eds.), *Basics and applications of photopolymerization reactions: Biocompatible photopolymers*, Research Signpost, Kerala, India **2010**.

[79] J. P. Fouassier, D. Ruhlmann, B. Graff, F. Morlet-Savary, F. Wieder, *Progress in Organic Coatings* **1995**, *25*, 235.

[80] G. Sagratini, G. Caprioli, G. Cristalli, D. Giardiná, M. Ricciutelli, R. Volpini, Y. Zuo, S. Vittori, *Journal of chromatography. A* **2008**, *1194*, 213.

[81] M. A. Lago, A. Rodríguez-Bernaldo de Quirós, R. Sendón, J. Bustos, M. T. Nieto, P. Paseiro, *Food additives & contaminants. Part A, Chemistry, analysis, control, exposure & risk assessment* **2015**, *32*, 779.

[82] A. Sanches-Silva, C. Andre, I. Castanheira, J. M. Cruz, S. Pastorelli, C. Simoneau, P. Paseiro-Losada, *Journal of agricultural and food chemistry* **2009**, *57*, 9516.

References

[83] S. Kim, K. Choi, *Environment international* **2014**, *70*, 143.

[84] A. Darvay, I.R. White, R. J. G. Rycroft, A. B. Jones, J. L. M. Hawk, J. P. McFadden, *British Journal of Dermatology* **2001**.

[85] J. Xue, Q. Wu, S. Sakthivel, P. V. Pavithran, J. R. Vasukutty, K. Kannan, *Environmental research* **2015**, *137*, 120.

[86] Y. Watanabe, H. Kojima, S. Takeuchi, N. Uramaru, S. Sanoh, K. Sugihara, S. Kitamura, S. Ohta, *Toxicology and applied pharmacology* **2015**, *282*, 119.

[87] D. Brunk, *Benzophenones named 2014 Contact Allergen of the Year* **2014**, http://www.edermatologynews.com/?id=372&tx_ttnews[tt_news]=241889&cHash=cb086f7e35 1cccbcfd9dbf5fa806762b.

[88] C. G. Williams, A. N. Malik, T. K. Kim, P. N. Manson, J. H. Elisseeff, *Biomaterials* **2005**, *26*, 1211.

[89] Saftey data sheet, *4-(2-hydroxyethoxy)benzaldhyde CAS: 22042-73-5*.

[90] R. Klos, H. Gruber, G. Greber, *Journal of Macromolecular Science: Part A - Chemistry* **1991**, *28*, 925.

[91] L. Pouliquen, X. Coqueret, F. Morlet-Savary, J.-P. Fouassier, *Macromolecules* **1995**, *28*, 8028.

[92] X. Coqueret, L. Pouliquen, *Macromol. Symp.* **1994**, *87*, 17.

[93] M. Visconti, M. Cattaneo, *European coatings Journal* **2004**.

[94] T. R. Crompton, *Additive migration from plastics into foods: A guide for analytical chemists*, Smithers Rapra Technology Ltd, Shawbury, U.K **2007**.

[95] ebrary, Inc, *Global legislation for food packaging materials*, Wiley-VCH, Weinheim **2010**.

[96] Du Pont GB925117.

[97] W.D. Davies, F.D. Jones, J. Garrett, I. Hutchinson, G. Walton, *Surface coatings international Part B: Coatings Transactions* **2001**.

[98] P. Xiao, H. Zhang, M. Dai, J. Nie, *Progress in Organic Coatings* **2009**, *64*, 510.

[99] J. Yang, R. Tang, S. Shi, J. Nie, *Photochemical & photobiological sciences Official journal of the European Photochemistry Association and the European Society for Photobiology* **2013**, *12*, 923.

[100] B. Neises, W. Steglich, *Angew. Chem. Int. Ed. Engl.* **1978**, *17*, 522.

[101] Z. Wang (Ed.), *Comprehensive organic name reactions and reagents*, Wiley, Hoboken, NJ **2009**.

[102] J. Hu, M. A. Fox, *J. Org. Chem.* **1999**, *64*, 4959.

References

[103] M. Nagaraju, A. Krishnaiah, H. B. Mereyala, *Synthetic Communications* **2007**, *37*, 2467.

[104] T. I. Briggs, G. G. S. Dutton, E. Merler, *Can. J. Chem.* **1956**, *34*, 851.

[105] E. Meneguzzo, G. Norcini, G. Li Bassi. Lamberti Spa WO2009135895.

[106] R. Noe, E. Beck, M. Maase, A. Henne. BASF WO03/0678785.

[107] D. S. Esen, F. Karasu, Arsu N., D. S. Esen, F. Karasu, N. Arsu, *Progress in Organic Coatings* **2011**, *70*, 102.

[108] C. Dworak, S. Kopeinig, H. Hoffmann, R. Liska, *J. Polym. Sci. A Polym. Chem* **2009**, *47*, 392.

[109] X. Allonas, J.Lalevee, F. Morlet-Savary, J.P. Fouassier, *Polimery* **2006**.

[110] C. Valderas, S. Bertolotti, C. M. Previtali, M. V. Encinas, *J. Polym. Sci. A Polym. Chem.* **2002**, *40*, 2888.

[111] U. Kolczak, G. Rist, K. Dietliker, J. Wirz, *J. Am. Chem. Soc.* **1996**, *118*, 6477.

[112] W. A. Green, *Industrial photoinitiators: A technical guide*, CRC Press, Boca Raton **2010**.

[113] B. D. Fairbanks, T. F. Scott, C. J. Kloxin, K. S. Anseth, C. N. Bowman, *Macromolecules* **2009**, *42*, 211.

[114] B. D. Fairbanks, E. A. Sims, K. S. Anseth, C. N. Bowman, *Macromolecules* **2010**, *43*, 4113.

[115] F. Sun, Y. Li, N. Zhang, J. Nie, *Polymer* **2014**, *55*, 3656.

[116] C. Heller, M. Schwentenwein, G. Russmüller, T. Koch, D. Moser, C. Schopper, F. Varga, J. Stampfl, R. Liska, *J. Polym. Sci. A Polym. Chem.* **2011**, *49*, 650.

[117] A. F. Senyurt, H. Wei, C. E. Hoyle, S. G. Piland, T. E. Gould, *Macromolecules* **2007**, *40*, 4901.

[118] J. F. Moulder, J. Chastain, *Handbook of x-ray photoelectron spectroscopy // Handbook of X-ray photoelectron spectroscopy: A reference book of standard spectra for identification and interpretation of XPS data*, Physical Electronics Division, Perkin-Elmer Corp; Perkin-Elmer Corporation, Eden Prairie, Minn **1992**.

[119] J. Qiu, J. Wei, *J. Appl. Polym. Sci.* **2014**, *131*, n/a-n/a.

[120] N. S. Allen, *Journal of Photochemistry and Photobiology A: Chemistry* **1988**.

[121] M. Visconti, M. Cattaneo, *Progress in Organic Coatings* **2000**, *40*, 243.

[122] S. Knaus, H. F. Gruber, *Pure Applied Chemistry* **1996**.

[123] W. A. Green, *Polymers Paint Colors Journal* **1994**.

[124] R. Liska, D. Herzog, *Journal of Polymer Science: Part A: Polymer Chemistry* **2004**.

[125] G. Ullrich, B. Ganster, U. Salz, N. Moszner, R. Liska, *J. Polym. Sci. A Polym. Chem* **2006**, *44*, 1686.

[126] K. Kojima, M. Ito, H. Morishita, N. Hayashi, *Chem. Mater.* **1998**, *10*, 3429.

References

[127] Fong-Yuan Ma (Ed.), *Corrosive Effects of Chlorides on Metals*, INTECH Open Access Publisher **2012**.

[128] R. Liska, *J. Polym. Sci. A Polym. Chem.* **2002**, *40*, 1504.

[129] C. Dietlin, J. Lalevee, X. Allonas, J. P. Fouassier, M. Visconti, G. L. Bassi, G. Norcini, *J. Appl. Polym. Sci.* **2008**, *107*, 246.

[130] S. P. Rannard, N. J. Davis, *Org. Lett.* **1999**, *1*, 933.

[131] K. M. Tomczyk, P. A. Guńka, P. G. Parzuchowski, J. Zachara, G. Rokicki, *Green Chem.* **2012**, *14*, 1749.

[132] H. A. Staab, *Justus Liebigs Ann. Chem.* **1957**, *609*, 75.

[133] A. El-Faham, F. Albericio, *Chemical reviews* **2011**, *111*, 6557.

[134] H. A. Staab, *Angew. Chem. Int. Ed. Engl.* **1962**, *1*, 351.

[135] J. H. Clements, *Ind. Eng. Chem. Res.* **2003**, *42*, 663.

[136] A. Williamson, *Philosophical Magazine Series 3* **1850**, *37*, 350.

[137] N. Prileschajew, *Ber. Dtsch. Chem. Ges.* **1909**, *42*, 4811.

[138] A. H. Hoveyda, D. A. Evans, G. C. Fu, *Chem. Rev.* **1993**, *93*, 1307.

[139] X. Hu, *Tetrahedron* **2004**, *60*, 2701.

[140] T. Corrales, F. Catalina, C. Peinado, N. S. Allen, *Journal of Photochemistry and Photobiology A: Chemistry* **2003**, *159*, 103.

[141] F. Catalina, C. Peinado, M. Blanco, T. Corrales, N. S. Allen, *Polymer* **2001**, *42*, 1825.

[142] F. Catalina, C. Peinado, M. Blanco, N. S. Allen, T. Corrales, I. Lukác, *Polymer* **1998**, *39*, 4399.

[143] G. Temel, N. Arsu, *Journal of Photochemistry and Photobiology A: Chemistry* **2009**, *202*, 63.

[144] B. A. Miller-Chou, J. L. Koenig, *Progress in Polymer Science* **2003**, *28*, 1223.

[145] J. G. Braks, R. Y. M. Huang, *J. Appl. Polym. Sci.* **1978**, *22*, 3111.

[146] D. Braun, I. Krämer, H. Pasch, *Macromolecular Chemistry and Physics* **2000**.

[147] V. P. Wittmer, *Makromol. Chem.* **1967**, *103*, 188.

[148] V. P. Wittmer, *Makromol. Chem.* **1967**, *103*, 188.

[149] L. J. Young, *J. Polym. Sci.* **1961**, *54*, 411.

[150] M. Podgórski, E. Becka, S. Chatani, M. Claudino, C. N. Bowman, *Polymer chemistry* **2015**, *6*, 2234.

[151] M. S. Karasch, F. R. Mayo, *Chem. Ind.* **1938**.

[152] L. M. Campos, K. L. Killops, R. Sakai, J. M. J. Paulusse, D. Damiron, E. Drockenmuller, B. W. Messmore, C. J. Hawker, *Macromolecules* **2008**, *41*, 7063.

References

[153] C. R. Morgan, A. D. Ketley, *J. Radiat. Cur.* **1980**.

[154] C. E. Hoyle, C. N. Bowman, *Angewandte Chemie (International ed. in English)* **2010**, *49*, 1540.

[155] N. Mosner, W. Schoeb, V. Reinberger, *Polymer Bullitin* **1996**.

[156] S. Reinelt, M. Tabatabai, N. Moszner, U. K. Fischer, A. Utterodt, H. Ritter, *Macromol. Chem. Phys.* **2014**, *215*, 1415.

[157] J. A. Carioscia, L. Schneidewind, C. O'Brien, R. Ely, C. Feeser, N. Cramer, C. N. Bowman, *J. Polym. Sci. A Polym. Chem.* **2007**, *45*, 5686.

[158] Q. Li, H. Zhou, D. A. Wicks, C. E. Hoyle, *J. Polym. Sci. A Polym. Chem.* **2007**, *45*, 5103.

[159] J. L. Ferracane, *Dental materials official publication of the Academy of Dental Materials* **2011**, *27*, 29.

[160] A. E. Rydholm, C. N. Bowman, K. S. Anseth, *Biomaterials* **2005**, *26*, 4495.

[161] T. M. Roper, C. Chandler, C. A. Guyman, C. E. Hoyle, S.E. Jönsson, *RadTech NA Tech. Conf. Proc.* **2004**.

[162] T. M. Roper, C. E. Hoyle, A. C. Guymon, *Polym. Prepr.* **2003**.

[163] A. A. Oswald, W. Naegele, *Makromol. Chem* **1966**.

[164] Q. Li, H. Zhou, C. E. Hoyle, *Polymer* **2009**, *50*, 2237.

[165] S. Reinelt, M. Tabatabai, U. K. Fischer, N. Moszner, A. Utterodt, H. Ritter, *Beilstein journal of organic chemistry* **2014**, *10*, 1733.

[166] I. V. Koval, *Russ. J. Org. Chem* **2005**.

[167] E. I. Miranda, M. J. Diaz, L. Rosado, J. A. Soderquist, E. I. Miranda, M. J. Díaz, I. Rosado, J. A. Soderquist, *Tetrahed. Lett.* **1994**, *35*, 3221.

[168] A. R. Jennings, D. Y. Son, *Chemical communications (Cambridge, England)* **2013**, *49*, 3467.

[169] G. Ducom, B. Laubie, A. Ohannessian, C. Chottier, P. Germain, V. Chatain, *Water science and technology a journal of the International Association on Water Pollution Research* **2013**, *68*, 813.

[170] H. E. Gottlieb, V. Kotlyar, A. Nudelman, *J. Org. Chem* **1997**, *62*, 7512.